THE UNIVERSITY OF HULL

Graded titanium based coatings by combining thermal spray and PVD technologies

being a Thesis submitted for the Degree of PhD Engineering Design and Manufacture

in the University of Hull

by

Fabrizio Casadei

July 2008

Content list

I - INTRODUCTION

There is a rapid growth in demand for improved surface performance in many priority industrial sectors. There have also been rapid developments in methods of surface engineering and in tribological understanding. There is accordingly an exciting opportunity for cost effective industrial exploitation of materials with desirable properties. Among these materials, titanium and its alloys occupy an important place: their use in sectors such as aerospace and biomedical has already started and they are very promising candidates for an increasing number of industrial applications, provided some weak points are solved, as will be discussed later.

Considering, for an example, the today's aerospace engine sector, titanium alloys are used in the cold sections of the engine, where a certain strength is needed. Their application is limited to operating temperatures below 550°C, due to degradation of mechanical properties and oxidation at higher temperatures. The alloys possess some excellent properties, including low density, high strength, and good corrosion resistance. In fact, the strength-to-density ratio of titanium alloys is the highest compared to all materials considered for current structural aero engine parts. Typical components in titanium include blades, vanes, discs, and casings in the fan and compressor stage of the engine.

The driving force to use titanium alloys in the engines is to a large extent based on the achieved weight reduction. This is particularly important concerning rotating parts, where reduced weight provides the means to decrease the dimensions of the total rotating assembly as well as containing parts. This, in turn, increases engine efficiency in terms of thrust-to-weight and so on. Consequently, there is a strong driving force within the aerospace engine sector to increase the use of titanium alloys. In this regard, future potential titanium applications include shafts, gears, and bearings.

A major problem considering the use and increased use of titanium alloys is due to their unfavourable tribological properties. In fact, in all applications that involve mechanical joints and fluctuating loads, the tribological performance, particularly in terms of fretting, wear, and fretting in combination with fatigue loads, is a seriously limiting

factor. A typical example of a fretting problem in combination with fatigue loads is found in the dovetail joint; i. e. the contact between fan blade and disc. This represents a severe case involving high energy critical components for which a failure is associated with a large human risk. Examples of other fretting and wear problems related to the introduction of titanium alloys in aircraft engines are contacts between shafts/splines, and contacts in bearings and gear boxes. Furthermore, within component systems lubricated with a liquid lubricant in a hydrodynamic regime, situations may occur where the lubricant is lost because of some mechanical failure. In these cases the tribological system changes from hydrodynamic to boundary conditions, and eventually, to a complete lack of lubrication. Under these conditions, the severe titanium-against-titanium contacts generate very high temperatures which are not bearable by these alloys in their untreated state.

This situation has led to an urgent need to develop suitable treatments and coating processes to improve the tribological properties of Ti alloys. However, development of coating processes is very complex and costly. The number of variants is huge, spanning from elementary process steps to macroscopic parameters, from material properties to behaviour in complex systems. Modelling tools, especially in the field of new surface treatments are very poor and they need to be developed to provide real benefits to designers for use on-line and failure analysis. Surface properties, such as friction coefficients, are common to many processes, but are difficult to deal with since they are aggregate properties. In addition, there exists a serious lack of fundamental design data; i. e. what properties or thickness of a coating are required in order to withstand fretting conditions with or without imposed fatigue loading. As a result, designers have little confidence in the use of coatings, and this is exacerbated by the titanium alloys' relatively low hardness and Young's modulus values, as well as a susceptibility to cold welding. Consequently, these alloys are expected to provide a poor degree of support to hard surface coatings, which are normally used to improve tribological properties. As an analogy, the situation can be compared to that of an egg; a too high concentrated load on an egg (a thin hard surface on a much softer bulk material) will cause a catastrophic failure. This view is supported by the limited amount of work on the fretting and wear fatigue of these alloys which shows that the effectiveness of hard coatings decreases rapidly with increasing contact pressure. A way to overcome the problems is to provide

a supporting layer between the hard coating and the titanium alloy. However, this is not a straightforward task.

Two types of solutions are currently being pursued:

- *Multilayer thin coatings, made up of various materials (TiN, TiC, TiCN, CrN, CrC, DLC) or different microstructures*
- *Chemical diffusion treatments of the titanium alloy substrate followed by deposition of hard thin coatings.*

Both approaches aim at realising layers with graded mechanical properties, going from the bulk toward the outermost surface, without significant discontinuities. The limiting factors consist in the exiguity of the thickness (< 10 µm) of such layers, in the inherent slowness (tens of hours) of the processes and in their unfavourable economy.

The present work aims at overcoming the above-mentioned limitations by stimulating and catalysing the introduction of state-of-the-art surface engineering technology into key industrial applications for titanium alloy components. The focus of this research is in developing an innovative surface treatment, consisting of two consecutive phases:

- deposition by Reactive Plasma Spraying (RPS) of a thick (hundred of micrometers) composite Ti/TiN coating on the titanium based substrate
- deposition by Physical Vapour Deposition (PVD) of a thin (a few micrometers) hard, TiN based coating, single or multilayer, on the already deposited thick coating.

In such a way, it is possible to obtain a hundreds of micrometers thick surface layer with a TiN phase increasing from the bulk toward the surface. The advantages of such an approach derive mainly from an increased compatibility between coating and substrate, better structural integrity of the coated system and yet likelihood of longer operational life due to the high thickness of the whole modified surface layer. Furthermore, the RPS technology looks competitive with other technologies from an economical point of view, especially because of the relatively short (a couple of hours) duration of the process.

This work was started with a through study of the literature, concerning titanium and its main alloys. It included chemical and physical properties, mechanical and tribological characteristics as well as characterization procedures, application case histories, and related treatment and coating technologies. The results of such a literature survey, which constituted the basis from which the experimentation, and in particular, the concept of "graded coatings", were conceived, are reported in detail in the following chapter.

II - LITERATURE SURVEY

The relevant literature is divided in three chapters. The first one deals with general information about titanium and its alloys and it covers eight areas: properties and preparation, effect of impurities, titanium classification, structures and stabilising elements, alloys classification, mechanical characteristics, chemical reactivity, thermal treatments. These areas are linked by the concept that there often is an important correlation between the titanium based materials (substrates and coatings) and the specific applications. Chapters 2 and 3, dealing with properties, industrial applications, and treatment/coating processes inherent the Ti-6Al-4V alloy, have been included, taking into account that it currently is the most employed alloy and it has been used as substrate material in the experimental part of this work.

1. Titanium and its alloys

1.1 Properties and preparation

Titanium (Ti), silvery grey metal of transition Group IV B of the periodic table, was discovered around 1790 in a mineral, known today under the name of Rutile (TiO_2). The metal was isolated in pure form in 1910 by the New Zealand-born U.S. metallurgist Matthew A. Hunter by reducing titanium tetrachloride ($TiCl_4$) with sodium in an airtight steel cylinder. After 1947 titanium changed from a laboratory curiosity to an important metal commercially produced by the Kroll process. Since 1950 the *Titanium Metals Company of America* introduced titanium into the market, as a structural material, its production has continuously grown by a yearly rate of about 8%.

The interest for titanium and its alloys is due mainly to the high strength, corrosion resistance, and low density (4.51 g/cm^3 for Ti; 4.43 g/cm^3 for the Ti-6Al-4V alloy, at 20°C). Thus, titanium is about half as dense as iron (7.87 g/cm^3) and less than twice as dense as aluminium (2.7 g/cm^3). The excellent corrosion resistance in many environments is due to the formation of a passive oxide surface film. No noticeable corrosion of the metal has been found after several years exposure to seawater. The metal has a very low electrical and thermal conductivity and is paramagnetic (weakly responsive to a magnetic field).

The combination of all these properties explains why titanium based materials are used for many parts of aircraft, spacecraft, missiles, and ships. Titanium is used in prosthetic devices also, because there is no reaction between it and fleshly tissues and bones.

Although titanium is the fourth most abundant (0.6%) element in the Earth's crust, after aluminium, iron, and magnesium, a few minerals only constitute a source of it with enough concentration to make the production process acceptable from an economic point of view.

Titanium with electronic configuration $(Ar)3d^24s^2$ exhibits three valence states (2, 3, and 4) in compounds of the TiO, Ti_2O_3, and TiO_2 types, respectively. The +4 oxidation state, as in the dioxide (TiO_2), is the most stable one.

Titanium is found combined in practically all rocks, sand, clay, and other soils. It is also present in plants and animals, natural waters and deep-sea dredging, meteorites and stars. The two prime commercial minerals are Ilmenite and Rutile:

- Ilmenite is a combined divalent iron with tetravalent titanium atoms usually expressed as iron titanate (FeO-TiO_2) containing about 32 % titanium and 37 % iron.
- Rutile is almost pure (98-99 %) titanium dioxide (TiO_2), with only small amounts of iron, silicon and other elements as impurities.

The production of titanium metal from its ores is accomplished in several steps, each involving chemical reactions and each designed to eliminate the gaseous elements oxygen and nitrogen coming from the chemical reactions. The titanium dioxide (TiO_2) prepared from the ore is first converted to titanium tetrachloride ($TiCl_4$) by reacting it with chlorine gas in the presence of a reducing agent, usually carbon. A sequence of distillations is carried out to remove impurities such as metal chlorides. Then, the high-purity $TiCl_4$ is reduced to metallic titanium by reaction with magnesium or sodium. The Kroll process, which is the most utilised in the world, uses molten magnesium and it is carried out at 900°C under an inert atmosphere (Ar). Another process, referred to as the iodide process, uses iodine in place of chlorine and it allows to obtain titanium with very high purity. The titanium tetraiodide (TiI_4) produced is then decomposed thermally under vacuum on the surface of a titanium wire, which acts as a nucleus for the growth of a long high-purity titanium crystal bar (Mc Quillan, 1956). Moreover, there are electrolytic methods to prepare high-purity titanium.

1.2 Effect of impurities

Titanium's purity is dependent on the purity of the titanium tetrachloride or iodide from which it was made, the purity of the magnesium or sodium reducing agent, and the purity of the atmosphere during the reduction process. **Table 1** reports a comparison between the impurities present in the high-purity titanium and in the commercial one, produced according to the iodide and Kroll methods, respectively.

Tab. 1 - Typical impurities in titanium produced by the "iodide" and Kroll processes (Adapted from Rassmann, Illgen, 1972, pp. 321-328)

Type of impurity	Iodide process (% by wt.)	Kroll process (% by wt.)
Mg	0.01	0.13
Si	0.01	0.05
Al	0.02	-
Fe	0.01	0.20
Ni	0.01	-
Co	-	0.02
Cr	0.01	-
Mn	0.005	0.02
C	0.01	0.08
N	0.02	0.04
O	0.02	0.11

Among the impurities, C, N, and O are elements that occupy interstitial sites within the metal lattice. The effects linked with interstitial elements on the deformation resistance of titanium have been investigated extensively (Conrad, 1981): it was pointed out that carbon, nitrogen, and oxygen linked with covalent bonds to their titanium surrounding atoms influence strongly (**Figure 1**) the resistance of the material at temperatures below about one half its melting temperature ($\sim 0.5\ T_{melting}$).

Fig. 1 - Effect of oxygen on tensile properties of pure titanium (Finlayand, Synder, 1950)

1.3 Titanium Classification

Metallic titanium is classified according to its purity:

1) High-Purity Titanium

Its purity is referred to the oxygen content that must not exceed 500 PPM. It is obtained electrolytically or by the iodide process, starting from special titanium sponges containing less than 0.1% by wt. O_2.

2) Commercially Pure (CP) and Modified Titanium

The CP titanium is classified according to the ASTM specification in four grades, identified by the impurities content (generally O, C, H, Fe, and N are the impurities considered).

Small amounts of interstitial impurities, as it was already pointed out, influence strongly the mechanical properties of titanium, e.g. it is observed an increase in the resistance to

breaking and yielding by increasing the impurities content. Therefore, it is preferred to determine each titanium grade according to its mechanical properties, in particular strength and ductility, rather than relying on the chemical analysis.

A comparison between two mechanical properties for the four grades of titanium and their maximum impurity contents are reported in **Tables 2** and **3**, respectively.

Tab. 2 - Mechanical properties defining the four titanium grades (Adapted from ASMI Handbook, 1994)

ASTM grade	Minimum resistance to Breaking (MPa)	0.2% resistance to yielding (MPa)
Grade 1	240	170-310
Grade 2	345	275-450
Grade 3	440	380-550
Grade 4	550	480-655

Tab. 3 - Maximum impurity contents in the four titanium grades (Adapted from ASMI Handbook, 1994)

ASTM Classification	Nitrogen % by wt.	Carbon % by wt.	Hydrogen % by wt.	Iron % by wt.	Oxygen % by wt.
Grade 1	0.03	0.10	0.015	0.20	0.18
Grade 2	0.03	0.10	0.015	0.30	0.25
Grade 3	0.05	0.10	0.015	0.30	0.35
Grade 4	0.05	0.10	0,015	0.50	0.40

All the alloys obtained by adding small amounts of palladium (Ti-0.2 Pd identified as ASTM Grade 7 and Grade 11) or molybdenum and nickel (Ti-0.3 Mo-0.8 Ni identified as ASTM Grade 12) are referred to as "modified titanium".

Going back to **Tables 2** and **3**, it is pointed out the following:

- Ti ASTM Grade 1 exhibits the highest purity and the lowest strength. It shows, among the four grades, the best ductility and formability at room temperature. This grade should be used when it is required maximum formability and a high corrosion resistance (due to the low contents of iron and interstitial elements).

- Ti ASTM Grade 2, with respect to Grade 1, has higher concentrations of oxygen and iron which are responsible for a higher resistance to breaking and yielding, but, at the same time, a lower ductility (20% elongation versus 24% of Grade 1) and a lower corrosion resistance.

- Ti ASTM Grade 3 has iron and oxygen contents which are lower than those of Grade 4 only. Thus, its strength results to be enhanced further at the expenses of the elongation ability and corrosion resistance.

- Ti ASTM Grade 4 has the highest iron and oxygen contents and it exhibits characteristics of higher strength along with a good ductility and moderate formability. However, its corrosion resistance is lower than that of the other Grades.

1.4 Structures and stabilising elements

Titanium exhibits two crystal structures: below 882°C, one hexagonal close-packed (HCP) called phase α; the other above 882°C, a body-centred cubic (BCC) or phase β (see **Figure 2**). **Figure 3** illustrates the phase diagram of the binary system Ti-O, from which it is possible to derive the transition temperature (882°C) of the two allotropic phases at atmospheric pressure. It is worth to remind that this temperature is called transition β (β transus) and it is defined as the lowest equilibrium temperature at which 100% of the material is in the form β.

Contaminants such as oxygen and nitrogen tend to increase the transition temperature up to 900°C, and an appreciable two-phase region, consisting of apparently pure titanium, can be observed.
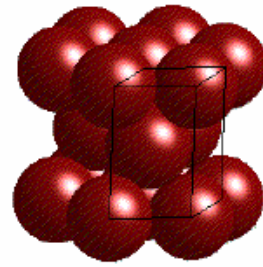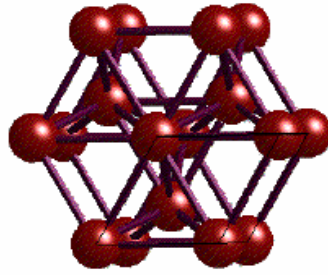
Hexagonal close-packed (HCP)
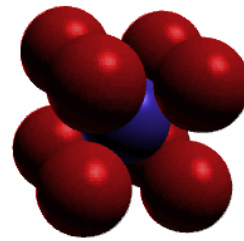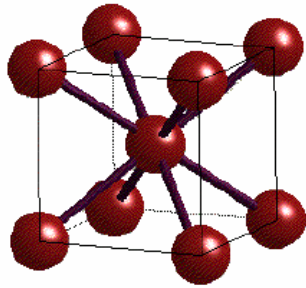
Body-centred cubic (BCC)

Fig. 2 - Crystal structures of titanium (Adapted from ASMI Handbook, 1994)
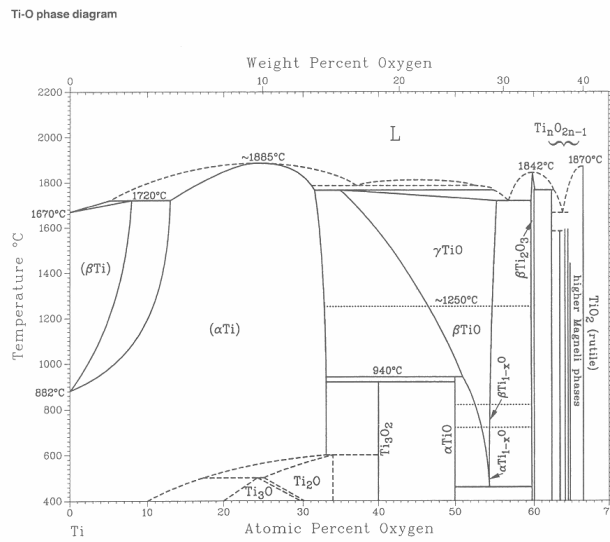
Fig. 3 - Phase diagram Ti-O (Murray, Wriedt, 1987)

Certain chemical elements dissolved in titanium may stabilise the two phases. They are divided in two categories, namely α and β stabilisers:

α stabilisers are generally simple metals (Al) or elements (N, O) that may occupy interstitial sites within the titanium crystal lattice (Molchanova, 1965). They are called also "s. p. elements" from their electronic configurations. Their presence causes an increase of the transition temperature (i.e. the temperature below which the α phase is stable).

β stabilisers are transition (Mo, V) or noble metals. Their presence causes a decrease of the allotropic transition temperature (i.e. the temperature at which the β phase becomes stable). The stabilisers of this type are divided into two groups: a) β-isomorphous elements (Mo, V, Ta) miscible in the β phase and b) eutectoid elements (Mn, Fe, Cr, Co, Ni, Cu, Si) which undergo eutectoid reactions with titanium. They show eutectoid temperatures up to 333°C that are lower than the transition temperature of pure titanium.

1.5 Alloys Classification

In titanium alloys, unlike pure titanium, the single phases α and β are separated by a two-phase region α + β, the width of which increases with increasing the concentration of the dissolved species (solute).

Titanium alloys are divided generally into five categories according to their microstructure states and type of stabilisers: α, β, α + β, near-α, near-β. The last two refer to alloys with such compositions so that place them near the phase boundaries α/(α + β) and (α + β)/β, respectively.

1. *Alpha* alloys

   Pure titanium and its alloys with αstabilisers such as Al, Ga, Ge, C, O, N, and Sn, alone or in combination possess a HCP structure below 882°C.

2. *Beta* alloys

   The solutes which stabilise the BCC phase β are transition metals of the V B (V, Nb, Ta) and VI B (Mo) groups and they (one or more) are present in large amount.

3. *α + β* alloys

These are alloys that at equilibrium, generally at room temperature, are made up of a mixture of α and β phases and they are obtained due to the presence of both types of stabilisers. The specific amount of β phase depends on the quantity of β stabilisers and thermal treatment. The α + β alloys can be produced without difficulty, except the Ti-6Al-4V (Salmon, 1979).

4. *Near-alpha* alloys

The alloys of this type form a limited amount of phase β only, and, thus, they may appear like the α alloys from a microstructure point of view.

5. *Near-beta* alloys

These constitute a metastable type of alloys which tend to retain the phase β upon cooling down to room temperature; however, secondary phases precipitate during thermal treatment.

The ratio among the quantities of the stabilisers in a given alloy is expressed as "equivalence" of stabilisers, referring to the two elements that are considered the most suitable: Al and Mo for stabilising the α and β phases, respectively.

According to Rosemberg (1970, pp. 851-859), the <u>equivalent aluminium concentration</u> in an alloy containing Al, Zr, Sn, and O is:

$$[Al]_{eq} = [Al] + [Zr]/6 + [Sn]/3 + 10 [O]$$

where the terms inside the square brackets indicate wt. percent concentrations.

The <u>equivalent molybdenum concentration</u> can be calculated from the data reported in **Table 4**. These values represent the amounts of transition elements to be added to titanium in order to decrease the rate of martensitic transition and, thus, allow the retention of the phase β at room temperature.

Tab. 4: Amounts of transition elements needed to retain the phase β at room temperature (Adapted from Molchanova, 1965)

Group	Element	Critical Concentration (wt.%)
V	V	15
	Nb	36
VI	Cr	8
	Mo	10
VII	Mn	6
VIII	Fe	4
	Co	6
	Ni	8

The <u>equivalent Mo concentration</u> is given by the following equation:

$$[Mo]_{eq} = [Mo] + [Nb]/3.6 + [V]/1.5 + 1.25\ [Cr] + 1.25\ [Ni] + 1.7\ [Mn] + 1.7\ [Co] + 2.5\ [Fe]$$

Utilising this method to compare, for example the following two alloys, it is obtained:

Ti-6Al-4V $[Al]_{eq} = 6.0\ \%$ $[Mo]_{eq} = 2.7\ \%$

Ti-6Al-6V-2Sn $[Al]_{eq} = 6.7\ \%$ $[Mo]_{eq} = 4.0\ \%$

1.6   Mechanical Characteristics

The higher purity grades (low content of interstitial elements) of metallic titanium show less strength, hardness and lower transition temperatures with respect to those of the lower purity grades.

In pure state titanium is ductile and it can be polished to a high lustre. Great importance for titanium derives also from its ability to be alloyed with most metals and some non-metals.

By alloying titanium, its tensile strength can be increased five fold to 14,000 kilograms per square centimetre.

The high solubility of oxygen and nitrogen in titanium confers on it unique properties; however, it may cause some uncommon problems also. For example, heating titanium in air at high temperature causes, beside oxidation, hardening as a result of O_2 and N_2 diffusion. It is formed a surface layer (contamination layer or alpha case) which lowers its resistance to fatigue and ductility. The oxide scale is removed before machining operations.

Between the alpha and near-alpha systems the alpha alloys containing Al, Sn, and/or Zr are preferable for both high temperature and cryogenic applications. Unlike the alpha-beta and beta alloys, the alpha alloys can be strengthened by thermal treatment. Generally, the alpha alloys are annealed or crystallised to remove the residual stress induced by cold working. These alloys possess good weldability because they are not sensitive to thermal treatment. Generally they exhibit poor forgeability with narrower forging temperature ranges than those of the alpha-beta or beta alloys; in particular at temperatures lower than the β-transus. The poor formability reveals itself with the tendency to form surface cracks or centre bursts in the material.

The alloys classified as near alpha or superalpha, which contain small amounts of β stabilisers (e. g. Ti-8Al-1Mo-1V or Ti-6Al-2Nb-1Ta-0.8Mo) and phase β in small quantity, behave as α and not as α-β alloys.

The α + β alloys can be strengthened by solution treating, carried out at elevated temperatures in the 2-phase α + β region and subsequent quenching in water, oil or other suitable materials, and by ageing. The result of quenching is that the phase β, present at the temperature of the solution treatment, may be retained or transformed in part upon cooling, either by a martensitic transformation or nucleation and growth.

The solution treatment is followed by the ageing at temperatures ranging between 480 and 650 °C, in order to precipitate the alpha phase and produce a fine mixture of phases α and β in the retained or transformed phase β.

The above described treatments may increase the strength of the α + β alloys in the order of 30-50 %, or even more, depending on the annealing or ageing conditions.

Regarding the Ti.6Al-4V alloy, the cooling rate in the case of quenching in water is not high enough to harden appropriately sections thicker than 25 mm. Increasing the content of β stabilisers the surface hardening of the alloy tends to increase: for example, Ti-5Al-2Sn-2Zr-4Mo-4Cr can be hardened homogeneously for sections up to 150 mm thick. With intermediate contents of β stabilisers, it is obtained the strengthening of a surface layer relatively thick, but its core properties, especially hardness and strength, remain about 10 – 20% lower with respect to the surface.

The strength which can be obtained by means of thermal treatments is a function also of the beta phase volume present at the temperature of the solution treatment.

The β metastable alloys are characterised by an elevated hardenability, and the metastable phase β is retained completely by quenching, in air in the case of thin sections or in water for thick sections.

The β alloys possess excellent forgeability; in the form of sheets these alloys can be cold worked more easily than those of the α or α-β types with high strength. The phase β usually is metastable and it tends to convert itself into an α + β equilibrium structure.

The main disadvantages of the beta alloys, with respect to the alpha + beta ones, are:

- higher density
- less thrust resistance
- lower ductility in the aged state.

The main advantages of the beta alloys are:

- high hardenability
- excellent forgeability
- good cold working formability in the solution treatment conditions.

As an example, it is reported a comparison between the mechanical properties of commercial pure (CP) titanium and its Ti-6-4 alloy of the α-β type: **Figure 4** shows the stress-strain curve relevant to Ti CP at both room and high temperatures. The

corresponding stress-strain curves for the Ti-6-4 alloy in the annealed state and after solution treating and ageing (STA) are shown in **Figures 5** and **6**, respectively.
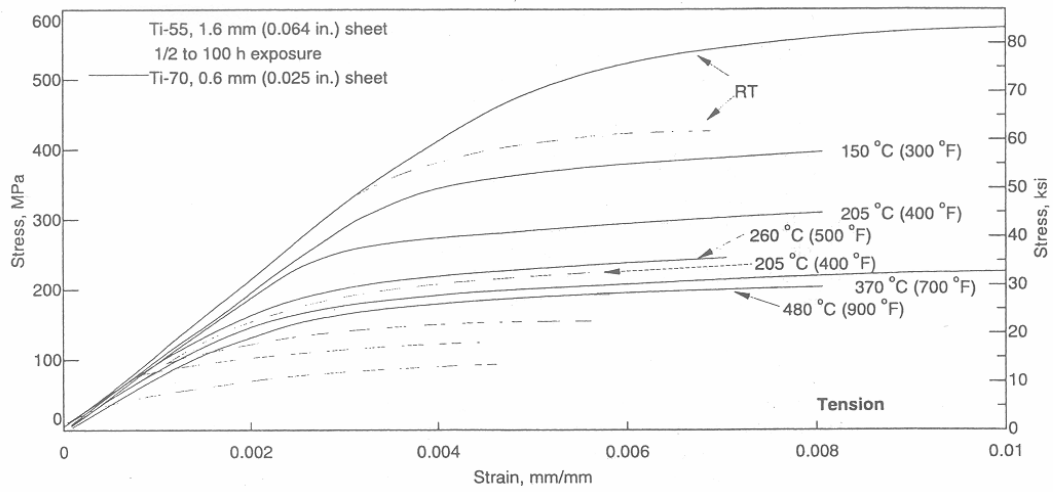
Fig. 4 - Stress-strain curves at room and elevated temperatures for CP titanium (Battelle Columbus Laboratories ed., 1963)
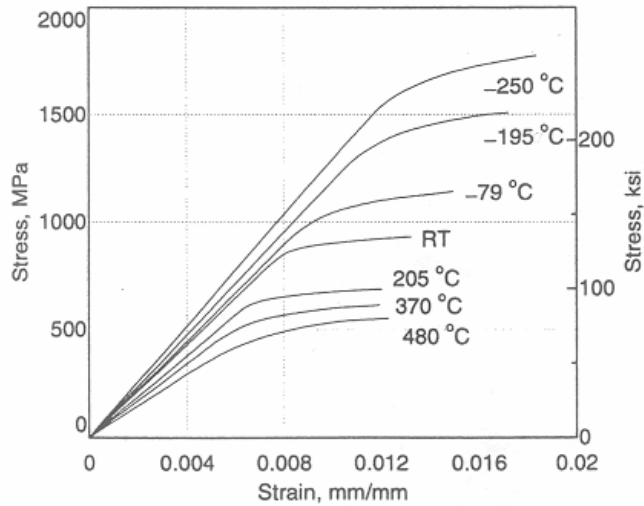
Fig. 5 - Stress-strain curves at room and elevated temperatures for Ti-6Al-4V alloy – annealed- (MIL-HDBK 5, 1991)
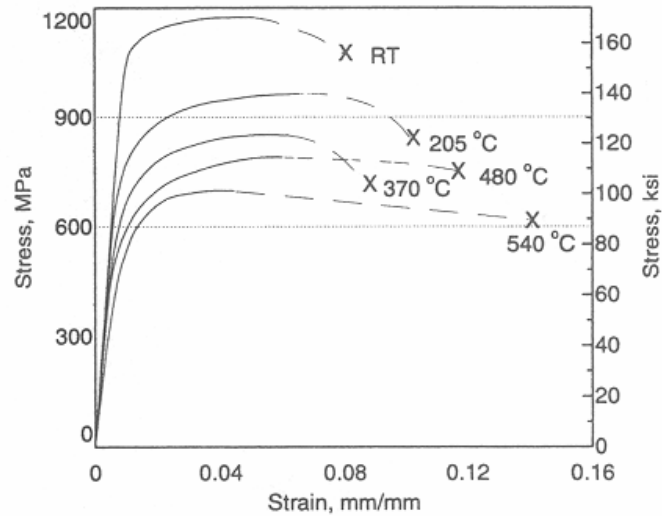
Fig. 6 - Stress-strain curves at room and elevated temperatures for Ti-6Al-4V alloy - solution treating and ageing- (MIL-HDBK 5, 1991)

1.7 Chemical Reactivity

1.7.1 Corrosion Resistance

Titanium and its alloys have excellent corrosion resistance in many environments because of the formation of a passive oxide surface film.

The oxides TiO, TiO_2, and Ti_2O_3 form naturally and instantly whenever the clean metal surface is exposed to even traces (p.p.m) of air or humidity (Kolachev et al., 1978, pp. 61-68). Oxidation at high temperature tends to promote the formation of crystalline TiO_2 as Rutile, while at lower temperatures it may form an amorphous Ti_2O_3 or TiO_2 as Anatase or a mixture of Rutile and Anatase.

The passive oxide TiO_2 is a type n semiconductor (Kolachev et al., 1993, pp. 27-30) and possesses a wide range of thermodynamic stability, as it is pointed out by the Pourbaix diagram (potential versus pH for the titanium-water system) shown in **Figure 7**: the oxide is stable at room temperature in the whole range of the pH scale for values of potential variable from strongly oxidising to moderately reducing.

The formation of hydride is expected under strongly reducing (cathodic) conditions. Although the film of oxide formed naturally has a thickness lower than 10 μm and it is invisible to the naked eye, it is stable with a continuous structure and strongly protective with a good adhesion. This oxide is resistant to hydrogen permeation, but it is attacked by a few substances, among which there are: concentrated hot hydrochloric acid, sulphuric acid, sodium hydroxide, phosphoric acid, and hydrofluoric acid.
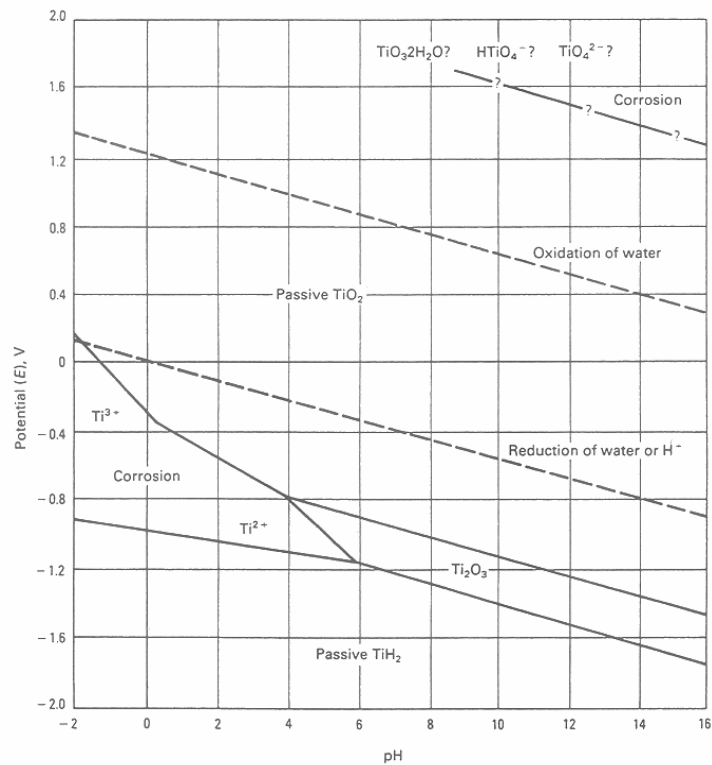
Fig. 7 - Pourbaix diagram for the system H_2O-Ti at 25 °C (Kolachev et al, 1993)

Generally the titanium metal and its alloys are resistant to corrosion in a brackish environment and in the presence of gases such as sulphydric acid and carbon dioxide up to a temperature of 260°C. However, titanium can be attacked by strongly oxidising or reducing environments: for example, under oxidising conditions, in complete absence of humidity, no protective surface film forms, while a process of in depth oxidation with a strongly exothermic reaction takes place.

Breaking of the passive film may take place also because of interaction with anhydrous oxidising agents such as concentrated nitric acid, non-oxidising watery environment, and due to pitting attacks or cracking in nearly neutral aqueous solutions (in particular in presence of halides). Finally, a continuous mechanical contact with other metals (wear) may prevent that the protective oxide is formed again in an uniform way and may speed up the corrosive process.

1.7.2 Influence of chemical composition on corrosion

The corrosion resistance of the oxide passive film remains essentially unchanged in the presence of minor (< 2-3%) alloying components or traces of impurities. For example, it has been pointed out (Covington, Schutz, 1981, pp. 163-180) that all the grades of metallic titanium, show the same wide range of corrosion resistance, independently of small variations in the iron content and interstitial elements (C, O, N), provided that there are the conditions of complete passivity (<< 0.04 mm/year). On the contrary, if titanium is not in passivity conditions but it exhibits a significant rate of corrosion (0.13 mm/year is the maximum corrosion allowed by designers), some alloying elements such as sulphur and iron speed up the corrosion rate.

Under reducing conditions, the corrosion resistance of the titanium alloys may be increased effectively by adding minor components such as nickel and palladium. Regarding the major components, it must be mentioned that in reducing aqueous acid solutions vanadium and molybdenum ($\geq$ 4%) increase the corrosion resistance, while additions of aluminium are detrimental.

1.7.3 Influence of Hydrogen

The surface titanium oxide is very effective in preventing hydrogen penetration in the interior of the material. The protective film (Covington, Schutz, 1982; Covington, 1975; Covington, 1979) is maintained by traces of oxygen or humidity in the same environment containing hydrogen. On the other hand, an atmosphere containing anhydrous hydrogen leads to the absorption of this gas, especially if temperature and pressure are increased.

The poor performance of titanium alloys in presence of hydrogen manifests itself at both high and low strain rates under load, and it is attributable to the precipitation of a hydride phase. Since in the titanium alloys the hydrogen solubility increases with temperature, the brittleness due to the presence of hydride decreases by increasing the temperature. Furthermore, at higher temperatures the hydride may become more ductile, reducing, thus, the initiation of brittleness breaking.

Damage due to hydrogen may take place whenever hydrogen is developed on the surface of a metallic material; for example, because of corrosive phenomena in an acid environment, galvanic processes, thermal treatment, pickling, and chemical treatments to remove the α-case.

Two types of hydrogen damage can be distinguished:

- *Swelling*, caused by the penetration of atomic hydrogen into the metal and its recombination to molecular state inside defective zones (holes, micro-cracks) present in the lattice, with localised pressure increase beyond elastic limit and yield point. This situation is responsible for strong localised strains, formation of cracks or breaking of the material.

- *Brittleness*, caused by penetration of atomic hydrogen into the metal and subsequent irreversible formation of brittle phases (hydrides) or reversible occupation of interstitial sites which cause a localised distortion of the crystalline lattice and a worsening of the mechanical characteristics (in particular the resiliency).

Since the hydrogen concentration has a relatively small effect on the hardness of the material, hardness testing is not a suitable method to estimate the amount of absorbed hydrogen. To this end a hot extraction technique in vacuum is used: a small sample is heated between 1100 and 1400°C for several minutes in order to release hydrogen that is determined by means of evolved gas (EG) measurements. In case its concentration is estimated to be high, a vacuum annealing for 2-4 hours is carried out. Maximum hydrogen content, according to current specifications, ranges from 125 up to 200 PPM, depending on

the type of titanium alloy. Above these limits, hydrogen makes brittle some titanium alloys, causing a decrease of the impact and traction resistance

A strong brittleness is observed in the various titanium Grades starting already with 30-40 PPM of hydrogen in presence of high residual stress or a stress raiser inclusion and high temperature. Such conditions induce hydrogen to migrate toward the inclusion, resulting in a significant localised increase of its concentration and the precipitation of hydrides.

Besides the brittleness problems, many beneficial effects (Kolachev et al., 1978), due to the presence of hydrogen, should be reminded. Among these it is worth mentioning the increase of the maximum deformation limit before the initiation of the first crack, the phase and structure deformations and the enhancement of the adhesion phenomena. These beneficial aspects have motivated a specific technology, referred to as *hydrogen technology* devoted to titanium based materials (Kolachev et al., 1993). It exploits the high diffusion mobility of hydrogen, according to which it may be introduced and removed easily. The *hydrogen technology* calls for the hydrogenation of the metal or alloy in a well defined range of concentrations and (after carrying out some technological operations taking advantage of the hydrogen presence), the annealing in vacuum to bring down the hydrogen content to safe values.

1.7.4 Contamination by the Environment

Titanium is chemically active at elevated temperatures and thus it may react with the many gases, such as O_2, N_2, H_2, H_2O, CO, and CO_2, usually present in the environment during thermal treatment.

The capture of oxygen or nitrogen at high temperature causes the formation of a surface film made up mainly of phase α: as it has been already pointed out, oxygen and nitrogen are α stabilisers and both contribute to the formation of the "α-case" layer, which is detrimental because of its brittle nature. Since the absorption rate of oxygen is higher than that of nitrogen, the predominant reaction is that involving oxygen. At a temperature of 955°C the α structure may extend down to 0.2-0.3 mm below the surface and it must be removed mechanically and/or chemically.

Nitrogen does not constitute generally a serious contamination problem; however, if a sufficient amount of it is adsorbed, hard and brittle nitrides such as TiN and Ti_xN_y are formed.

Adsorption of H_2 gas by titanium alloys is strongly dependent on temperature, hydrogen pressure and its humidity or oxygen content, surface characteristics /composition of the alloy and nature of its surface oxide.

Without interference due to the oxide film, the hydrogen concentration in titanium is directly proportional to the square root of the H_2 partial pressure. It was demonstrated that a 2% H_2O content in 5.5 MPa of H_2 at 315°C retards the hydrogen capture by the Ti CP.

1.8 Thermal Treatments

Titanium alloys are treated thermally to obtain microstructures and sets of mechanical properties specific for a given application.

Thermal treatments may be also combined with a sequence of specific thermo-mechanical treatments to improve microstructure and properties. The results depend, to a large extent, on the particular composition of the alloy and effects of alloying elements on the α-ß phase.

Different thermal treatments are employed for the various titanium alloys according to their compositions and microstructures. Therefore, some alloys may undergo unique thermal treatments meant to improve specific properties such as creep and fatigue resistances.

Thermal treatment conditions may be very stringent if it is required to improve specific properties: for example, to obtain the maximum creep resistance for the IMI 834 alloy, the temperature of the solution treatment must be controlled within a range of ± 5°C.

Thermal treatments generally applicable to titanium alloys are classified as shown in **Table 5**. **Table 6** summarises the typical thermal treatments carried out in the case of titanium alloys of the α-ß type.

Tab. 5 - Heat treatments on Ti alloys (Adapted from ASMI Handbook, 1994)

Heat treatments	Aim (Effect)
Stress-reliving	Reduce the undesiderable residual stresses developed during fabrication (welding, forming, ..)
Annealing	Produce an acceptable combination of ductility, machinability, and dimensional and structural stability especially in alpha-beta alloys under less stringent processing rules than those used to generate optimum strength or special property combinations
Ageing combined with	Increase strength
Solution treatment	Optimize special properties such as fracture toughness, fatigue strength and high-temperature creep strength

Tab. 6 - Summary of heat-treatments for α–β alloys (Adapted from ASMI Handbook, 1994)

T: temperature; t: time; β_T: β-transus temperature

Heat-treatment designation	Heat-treatment cycle	Microstructure	Effect
SR Stress Reliving	• T=480/705°C • t= 30 min. to 4 h • furnace (slow cool) or air cool	No significant changes in microstructure are observed	Relives residual stresses from welding, forming, etc. This cycle only provides a partial stress relief. A full anneal must be used for full stress relief. Low strength, good ductility

MA Mill Anneal or Full Anneal	•T=650/815°C • t= 30 min to 4 h •air cool or slow cool	Incompletely recrystallized alpha with a small volume fraction of small beta particles	Most common heat treatment, has good overall properties combinations. Low strength, good ductility
RA Recrystallization Anneal	•T= 25/55°C below β_T • t= 1 to 1 4 h • air cool to 50°C or slow cool	Equiaxed α (Rx coarse) with small amounts of beta phase at grain-boundary triple points	Usually used for ELI material. Strength comparable to above conditions, but improved damage tolerance. Fracture toughness, fatigue crack growth strength reduced crack growth rates and ductility. Strength is lower for ELI material.

DA
Duplex Anneal
	•T= 25/55°C below β_T
	• t= 1 h
	• air cool
	•overage
	   T= 600/760°C
	   t= 2-4 h
	• air cool
		Primary equiaxed alpha + Widmanstätten α–β regions	Improved damage tolerance (strength, creep strength, fracture toughness, fatigue)

BA
Beta Anneal
	•T= 25/55°C below β_T
	• t= 1 h
	• air cool
	•overage
	   T= 600/760°C
	   t= 2-4 h
	• air cool
		Widmanstätten or alfa basket weave plus beta colonies	Used to maximize damage tolerance properties. Maximum of fracture toughness, fatigue crack growth strength, with lower fatigue strength and ductility

STA Alpha-Beta Solution Treat and Age	•T= 15/55°C below β_T • t= 1 h	Primary equiaxed alpha + alpha tempered (α') or alpha	Highest strength condition, but less ductility and lower

	•air cool or water quench	Widmanstätten + beta	fracture toughness and fatigue crack growth strength than annealed. Good combination of fatigue and creep
	•age		
	T= 480/650°C		
	t= 4-8 h		
	• air cool		
SR Stress Reliving	•T=480/705°C • t= 30 min. to 4 h • furnace (slow cool) or air cool	No significant changes in microstructure are observed	Relives residual stresses from welding, forming, etc. This cycle only provides a partial stress relief. A full anneal must be used for full stress relief. Low strength, good ductility
MA Mill Anneal or Full Anneal	•T=650/815°C • t= 30 min to 4 h •air cool or slow cool	Incompletely recrystallized alpha with a small volume fraction of small beta particles	Most common heat treatment, has good overall properties combinations. Low strength, good ductility
RA Recrystallization Anneal	•T= 25/55°C below β_T • t= 1 to 1 4 h • air cool to 50°C or slow cool	Equiaxed α (Rx coarse) with small amounts of beta phase at grain-boundary triple points	Usually used for ELI material. Strength comparable to above conditions, but improved damage tolerance. Fracture toughness, fatigue crack growth strength reduced crack growth rates and ductility. Strength is lower for ELI material.
DA Duplex Anneal	•T= 25/55°C below β_T • t= 1 h • air cool	Primary equiaxed alpha + Widmanstätten α–β	Improved damage tolerance (strength, creep strength,

	•overage
	
	  T= 600/760°C
	
	  t= 2-4 h
	
	• air cool
		regions	fracture toughness, fatigue)

BA
Beta Anneal
	•T= 25/55°C below β_T
	
	• t= 1 h
	
	• air cool
	
	•overage
	
	  T= 600/760°C
	
	  t= 2-4 h
	
	• air cool
		Widmanstätten or alfa basket weave plus beta colonies	Used to maximize damage tolerance properties.
			Maximum of fracture toughness, fatigue crack growth strength, with lower fatigue strength and ductility

STA
Alpha-Beta Solution Treat and Age
	•T= 15/55°C below β_T
	
	• t= 1 h
	
	•air cool or water quench
	
	•age
	
	  T= 480/650°C
	
	  t= 4-8 h
	
	• air cool
		Primary equiaxed alpha + alpha tempered (α') or alpha Widmanstätten + beta	Highest strength condition, but less ductility and lower fracture toughness and fatigue crack growth strength than annealed.
			Good combination of fatigue and creep

2. Ti-6Al-4V (Ti 6-4) ALLOY

2.1 Industrial Applications

This titanium alloy, which contains 6% aluminium and 4% vanadium by weight, is characterised by an excellent combination of specific resistance (resistance/density = 25 * 10^6 mm), toughness, stability up to a temperature of 400°C, and an excellent corrosion resistance. It is the mostly used one among the titanium alloys (50% of the titanium produced worldwide is in the form of Ti-6Al-4V).

It is mainly (80% of the worldwide production) used by the aerospace industry, while surgery products (prosthesis) hold the second place (3%) and the remaining 17% is utilised in various sectors of the mechanical and chemical industries (i.e. high performance and racing cars, sport items, offshore).

Its high cost is the main factor to forbid a wider use: a cost comparison of products realised with different materials is reported in **Table 7**.

Tab. 7 - Costs of Ti 6-4 products compared to those of aluminium, stainless steel, and nickel based materials (Adapted from Donachie, Jr., ed., 1988)

Product	Material	Cost (US $/Kg)
Die forging	Ti 6-4	66
	Al	22
	stainless steel	17.5
Sheet	Ti 6-4	35
	Al	4.5-9
	stainless steel	6.5
	Inco 718	22
Forged block	Ti 6-4	17.5
	Al	5.5-6.5
	stainless steel	5.5-6.5
Cable(0.625 cm.)	Ti 6-4	57
	Al 7075	5
	stainless steel	16.5
Extrusion	Ti 6-4	28.5-33
	Al	4.5-9
	stainless steel	6.5-9
	300 serie	

The alloy is available in the form of various types of machined products (bars, sheets, rods, etc.) with properties varying according to the content of interstitial elements and to the thermo-mechanical processes it has been exposed to.

All types of products are used by the aeronautical industry, while in the space applications the alloy is employed for the production of rocket engines, wings, missile fuselages, housing of optical sensors. Initially, in the fifties, this alloy was used for compressor blades in the gas turbine engines; nowadays it is used for airplane structures and in turbine engine components, which include blades, discs, and wheels. Furthermore, the super plastic characteristics of the alloy, which are obtained by means of special treatments leading to an equiaxial fine grain structure, combined with the good characteristics of diffusion bonding, allow the realisation of very complex structures, exploited more and more often for aerospace applications and, in particular, in the construction of military aircrafts.

The casting pieces used for aerospace applications include large size structural components, each one of which may weigh as much as 135 Kg, and small components such as the switch guards which weigh less than 30 g.

Ti 6-4 castings are used to join the main external tanks to the Space Shuttle.

2.2 Relationship between alloy properties and structures

Since the Ti 6-4 is an alloy of α- ß type it presents different volume fractions of alpha and beta phases according to the thermal treatment that it has undergone and to the content of interstitial elements (oxygen in particular).

The amount of equiaxial phase α and the granularity or subdivision state of the converted phase ß determine the properties of the alloy. A comparison between the advantages derived from the presence of equiaxial or acicular microstructures is shown in the following layout:

Alloy microstructure	
Equiaxial	**Acicular**
Advantages	
• High ductility and formability • Higher resistance (thermal treatment being equal) • Better hydrogen tolerance • Better low-cycle fatigue characteristics	Superior creep properties Higher toughness values to fracture

The Ti 6-4 alloy in the annealed condition possesses strength characteristics which derive mainly from the presence of substitutional and interstitial alloying elements, contained as solid solutions in both the α and β phases.

As already mentioned, the interstitial elements (O, N, H) increase strength and decrease ductility; while the effect of aluminium, the most important substitutional element, is that of increasing strength linearly.

Aluminium in the Ti 6-4 alloy shows a tendency to promote an ordered phase (α_2) forming Ti_3Al.

Precipitation of this compound, which has been verified experimentally in alloys containing less than 0.2 wt.% of oxygen (Welsch et al., 1977, pp. 169-177) takes place at ageing temperatures ranging between 500 and 600 °C, and it is caused by an increase of oxygen concentration, since it decreases the solubility limit of aluminium in the phase α of titanium. However, it is worth mentioning that the oxygen content remains within acceptable values for this type of alloy.

The presence of an ordered phase gives a contribution of about 15-35 MPa to the alloy strength.

2.3 Elastic properties

Young's modulus, E, at room (298°K) temperature of pure titanium ranges between 100-110 GPa, which is in agreement with the calculated value for the single crystal of titanium along the direction perpendicular to the crystallographic c axis. For the single crystal, E varies according to the sample orientation as it is the case for the Poisson's modulus, ν: typical values of this last parameter for the polycrystalline titanium range between 0.32 and 0.36.

At room temperature the shear modulus, G, for titanium varies between 42 and 45 GPa according to the interstitial impurities and the bulk modulus (expressed as the reciprocal of the compressibility in the elastic range) varies between 106 and 108 GPa.

The Ti 6-4, among the titanium alloys, is positioned at an average value of E, as it is shown in **Table 8**.

Tab. 8 - Young modulus (E) and shear Modulus (G) of some titanium alloys at room temperature (Adapted from Donachie, Jr., ed., 1988)

Alloy	Condition	Young modulus, E (traction) 10^{10} N/m^2	Young modulus, E (compression) 10^{10} N/m^2	Shear modulus G 10^{10} N/m^2
Ti-5Al-2.5Sn	Annealed	10.9	-	4.8
Ti-8Al-1Mo-1V	Annealed	12.1	12.4	4.6
Ti-6Al-4V	Annealed	11	11.4	4.2
	Aged	11.4	-	4.2
Ti-10V-2Fe-3Al	Aged	11	11.2	-
β-III Ti-45Sn-6Zr-11.5Mo	Annealed	8.3	7.6	2.7
	Aged	10	11	4.1

However, the value of E for the Ti 6-4 alloy is relatively low when compared with those of steel or nickel alloys, as it is shown in **Table 9**.

Tab. 9 - Values of E, G, and ν of some metallic alloys (Adapted from Donachie, Jr., ed., 1988)

Alloy	Young Modulus, E [GPa]	Shear Modulus, G [GPa]	Poisson Ratio,ν
Ti-6Al-4V	105-116	41-45	0.26-0.36
Duraluminium	72	26-27	0.34
Nickel alloys	200-222	76-85	0.31-0.32
stainless steel	190-215	74-83	0.27-0.30

At cryogenic temperatures the E variation for the Ti 6-4 alloy is shown in **Figure 8**, whereas the E, G, and ν values in the temperature range between - 196 and 800°C are reported in **Table 10**.
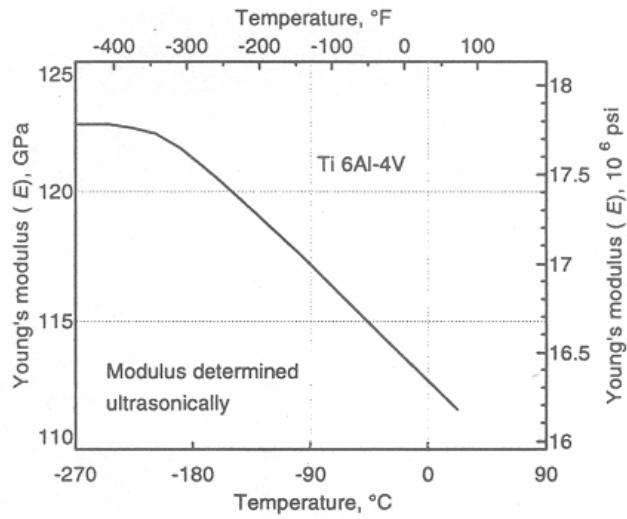
Fig. 8 - E variation for the Ti 6-4 alloy at cryogenic temperatures (Donachie, Jr., ed., 1988)

Tab. 10 - E, G e ν values for the Ti-6Al-4V alloy at different temperatures (Adapted from Donachie, Jr., ed., 1988)

Temperature [°C]	Young Modulus, E [GPa]	Shear Modulus, G [GPa]	Poisson Ratio,ν
-196	114.9	46.6	0.23
0	105.0	42.8	0.23
200	94.7	38.5	0.23
400	84.1	34.2	0.23
600	74.2	30.0	0.24
800	62.8	-	-

2.4. Tribological Properties

2.4.1 Friction and Wear

The excellent mechanical characteristics of titanium and its alloys go together with the poor tribological properties in terms of low resistance to adhesion wear and surface fatigue. Such a situation restricts the number of applications, unless special treatments or surface coatings are carried out.

Theoretical calculations have pointed out that metals with lower breaking points and poorer shear resistance have higher friction coefficients (μ). Among the materials with a compact hexagonal structure, titanium shows relatively low values of both breaking point and shear resistance; therefore, a high friction coefficient is expected. Actually, it was found a value of $\mu = 0.6$ for sliding titanium against titanium in air (Miyoshi, Buckley, 1982, pp. 15-23) and in vacuum (Buckley, 1981, p. 353).

The material transfer of titanium sliding against the surface of a non metallic material is quite likely to all those materials which are characterised by a low traction resistance. The titanium oxide film that forms easily on the titanium surface is transferred to the surfaces of non metallic materials such as polymers and it adheres to them, causing a severe adhesion wear (Buckley, 1981).

The addition of a lubricant reduces both the wear damage and the friction coefficient with respect to the unlubricated conditions. However, at elevated temperatures reactions between the titanium surface and the lubricant may take place, causing a degradation of the lubrication performance.

In **Figure 9** it is shown the modest decrease of the friction coefficient observed in a Ti 6-4 sample by adding a poly-perfluoro-alchyl-ether lubricant (Snyder, Dolle, 1975, pp. 171-180); a more substantial decrease takes place if the sample surface is modified by the ion implantation process (Kustas et al., 1992, pp. 100-105; Jamal et al., 1980, pp. 245-254), also shown in the same **Figure 9**.
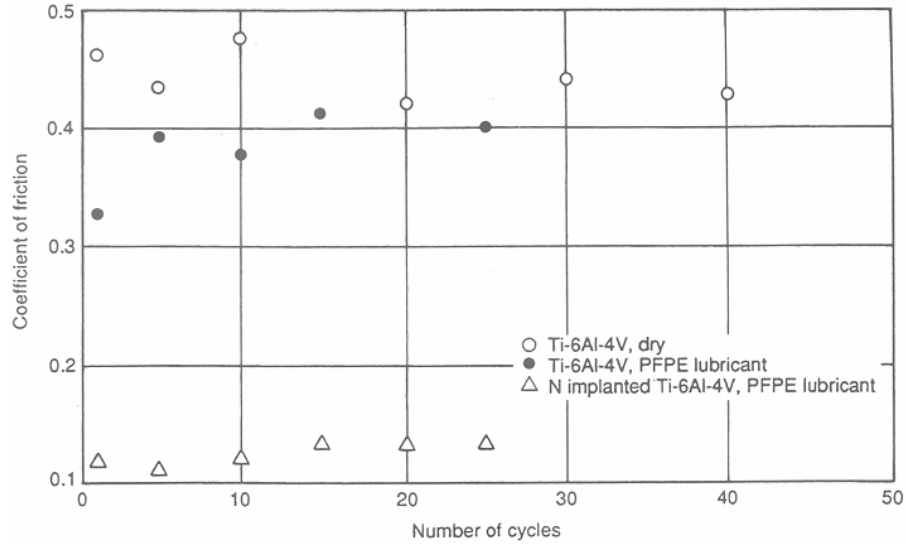
Fig. 9 - Comparison among the friction coefficient variations for Ti-6Al-4V (on air), Ti-6Al-4V lubricated with PFPE, and Ti-6Al-4V N implanted and lubricated with PFPE. Material utilised as counterpart: WC-Co. Sliding speed 1mm/s; load 5 N (Jamal et al., 1980, pp. 245-254)

2.4.2 Fretting

The Ti 6-4 alloy is widely used for making turbine engine components, in particular blades and discs. These components are liable to fretting phenomena which take place, generally, almost in the contact points of any mechanical structure, whenever small amplitude displacements (or vibrations with apparent absence of displacements) occur. After-effects of fretting are:

- dimensional tolerance variations, as a consequence of surface wear, which cannot be borne by the high speed engines.
- the arising of microcracks, which may propagate, because of fatigue, within components exposed to alternating mechanical stress and lead eventually to breakage. It is estimated that at least 30% of starting fatigue failures in the turbine engines are due to fretting (Chamont et al., 1988, pp. 1883-1888).

Fretting is observed in the turbo engines in the following contact points:

- between the root of the fan blades, compressor or turbine and the slots in the disc;

39

- between the bearing ring and the surfaces of the rotating pivots of the turbine shaft or compressor;
- in the assembly and clamping points of the shafts by means of bolts.

In the turbine engines, the most critical fretting problems may appear between the root of the fan blades or compressor and the disc slots, which are made up of titanium alloys such as Ti 6-4 or IMI 685 (Ti-6Al-5Zr-0.5Mo-0.25Si), both very sensitive to fretting. The initiation of cracks in these components, if not detected in time, may lead to brakeage of parts, due to the elevated cyclic stresses, and, as a consequence, cause serious damage to the whole compressor.

The solution to these fretting problems has been sought in part by employing coatings (for example self-lubricating paints containing molybdenum disulfide or graphite or deposited by plasma spraying) which, by acting as a third body between the two wearing surfaces, prevent the metal to metal contact.

Sand blasting of the contacting surfaces is an alternative solution. In fact, such an operation causes a hardening of the surfaces due to deformation and compression stresses on and immediately below the surface of the material, resulting in an increase of the fatigue and fretting resistance.

Specific investigations, relevant to fretting in the turbine engines, have been carried out by Chamont et al. (1988, pp. 1883-1888) who, in a first attempt, coupled the fan blades (made up of Ti 6-4 alloy, coated with a plasma sprayed layer of copper-indium-nickel and lubricated with a paint containing molybdenum disulfide) with a disc slots, consisting also of a Ti 6-4 alloy which had been sand blasted using 315 µm steel balls.

The study of testing parameters simulating the fretting conditions has led to the selection of a very high (from 400 to 500 MPa) contact pressure, elevated displacement amplitude (up to 150 µm), and low temperature ($\leq 100°C$).

The roughness of the plasma coating allows a good adhesion of the subsequent layer of self-lubricating paint and the supply of it. However, after a prolonged time of severe working conditions it is first observed a wearing of the paint and then of the sprayed layer, resulting in a deterioration of the disc slots and the material (alloy) at the root of the blades.

In another case, smaller compressor blades, constituted also by Ti 6-4 alloy, the root of which had been sand blasted (using 160 µm glass balls) and coated with a self-lubricating paint containing graphite. The tests were carried out at lower contact

pressures (from 200 to 300 MPa) and displacement amplitudes (up to 20 µm) and at a higher operating temperature (≤ 450°C) with respect to the first case.

Some significant damages, very much localised at the root of the blades and with different extents of deterioration at higher loads, were observed in this case too, after a certain period of working time. Such damages, gathered on those zones where the paint is mostly worn out, may go down to the substrate with seizure effects and sometime initiation of cracks at the boundary of the contact area due to the elevated load. The cracks subsequently propagate by a low or high fatigue cycle and may cause the brakeage of the blade root, as shown in **Figures 10** and **11**.
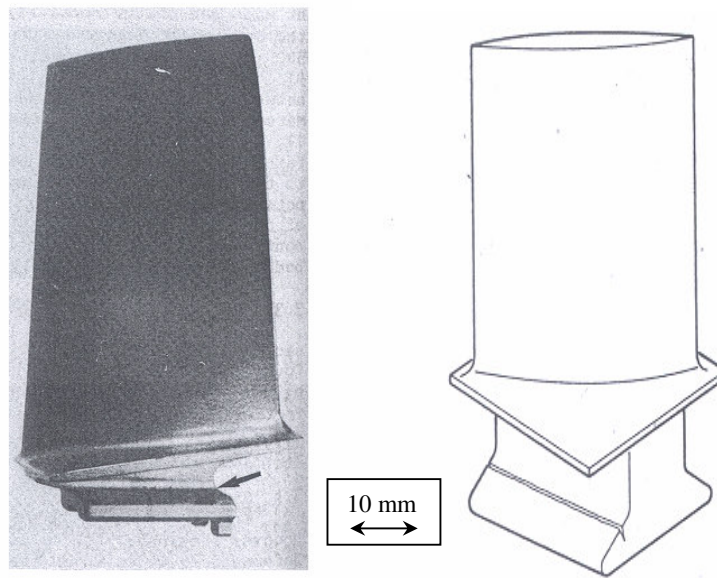
Fig. 10 - Scheme and sample of compressor blade with fretting damage on the root (Chamont et al. 1988, p. 1878)
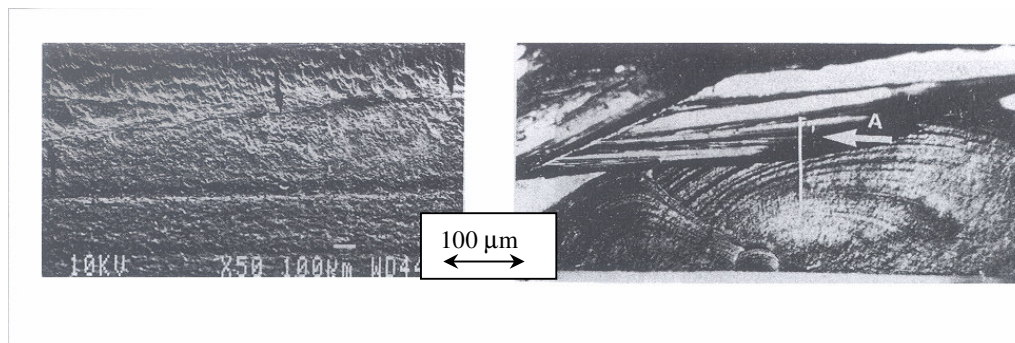
Fig. 11 - Fretting damage on root blade (left); fracture surface with crack initiation near the contact area (right) (Chamont et al. 1988, p. 1887)

Simulating tests have been carried out in the laboratory using coated and uncoated samples made of the same material of the real components. The results of these tests have pointed out, after a limited number of sliding strokes, the presence, on the uncoated samples, of deep lines and signs of surface plastic deformation which indicate that very thin layers of the material slip one over the other one (**Figure 12**). On the contrary, in the case of coated samples, wear of the coating, down to the substrate, was observed only after some millions of cycles. The SEM micrograph, shown in **Figure 13**, points out that the damages undergone by the alloy substrate are much less severe than those observed on the uncoated samples.
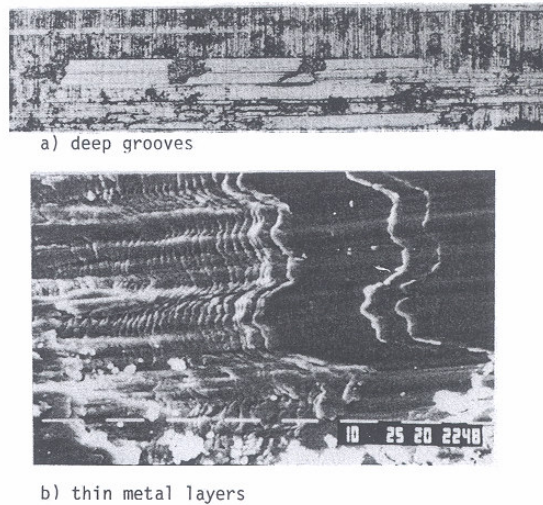
Fig. 12 - Wear damage after sliding (uncoated material) (Chamont et al. 1988, p. 1888)
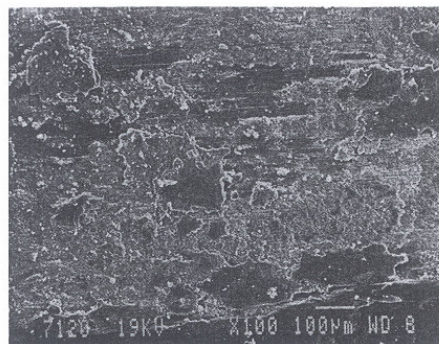
Fig. 13 - SEM image of a coated sample after wear test (Chamont et al. 1988, p. 1888)

2.5 Corrosion

The corrosion resistance of the Ti 6-4 alloy appears to be quite high when compared to other alloys. Such a high resistance is due to the surface oxide (mainly TiO_2 as Rutile)

which forms under normal environmental conditions, even at low temperatures, as a consequence of the oxygen diffusion toward the interior of the material.

The oxidation behaviour of the Ti 6-4 alloy is like that of pure titanium (Motte et al, 1976, pp.113-125): weight variation of some alloy samples as a function of time and at different temperatures is shown in **Figure 14-a**; thickness variation of the oxide as a function of the oxidation time is reported in **Figure 14-b**. By increasing the temperature, the oxidation reaction kinetics shows different behaviours for different temperature ranges: logarithmic for temperatures ranging between 300 and 500°C, parabolic for temperatures ranging between 500 and 750°C, and linear for temperatures higher than 750°C.

Oxidation in terms of (a) weight gain and (b) oxide thickness. The oxide forms multilayered structures and spalls off easily. In addition, oxygen is readily taken up into solution in the surface layer of the alloy and may reach 33 at.%. It is the cause of the surface alpha-case with its severe embrittlement.
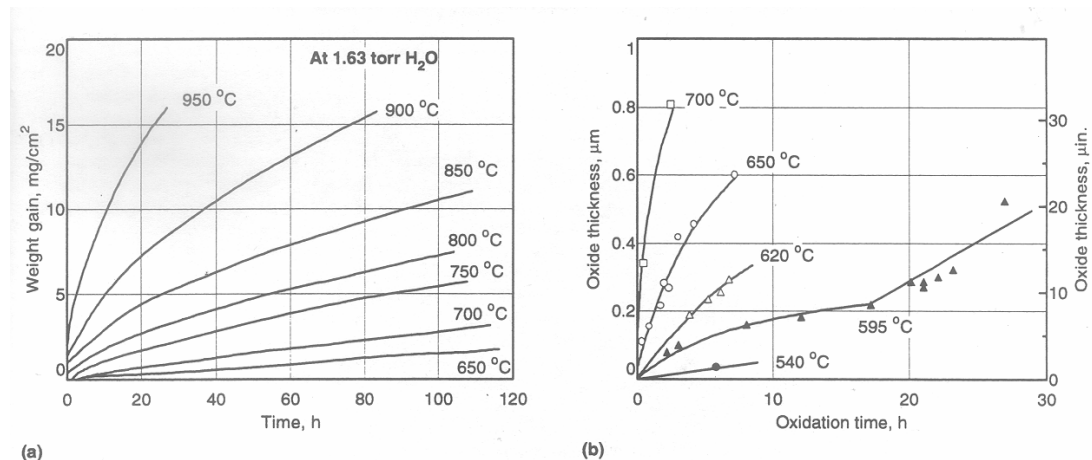
Fig. 14 - Oxidation of Ti-6Al-4V alloy: a) oxidation curves; b) Oxide thickness (Motte et al, 1976, pp.113-125)

At temperatures higher than 400°C, surface oxide breaks and some oxygen diffuses into the metallic underlayer, causing the formation of a surface layer known as α-case, which is responsible for a severe brittleness.

Over 500°C the oxide grows as a multi-layer, porous and non protective scale which causes brittleness.

Thin surface layers of TiO_2, smaller than 100 nm, may be formed by anodising to avoid the brittleness due to oxygen. This treatment is very useful in the case of components undergoing rubbing.

The Ti 6-4 alloy is strongly resistant to a vast majority of chemical agents in aqueous solutions up to temperatures near their boiling points; it has excellent resistance to sea

water corrosion and cooling liquids (with low freezing point), oxidising acids and aqueous solutions of chlorides, wet chlorine gas and sodium ipochlorite. It is, however, affected by inorganic reducing acids such as hydrofluoric (HF), hydrochloric (HCl), sulphuric (H_2SO_4), phosphoric and organic acids such as oxalic [$(COOH)_2$] and formic (HCOOH).

In particular, the hydrofluoric acid attacks the alloy in a very aggressive way in the whole range of possible concentrations and temperatures because the fluoride ion (F^-) forms with titanium very stable and soluble complexes. The addition of oxidising species (for example HNO_3), slows down the hydrogen capturing process and the corrosion process in HF solutions; however, it is not able to stop them.

In very diluted solutions of HF the corrosion process may be forbidden in presence of metallic ions such as Fe^{3+}, Al^{3+} and Cr^{6+} that form complexes with the fluoride ion removing it from the reaction environment. In absence of these metallic ions, the solutions containing more than 20 ppm of F^- ions may attack titanium and its alloys when the solution pH is lower than 6-7.

The Ti 6-4 alloy is generally free from galvanic corrosion when it is in contact with other structural materials; in this aspect it is consistent with nickel and stainless steel alloys. However, if it is in contact with less noble metals (carbon steels, aluminium, magnesium alloys) the galvanic attack may be speeded up.

2.6 Hydrogen damage

The Ti 6-4 alloy is slightly sensitive to hydrogen damages.

The species responsible for the brittleness is the titanium hydride which forms as a consequence of hydrogen diffusion into the material during exposure to hydrogen gas or hydrogen coming from a cathode process.

The growth rate curves of the cracks as a function of temperature, shown in **Figure 15**, may present a peak which is indicative of the phenomenon dependence on two parameters: hydrogen diffusion and hydride formation. The noticeable decrement, observed in all experimental curves (except the case of the Ti-5Al-2.5Sn alloy at 0.9 atmosphere of H_2 which shows a continuous growth) is likely due to the nucleation difficulty of the hydride at higher temperatures. It takes place a separation of phase containing hydride for a hydrogen concentration that depends on the alloy composition as well on the metallurgic history of the sample.

Ti-6Al with a continuous α phase and Ti-6Al-4V exhibit a maximum in crack growth susceptibility near 0 °C (32 °F), whereas Ti-6Al-6V-2Sn with continuous β phase exhibits a maximum near 50 °C (120 °F). No maximum was observed for Ti-5Al-2.5Sn at the temperatures tested. All crack-growth rates correspond to an applied stress intensity near 50 MPa√m (45 ksi√in.).
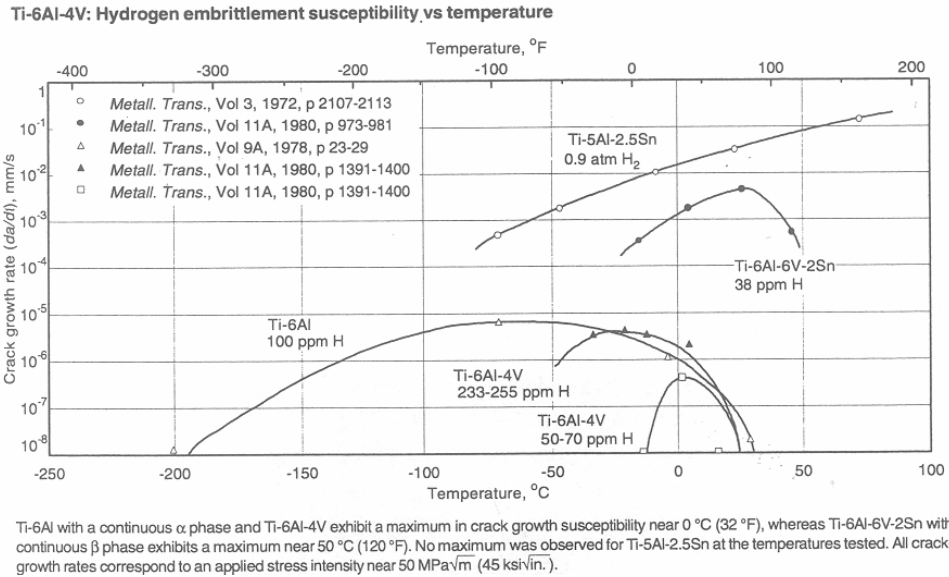
Fig. 15 - Growth rate curves of the cracks as a function of temperature Ti-6Al-4V and other Ti alloys (Moody, Costa, 1991)

2.7 Mechanical properties

The traction resistance at room temperature of the Ti 6-4 alloy is influenced by the thermal treatment (microstructure), composition (especially oxygen content), and texture (in particular in the sheets).

The thermal treatment may change the value of the breaking point in the order of 200 MPa or even more, whereas the oxygen content contributes for about 70-100 MPa. The textured sheets may show variations in the order of 200 MPa according to direction.

A comparison of breaking points among various materials is reported in **Table 11.**

Tab. 11 - Breaking points of various materials (Adapted from ASM Handbook, 1990)

Material	Breaking Point [MPa]
Ti-6Al-4V	895-1250
titanium alloys	240-1500
alloyed steel	100-2300
aluminium	70-700
copper	170-1500

45

Table 12 reports the lowest and average values of traction properties of the Ti 6-4 alloy in different thermal treatment conditions and in the case of low oxygen content.

Tab. 12 - Tensile properties of the Ti-4Al-6V under different conditions of thermal treatment (Adapted from ASM Handbook, 1990)

Alloy	Condition	(Ultimate Tensile S.) [Mpa]	0.2% offset (Tensile Yield S.) [Mpa]	Elongation (%)
6Al-V	Annealed	900-993	830-942	14
	Solution treatment +Ageing. (STA)	1172	1103	10
6Al-4V (low oxygen content)	Annealed	830-896	760-827	15

The Ti 6-4 alloy was initially developed for aerospace applications in which temperatures must not go over 350°C; the deterioration of tensile properties is evident with the temperature increase, as it is pointed out in **Figures 16** and **17** that report the typical tensile/yield behaviour and that of the alloy in STA (solution treated and aged) conditions, respectively.

Fig. 16 - Tensile strength vs. temperature for Ti-6Al-4V mill annealed (ASM Handbook, 1980)

Ti-6Al-4V: STA tensile strengths vs temperature

STA condition—1 h at 955 °C (1750 °F), water quench, age 4 h at 525 °C (975 °F) and air cool.
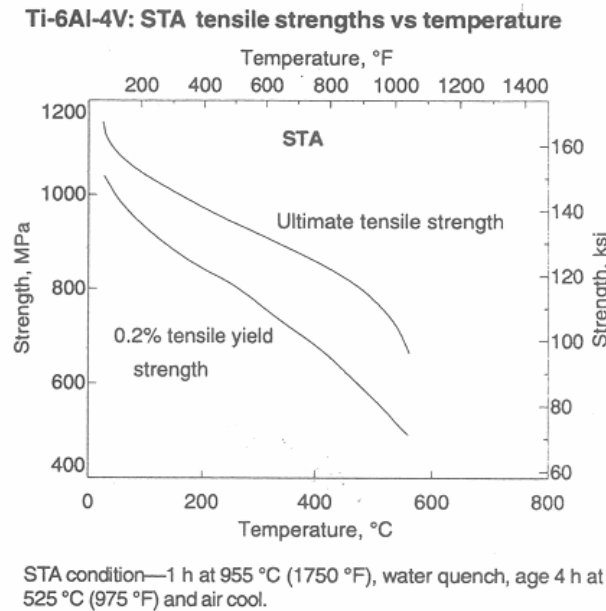
Fig. 17 - Tensile strength vs. temperature for Ti-6Al-4V STA conditions (ASM Handbook, 1980)

The compressive yield stress of the alloy depends on the thermal treatment conditions, but it is always slightly higher than the corresponding tensile properties. That makes the Ti 6-4 alloy an ideal material for structural design. In fact, the austenitic stainless steels show compressive stress properties that are a third only of their corresponding tensile properties, in all conditions of thermal treatment.

The compressive, like the tensile yield, varies linearly with temperature, up to 540°C.

2.8 Creep behaviour

As it has been already pointed out, the Ti 6-4 alloy is used up to a temperature of about 300-350°C. As an alloy of the $\alpha-\beta$ type, its creep properties are at an intermediate stage between those (the best ones) of an α alloy and those of a β alloy. The optimum creep properties can be obtained by converting an equi-axial structure into an acicular one.

2.9 Fatigue behaviour

It is necessary to take into account yield stress, grain sizes, and material microstructure of the material, in order to estimate its fatigue behaviour. There is evidence that the Ti 6-4 alloy , in the form of bars, possesses HCF (High Cycle Fatigue) (10^7 cycles)

resistance, obtained by means of fine grain equiaxial structures or by quenching treatment, carried out from the β phase to the production of the fine acicular α' phase.

There is agreement that microstructures of the Widmanstätten or α+β colonies type have a fatigue resistance lower than the previous microstructures.

Generally, all the microstructure parameters that increase the yield point and/or decrease the creep, improve the HCF resistance.

The LCF (low cycle fatigue) failure often occurs at less than 10^4-10^6 cycles. The LCF is sensitive to the thermal treatment that the alloy has undergone and to its microstructure characteristics. The α-β annealing thermal treatment provides a higher fatigue resistance (84,370 cycles as an average value, with an amplitude of sinusoidal strain equal to ± 0.006 and with a frequency of 28.6 Hz) with respect to the recrystallization annealing (58,840 cycles) or β annealing (42,720 cycles) (Gilmore, Imam, 1982, p. 637).

The surface residual stress is the main factor to influence the fatigue behaviour and it is also a more powerful gauge than the surface roughness, although residual stress and roughness are, in many cases, strictly correlated.

Combined effects of residual stress, cold working structure, and surface roughness converge on the HCF resistance. The surface effects on the HCF are summarised in **Table 13**.

Tab. 13 - Surface effects on HCF (high cycle fatigue) behaviour (Adapted from Gilmore, Imam, 1982)

Surface effect	Cracks nucleation	Cracks propagation
Roughness	Speeds up	No effect
Cold working	Slows down	Speeds up
Compressive residual stress	Small or no effect	Slows down

Surface treatment processes of sand blasting and finishing interact in a complex way in influencing fatigue resistance. For example, sand blasting raises the fatigue resistance at room temperature of an electrolytically polished surface having a fine lamellar microstructure. Further electrolytic polishing
has an additional effect, whereas a stress relief process, carried out on the sample after its sand blasting reduces fatigue resistance to a lower level than the starting baseline of the electrolytically polished sample. In this case, by adding another electrolytic

polishing treatment it is possible to restore almost completely the benefits obtained with the sand blasting.

Table 14 shows the fretting-fatigue resistance of titanium and its alloys as a function of the surface treatment.

Tab. 14 - Fretting-fatigue resistance as a function of surface treatment (Adapted from Taylor, 1981, p. 177)

Surface Treatment	Normal Pressure [MPa]	Fretting-fatigue resistance 3×10^6 cycles [MPa]	
		20°C	400°C
None	35	220	220
Sand blasting	35	270	240
Sand blasting + Cu-Ni-In	35	320	245
None	140	215	190

2.10 Thermal treatments

The Ti 6-4 alloy is generally used in the mill annealed condition; it has a limited hardening susceptibility and it is sometime used in the STA (solution treatment and ageing) condition. In this last case it is possible to obtain resistances up to 1100 MPa in sections with a thickness ranging between 12.7 and 19 mm.

The beta-annealing (BA)* treatment, which gives a completely transformed beta structure, optimizes properties such as fracture toughness, that becomes the highest, and the growth rate of the cracks, that becomes the lowest. All this goes together with a reduction of ductility (although the material maintains 5% of elongation) and fatigue resistance.

Performance in terms of fatigue resistance can be improved by quenching in water from a temperature higher than the β-transus and equal to 995°C.

The improvement obtained by recrystallization annealing (RA) on the fracture toughness and growth rate of cracks is lower than that obtained by beta annealing (BA), but, on the other hand, ductility and fatigue resistance are improved.

The best result on the above mentioned properties may be obtained with both the BA and RA treatments if an ELI (extra-low-interstitial) alloy with a low oxygen content is utilised.

Finally, thermal treatments should be carried out in environments free of reducing gases and other contaminants which might favour an excessive hydrogen adsorption.

3. Treatment and coating processes for the Ti6Al4V alloy

3.1 Introduction

As it has been already pointed out, although titanium alloys have interesting mechanical and physical features, their surface properties are lacking and, thus, their use is restricted to non-tribological applications. In fact, titanium alloys do exhibit characteristics opposite to those required by tribological materials, i.e. low friction coefficients and/or elevated wear resistance.

Such a situation is complicated by titanium and its alloys not being lubricated efficiently by conventional oils, greases, or solid lubricants (Bucholtz, Kustas, 1996, pp. 330-337): titanium friction coefficient in presence of oil lubrication is higher than 0.1 (Tian, Saka, Suh, 1989, p. 289), whereas in case of solid lubrication it is MoS_2 only to give friction coefficients lower than 0.1, but the life of the lubricating coating is unsatisfactory (Seitzman, Bolster, Singer, 1996, pp. 10-13). The operational life of MoS_2 (and some other lubricants) may be improved to some extent by modifying initially the metal surface, that's hardening it or generating an intermediate layer (Budinsky, 1991, p. 203). Even better results, in terms of life and friction coefficient, are obtained by depositing MoS_2 by the IBAD (ion beam assisted deposition) technique, as it will be described later in detail.

In aeronautical applications (Bill, 1985, pp. 283-301), the wear problem of components which are made up usually of Ti-6Al-4V alloy in the hardened condition is a critical factor. In particular, for bolt fixed parts, pinned joints, spline couplings and gripped components which are used in airplane's structures and engines.

Vibrations, fluctuating major loads and misalignments between rotating components, inherent in any type of airplane, promote small amplitude oscillations between the coupled surfaces, resulting in a very serious fretting problem.

The surface modification by means of specific treatments increases generally the wear resistance, reduces the friction coefficient and decreases the material transfer (adhesive wear).

The titanium poor tribological characteristics are caused by three main factors (Peacock, 1997, pp. 22-25) that will be briefly described:

i)   *the electronic configuration of the metal*, which has 2 electrons only in the d orbitals out of a maximum of 10. The low filling of the d orbitals confers a greater

reactivity to the metal. Partial filling of these orbitals by means of alloying elements tend to reduce such a reactivity;

ii) *the titanium crystalline structure*, hexagonal in the commercially pure (CP) metal, with a c/a ratio equal to 1.587. Since such a ratio is lower than the ideal one for a compact hexagonal structure, it results into a slippage not only across the basal plane. Titanium alloys show different slipping systems, which give a slightly better wear resistance with respect to the CP;

iii) *the traction and shear resistance,* relatively low in the CP titanium. Because of the bonds generated during the sliding against other metals, breakages may occur in the titanium substrate rather than at the interface. This results into metal transfer, surface damage, and elevated wear rates. The strength may be improved by forming alloys, especially in the case it is developed a significantly harder layer with a satisfactory thickness.

These problems can be overcome by isolating the titanium surface entirely from the tribo-system by means of a suitable coating.

The criteria for the coating selection may be dictated by the following procedure:

<u>End use.</u> The mechanism of wear and its severity, the type of the required protection, or other specific properties must be evaluated with respect to the proposed surface engineering system. However, it is not sufficient to examine the surface properties of the coating separated from the substrate. Titanium has a low elastic modulus and this, combined with a relatively low hardness, causes a higher under load deflection when compared to steel. Thin coatings, in particular, cannot be borne appropriately by the titanium substrate and under higher loads they will collapse as "ice on mud" (Peacock, 1997, pp. 22-25).

Operational environment, temperature, and presence of corrosive media must be controlled with respect to the potential life of the system.

<u>Configuration and size of components.</u> It is necessary to make sure that the selected process for producing antiwear coatings is suitable for the components' to be coated. i.e. 'Line of sight processes (e. g. thermal-spraying) may not be suitable for coating internal, hidden surfaces or bores.

<u>Unfavorable side effects.</u> Surface modifications may determine a reduction of mechanical properties; in particular, ductility and resistance to fatigue crack

propagation. The titanium corrosion resistance in a specific environment can be modified by means of coatings or surface alloying elements.

3.2 Treatment and coating technologies

Various technologies, which are listed in **Table 15**, are currently utilized for modifying the tribological properties of titanium alloys.

Tab. 15 - Main treatment and coating technologies

1. **PVD (Physical Vapor Deposition)**
♦ Evaporation
° electric resistance process
° induction process
° EB (electron beam) gun **-**shallow cathode
-filament   self accelerated
work accelerated
° arc
♦ Sputtering
° diode
° magnetron
° ion beam
° triode
♦ Ion plating
2. **IBD (Ion Beam Deposition)**
3. **Ion Implantation**
4. **CVD (Chemical Vapor Deposition)**
5. **Thermal Spraying**
6. **Thermo-chemical Treatments (including those assisted by plasma or laser)**
♦ Nitriding
° Ionic or Plasma nitriding
° Gaseous nitriding
° Liquid nitriding
° Laser (Laser nitriding)
♦ Ionic carburizing
♦ Laser borating
7. **Chemical and Electrochemical Processes**
8. **CVD (Chemical Vapor Deposition)**

Advantages and limits of some listed techniques are reported in **Table 16**.

Tab. 16 - Advantages and limitations of the surface modification treatments for titanium alloys

Technique	Advantages	Limitations
PVD		
Sputtering	• Low temperature process • Feasibility for multilayer coatings • Coatings composition suitable to specific requirements	• Thin coatings • Low deposition rate
Evaporation	• Wide choice of available materials • Tailoring compositions to specific requirements • High purity of coatings • Low cost process	• Thin coatings • Sharp interfaces (except for the ion-beam assisted technique)
Ionic Implantation	• Low temperature process • Efficient on final shape components • Feasibility of unique alloys formation • Graded interface	• Line of sight* • Shallow modified surface area • High cost
Thermal-spraying		
	• High deposition rate • Thick coatings • Intrinsic porosity suitable to retain the lubricant • Low cost process	• Intrinsic porosity of coatings • Rough surface finish • Possible adhesion problems • Difficulty in controlling composition of coatings • Line of sight[1]
Thermo-chemical Treatments		
Nitriding, carburizing, borating	• Substrate conversion with graded interface • Thick zones of modified surface	• Possible hydrogen brittleness problems which restrict the selection of titanium alloys • High process temperature may cause deformation of components and degradation of mechanical properties
Chemical and electrochemical Depositions		
	• No problem of line of sight* • Low cost process	• Possible hydrogen brittleness problems which restrict the selection of titanium alloys • Sharp interfaces

---

[1] Military term. In any system where the material to be deposited is "shot" over the substrate, a limit may be represented by the relative angulations that must be maintained between the depositing device and the substrate so that a satisfactory coverage is obtained.

3.2.1 Physical Vapour Deposition technologies

Physical Vapour Deposition (PVD) is a term used to describe a wide range of coating techniques which share the feature that the coating process is carried out under vacuum with at least one of the depositing species being thermally evaporated or removed by momentum transfer from a solid surface.

The PVD-technology can be divided into four main categories: evaporation, sputtering, ion plating, and ion beam deposition. However, due to the large number of process layouts, developed during the last decades, some of the various PVD methods are often classified and described on the basis of fundamental characteristics regarding the mechanism of coating formation. For example, the evaporated or removed species may directly reach the substrate to form a coating or it may first react with other species present in the deposition chamber. In the first case we are dealing either with a simple evaporation or sputtering, while in the second case a reactive evaporation or reactive sputtering are taking place. Furthermore, either evaporation or sputtering may be used in conjunction with ion plating and/or ion beam deposition. Finally, both evaporation and sputtering processes may be assisted by the action of a glow discharge or plasma, in which case the process is referred to as Plasma Assisted Physical Vapour Deposition (PAPVD). These refinements have spawned a large number of variant/hybrid techniques, the denominations of which are generally associated with the name of the energetic source or particular configuration utilised, e.g. resistive evaporation PVD, electron beam PVD, arc PVD, magnetron sputtering, diode sputtering, etc. All these variants have generally a large influence on the physical and mechanical characteristics of the coatings obtained and also on their state of stress.

PVD-evaporation

It is also referred to as Vacuum Deposition. Preparation of thin films by this technique is done by converting a solid material to a stream of vapour under a vacuum normally in the 10^{-7} torr (13 µPa) to 10^{-6} torr (0.13 mPa) range. The process is schematically illustrated in **Figure 18**.
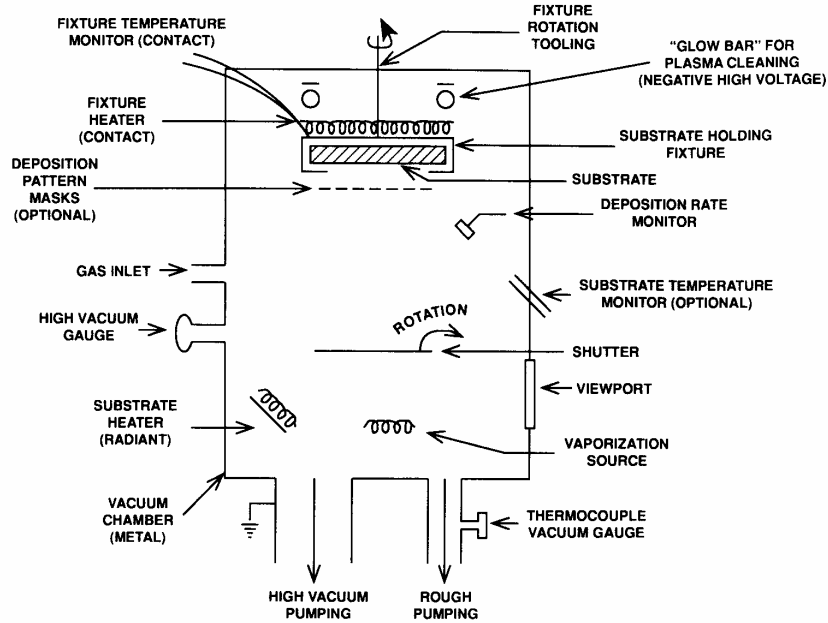
Fig. 18 - Schematic layout of vacuum deposition process

In resistance heating evaporation, the material to be evaporated is held by a refractory metal crucible which is heated to the vaporization temperature by large currents passed through it. An improved method involves heating the coating material directly by an electron gun using a magnetic field to direct the electron-beam (EB) path into the crucible. The current of the EB is typically 1 A accelerated through 10 kV. To avoid damage of the coating because of the ionisation radiation of the EB, an alternative heating method utilises a radio frequency (RF) spiral which surrounds a BN crucible and it gives, by induction, energy to the material inside the crucible. In the laser-PVD it can be used a continuous wave laser or a pulsed one to evaporate the coating material from a crucible or remove it from a suitable target. In this case the term LAD (Laser Ablation Deposition) is used.

In all the above variants, the temperature of the substrate may vary from ambient up to 500 °C. However, components to be coated are generally preheated in vacuum, for degassing and surface activation, and are rotated within the evaporate cloud during the deposition process. These methods allow relatively low vapour pressure metals such as Al, Ti, Cr, Mo, Pt, W and some insulators such as Al_2O_3 and SiO_2 to be evaporated. It is important to note that in thermal evaporation the depositing atoms have impact energies in the order of kT (where k is Boltzman constant and T is temperature) and, thus, they are limited by the temperature necessary at the source for vaporization. Also,

because of the wide difference in vapour pressure between most elements, only a relatively small number of alloys can be prepared using a single source of material. The deposition rate depends to a large degree on the physical properties of the coating material. High vapour pressure materials such as Zn have deposition rates which can reach 50 µm/s; however high melting materials have deposition rates ranging between 0.1 to 0.3 µm/min.

The reactive evaporation is carried out utilising a partial pressure of a reactive gas, introduced into the deposition chamber. In such a way the metal vapour, produced directly as in simple evaporation, reacts on the substrate with the reactive gas to form the coating. Such a process allows to obtain oxide, nitride, or carbide based coatings, using as reactive gases oxygen, nitrogen, and hydrocarbons, respectively.

PVD-Arc

Normal arcs in a gas atmosphere between a negative cathode and a positive anode with low voltage (order of magnitude 20 V) and high amperage (order of magnitude 100 A) are generally well known. However, in a low-pressure atmosphere or a vacuum, an arc with the same electrical characteristics changes its physical appearance at the cathode. The arc no longer attacks the entire cathode, it moves around attacking only small spots of some micro-millimetres in diameter; the so-called cathode spots. Such a cathode spot exists only for some 5-40 ns and is then replaced by one or more new cathode spots in the immediate vicinity. It is possible to trace the path of the arc moving very quickly over the cathode. The total electrical power of the arc concentrated in one such microscopic crater of a cathode spot causes momentary power densities in the order of 10^9 W/cm^2. As a result the solid cathode material is suddenly evaporated; the vapour particles are ionized several times and accelerated tremendously in a heated ion cloud in front of the cathode spot –the so-called plasma. Mostly ionized vapour is emitted although there are individual emissions of molten droplets some of which are incorporated in the coatings.

Since the vapour particles are produced from the solid cathode material the physical arrangement of cathodes in a vacuum chamber can be varied.

The vast acceleration of the ions is particularly striking. The energy content of the emitted vapour cloud is more than 100 times higher than for conventional evaporation from a crucible even before the ions have been accelerated by the bias voltage. This clearly indicates that the arc process attains very good coating results even at low bias

voltages. A distinctive feature is that coatings deposited at temperatures of 200°C are characterised by good adhesion. This means that a number of steels (cold worked steels) can be coated without loss of hardness or distortion.

In PVD equipment, e.g. for TiN coating, the cathode is a solid piece of titanium with a simple circular or rectangular shape. The vacuum chamber walls act as the anode. The arc is ignited with an ignition trigger as a result of a brief contact with the cathode. Static magnetic fields behind the cathode assure uniform cathode erosion over the entire surface in the case of an uncontrolled arc – the so-called "random arc". Locally variable magnetic fields are used if one wishes to control the arc's erosion at the cathode surface. This technique, the so-called "steered" arc, has been technically developed to such an extent in recent years that the path of erosion of the cathode spot over the cathode surface can be controlled in a reproducible manner. Another feature of the steered arc is that it reduces the surface roughness of produced coatings and offers promising application possibilities for cathodes made up of segment of different materials.

Erosion of the cathode by a vacuum arc causes a flow of material in three forms: Ions, uncharged metal vapour and molten metal micro-particles (droplets). In the case of titanium the contribution of the mass flow in the form of ions to the total erosion rate is approximately 80%. Multi-charged ions are predominant in the generated metal plasma. Ion with five or six unit charges can even be detected in materials with a high melting point (e.g. tungsten and molybdenum).

Another feature of arc evaporation is the emission of droplets which decreases as the melting point of the material to be evaporated increases. However, methods are now available for influencing droplet size and frequency. The influence of the droplets (which primarily form during the ion bombardment phase before the actual coating process) on the performance of the coated tool depends on the type of application.

The negative role of the droplets should not be overrated in the case of machining and cutting tools since arc coated tools attain a very long life even if droplets are present. Adhesion, stoichiometry, coating thickness, coating thickness distribution and stress condition are more important coating features which govern the performance of coated tools.

In the case of forming tools the higher coating surface roughness resulting from droplets can have an effect. However, the surface quality attained after a subsequent polishing step, which is normal practice for forming tools, permits the successful use of tools also for this application.

Prior to actual hard coating any microscopically thin oxides film and impurities adhering to the substrate are removed by intensive ion bombardment at a high bias voltage. During subsequent coating the high ion current density of the Arc PVD Process ensures that loose coating particles are removed and that the hard coating is compressed. The effect of the ions can be compared to the coating being carefully hammered on to the surface of the component. This compression also ensures that the chemically correct amount of nitrogen is always exactly included – Arc PVD coatings are stoichiometric and largely independent of the adjusted nitrogen pressure.

However, the most significant advantage of the Arc Process is that adhesive layers can be deposited at substrate temperatures of around 200°C. This again is due to the uniform high-energy ion bombardment; the substrate surface is changed microscopically – to a depth of few nanometers – to create ideal growth conditions for the hard material which actually alloys with the surface. Uniform ion bombardment during coating leads to a favourable stress pattern in the hard coating so that flaking and microcracks are avoided. And, to repeat, this all takes place at low coating temperatures too.

TiN coatings which have been available for wear protection since the beginning of the eighties are acknowledged and used all over the world. However, there are certain application cases where TiN coatings are only partly successful and are surpassed by other hard coatings.

TiAlN

The addition of aluminium to the hard coating increases the hardness and, above all, the oxidation stability of the coating. As a result tool life is considerably longer than that attained with the TiN coatings especially in the case of cutting tools in the higher cutting speed range. Coating properties depend greatly on the aluminium percentage in the coating. In general rougher coatings are deposited at higher aluminium percentages and the deposition rate is increasing simultaneously. TiAlN coatings can be used for wear protection up to a certain maximum aluminium content.

CrN

The coating thickness is increasingly important in case of exposure to abrasive loads such as those frequently encountered in the paper, textile and plastic industry applications. TiN coatings normally exhibit compressive stresses and consequently only

coating thickness up to 10 μm is applied for practical use. CrN coatings are characterised by low stress structure which permits coating thicknesses up to 50 μm. Another plus point is the high oxidation stability of CrN. However, adhesion can be slightly poorer than that of TiN depending on the substrate particularly at low coating temperatures. On the other hand, supported by the higher coating thickness, CrN coatings exhibit better corrosion resistance than TiN especially in aqueous solutions. The best proof of this is that CrN coatings show much better results in salt spray tests. If CrN is compared to conventional hard chrome plating it is apparent that:

- CrN is twice hard
- CrN coatings are free from cracks
- CrN coatings are applied in environmentally compatible manner.

TiCN

Carbonitrides have proved to be suitable hard material for thin coatings since the inclusion of carbon in the metal nitride lattice substantially increases the hardness. In the case of arc coating, the carbonitride layer is produced by introducing a reactive gas containing carbon into the coating chamber during the process. The variation of the N/C ratio governs the properties of the coating.

For milling operations TiCN coatings offer a longer tool life and, at the same time, a higher cutting speed than TiN. Furthermore, they are characterised by low surface roughness, good adhesion and a low friction coefficient. The TiCN coating deposited with the arc technique has a hardness of HK 3000-4000 and the critical load determined by means of the scratch test is approximately 70 N.

Other coatings under development

Coatings with mixed metal structures TiZrN have proved to be very successful on punches for stamping laminations. Twice as many laminations have been produced with a TiZrN coated tool.

TiBN coatings, with their striking roentgen-amorphous structure, showed similarly high resistance to wear in punching test. This very interesting coating combination is being further developed.

The progress made by the Arc PVD Process in the field of diamond-like coatings is also very promising. Highly resistant coatings with a hardness of almost 7000 HK 0.05 and

an extremely low friction coefficient of 0.05 (against 100Cr6) are obtained with a carbon cathode and without any addition of hydrogen. At present these coatings are restricted to flat substrates for reasons relating to the process.

PVD-Sputtering

The "simple" sputtering deposition process consists in bombarding the solid source called target (material to be deposited) with inert gas ions and neutrals of high kinetic energies. The ions, usually generated in a glow discharge, are accelerated toward the target (cathode) through a potential gradient. The potential may be D.C. for metals and R.F. for insulators and semiconductors. Momentum transfer ejects the atoms at the target surface, with sputtering yields of 3-10 atoms/ion and with kinetic energies normally in the 1-10 eV range, with an energy tail extending to about 1 keV for sputtering in a low-pressure environment. Atoms, and in some cases molecules, are removed from the target surface with a square cosine distribution. Another sputtering mode approach allows the substrate holder to be rotated in front of several targets of different materials, at slow rates for sequential sputtering, or at high rates for "contemporaneous" multi target sputtering.

Deposition rates are normally in the range of 0.03 up to 10 µm/h and they are fairly constant and easy to control.

When compared with other deposition methods for thin coatings, sputtering offers the following advantages:

- it is possible to deposit a large number of materials (metals, semiconductors, insulators, alloys, and compounds). Particularly valuable are those with high melting temperature such as nitrides, carbides, and other insulating compounds which cannot be evaporated thermally

- the targets are typically 10 cm in diameter; however they may be made with hundreds cm in diameter and in various shapes in such a way that it would be possible to coat substrates with large dimensions. Components, large as an airplane wings, can be coated and production can be speeded up by utilizing moving strips and vacuum systems equipped with "air to air load-locks"

- the gaseous environment is very useful to clean the substrate surface by means of ionic bombardment and to remove damaged material from the surface of substrates smoothed by sputter etching

- the gas may be used not only to bombard the target, but also to react with it as it is the case regarding the deposition of oxides and nitrides

- the gas for the bombardment of the target or other gases directed toward the substrate can be used to maintain an overpressure, for example, of Hg or As for forbidding the evaporation of high vapour pressure elements in (HG, Cd) Te and GaAs coatings, respectively

- the elevated number of process parameters can be used in such a way to tailor them to the properties of the coating. Key parameters are the arrival rate of the coating species; the temperature and the surface potential of the substrate; the pressure of the sputtering gas and the partial pressures of other elements in the gaseous state; the voltage applied to the targets and the parameters linked with equipment for keeping impurities to the lowest possible levels (cold traps, speed of vacuum pump, methods for removing contaminants, out gassing etc.)

- flexibility of the target and of the configurations for sputtering in relation with the design requirements. As far as this last advantage is concerned, it should be noted that, in addition to the normal configuration of diode with anode and cathode in parallel, there are various configurations of triode that permit to plan the plasma discharge independently from the voltage applied to the target. Such an independence allows to keep very low the gas pressures (0.1 mtorr) and also to bombard the target at low voltage

- the coating adhesion is generally very good.

The simplest case of glow discharge sputtering (GDS) is constituted by the diode in D.C. configuration (**Figure 19**).
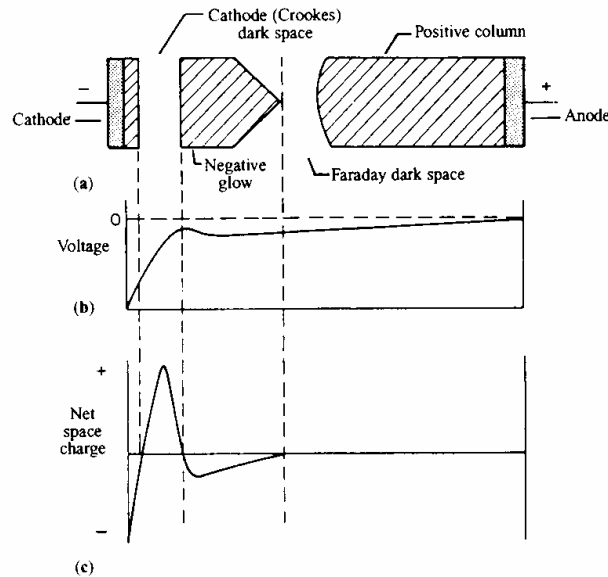
Fig. 19 - Glow discharge sputtering (GDS) with diode in D.C. configuration (Wasa, Hayakawa, 1991)

On the left, near the cathode, there is a zone made bright by the neutralization of ions. Hardly on the right there is the dark zone of the cathode, in the interior of which most of the potential drop takes place; such a drop serves the purpose of accelerating the ions toward the surface of the target. More to the right it is visible the negative discharge, the dark zone of Faraday, and the anodic discharge. As soon as an ion hits the cathode, in addition to the heat generation and to the removal of atoms and ions, there is a certain probability (5-10%) that secondary electrons are emitted. These are accelerated and, passing through the cathode dark zone, penetrate into the negative discharge. Here they generate ions, approximately 10-20 ions/electron. In such a way the secondary electrons support the discharge. In the case of self sustained plasma the zones downstream from the negative discharge do not play an important role. For this reason the trend is to bring the anode near the cathode, eliminating the anodic discharge and narrowing the zone of negative discharge. As a consequence, in the sputtering deposition, the substrate is dipped in this last zone. Around it, a further dark zone develops, with a thickness that is a consequence of the potential at which the substrate is kept. Such a potential (called bias) defines also the type and the energy of the charge carriers reaching the material to be coated.

In addition to the diode configuration, which has the undisputable advantage to be constituted by a simple set-up, other techniques of sputter deposition have been

63

developed: RF-sputtering, triode-sputtering, and magnetron sputtering. The main advantage in utilising radio frequency discharge (RF-sputtering) consists in the possibility of using non conductive materials as targets, since the electric coupling occurs by means of an inductive impedance (operating frequencies exceed 50 kHz). Furthermore, the electrons in the negative zone have enough energy for ionising directly the gas atoms and sustaining in such a way the discharge. Therefore, it is possible to operate with less electronic density and, as a consequence, at a lower pressure. A restriction, deriving directly from the utilization of non conductive targets, is constituted just by the poor thermal conductivity of these materials. The thermal conditions that they must undergo during the bombardment may originate such a stress conditions as to lead to their breakage.

In the triode configuration (triode-sputtering), a second cathode (a conductive material kept at a certain bias potential or a thermo ionic source, according to circumstances) serves the purpose of sustaining the discharge while the target draws out ions from the plasma. The second source of electrons allows to keep low the pressure (down to 0.001 Pa) or, alternatively, to operate with very moderate voltages (40 V). By varying the emission of the electronic source it is possible to obtain high ionic densities on the target and on the substrate, keeping low the potential between the electrodes.

In RF sputtering with D.C. bias or just RF samples can be coated without the need for rotation, because the emitted species leave the target at every possible angle. Most of the sample surface is in straight line of sight with some part of the target. Since the average free path of the emitted species is relatively small (< 1 cm), the emitted material shall be distributed at random directions because of the collisions with the plasma particles. Such a scattering allows the emitted species to reach those surfaces which are not in straight line of sight with the target.

Another process variant is the magnetron sputtering which allows to increase the deposition rate by a factor of 100. Therefore, for example, Al and its alloys can be deposited up to rates of 60 µm/h. The magnetron sputtering is different from the other techniques since the plasma is restricted in the zone immediately adjacent the target. The restriction is obtained by establishing a strong magnetic field above the target surface so to compel the secondary electrons, coming from it, to scour spiral form paths that maintain themselves near the cathode. In such a way most of their energy shall be dissipated just in the target zone, increasing the sputtering rate and, as a consequence, the deposition rate. Typically, ions are drawn out from the plasma by applying to the

substrate a potential of negative bias (50 - 500 V); in spite of that, the current of incident ions is rather low (0.05-0.10 ions per each atom deposited). If such a current could be increased without raising the energy of the incident ions (that is without increasing the bias voltage) it would be possible to obtain more dense coatings with a more regular crystalline structure. For this reason the *unbalanced magnetron sputtering* techniques, initiated by Window and Savvides, have been developed.

The large variety of interactions that may take place between ion beam and target are summarised in **Figure 20**. The number of atoms per incident ion emitted by the target depends on the material to be deposited. The most important process parameters are again: substrate temperature, pressure in the deposition chamber and bias voltage [potential gradient between target (cathode) and substrate (anode)].
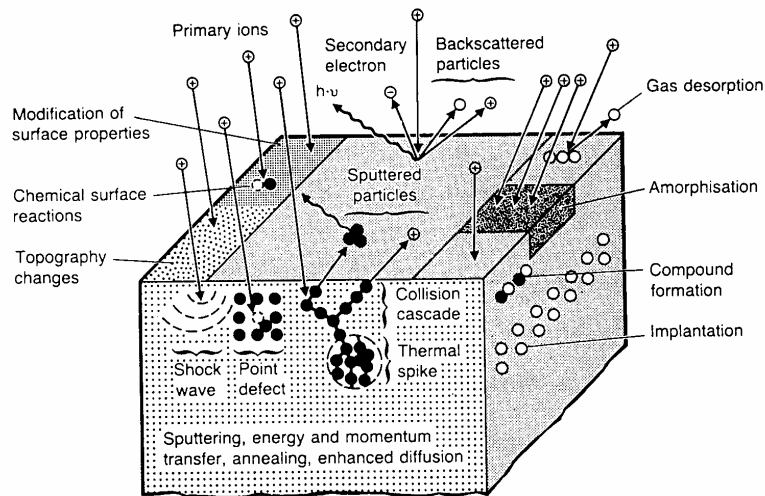

Fig. 20 - Main interactions between ion beam and substrate (Weissmantel, 1983, p. 300)

In conclusion, an increase of the substrate temperature causes an increase of the coating density. The pressure plays a diametrically-opposed role: its increasing causes a reduction of the average free path of atoms/ions and, thus, they reach sooner a sort of thermal equilibrium (reduction of their speed to a value linked to the temperature inside the deposition chamber). As a consequence, the energy of the species impacting on the substrate will be less and the coating will result less dense.

Microstructure changes, similar to those due to temperature and pressure just described, are reproducible by applying to the substrate a negative bias potential. An increasing of

65

the scalar value of the potential corresponds to an increase in the coating density, as it was demonstrated by Mattox in some deposition experiments of tantalum.

A disadvantage to mention about GDS is that it is a "dirty process" due to the sputtering gas impurities, necessary heating and outgassing of the apparatus components, and impurities in the target material. All these factors cause the introduction of impurities into the coating during its growth. In every case the deposition processes present peculiar contamination problems; as far as the GDS is concerned, the contamination problem has been in part solved by using on the substrate, as it was previously discussed, a small voltage bias to draw out atoms or molecules of ionised gas which are capable of removing those impurities weakly bonded during the film growth by bombardment at low energy.

The physical changes in the surface topography and composition changes due to the different sputtering yields must be taken into account in any method of surface modification that involves ionic bombardment. The complex compositional changes, as a consequence of bombarding a multi-component target (for example brass) depend on the different removal yields among the elements present in the target matrix. The thickness of the modified layer and its growth with time depend on the sputtering yields of the surface elements and the diffusion of elements toward the surface through the modified layer. It is difficult to model such a process due to its dependence on temperature and crystallinity.

As soon as the thickness of the film increases beyond 0.5 µm various characteristics of growing unusual crystallographic defects are formed within the matrix of the deposited coatings. These defects may be due to different causes, among the most commune ones there are topographical surface effects (micro scratches, irregularities, impurities and contaminants) and spots of fault growth of the crystalline film which become favoured sites for nucleation. On these sites an accelerated growth with respect to the matrix growth takes place. As a consequence such crystallographic defects spread over the matrix surface.

PVD-ion plating

Normal deposition by evaporation in a vacuum is not adequate for wear-resistant coatings. The metal vapour which builds up the hard coating must consist of high energy vapour particles. High-energy means particles with a high velocity. This is achieved by charging the vapour particles with a positive potential (ionisation) and

accelerating the ions by means of a negative voltage, applied to the substrate and called bias. Coating with partly ionised metal vapour at bias voltage is termed *ion plating*. The kinetic energies of the ions are in the 100 to 300 eV range. The shallow implantation of the more energetic ions, gives ion-plated material an excellent adhesion to substrates to which it normally would not adhere.

Three coating generation processes are suitable for ion plating: the first two, namely evaporation from a crucible and sputtering in a glow discharge have been already described in some detail. The third one is evaporation using a so-called *vacuum arc*, which depends on phenomena also associated with glow discharge sputtering. In arc deposition process the metal is simultaneously evaporated at microscopically small areas and the vapour particles are ionised and accelerated all in one single work stage.

Normal arcs in a gas atmosphere between a negative cathode and a positive anode with low voltage (order of magnitude 20 V) and high amperage (order of magnitude 100 A) are generally well known. However, in a low-pressure atmosphere or a vacuum, an arc with the same electrical characteristics changes its physical appearance at the cathode. The arc no longer attacks the entire cathode, it moves around attacking only small spots of some micro-millimetres in diameter, the so-called cathode spots. Such a cathode spot exists only for some 5-40 ns and is then replaced by one or more new cathode spots in the immediate vicinity. This deposition method is based on the possibility of producing coatings by utilising the charged species forming the electric arc. It is possible to trace the path of the arc moving very quickly over the cathode. The total electrical power of the arc concentrated in one such microscopic crater of a cathode spot causes momentary power densities in the order of 10^9 W/cm^2. As a result the solid cathode material is suddenly evaporated; the vapour particles are ionised several times and accelerated tremendously in a heated ion cloud in front of the cathode spot - the so called plasma. The kinetic energies of the ions are in the 100 to 300 eV range. Mostly ionised vapour is emitted although there are individual emissions of molten droplets some of which are incorporated in the coatings.

It is possible to control both the path that the coating material does between the source and the substrate and its energy of impact on the substrate. The capability of measuring out the energy of the incident beam allows the formation of coatings with higher density, purity, and adhesion. The path control is also used for minimizing the problem of the droplets (micro and macro particles) which, coming out from the electrodes, may be incorporated in the coating, worsening its mechanical and adhesion characteristics.

The higher reactivity of the vapour produced by electrical arc, due to the large presence of ionised species, makes possible to produce coatings made up of stoichiometric compounds and much better results than those obtained with simple evaporation or magnetron sputtering. The vast acceleration of the ions is particularly striking. The energy content of the emitted vapour cloud is more than 100 times higher than for conventional evaporation from a crucible even before the ions have been additionally accelerated by the bias voltage. This clearly indicates that the arc process attains very good coating results even at low bias voltages. A distinctive feature is that coatings deposited at coating temperatures of 200 °C are characterized by good adhesion.

The most used type of arc is the so-called cold cathode which is kept at a temperature lower than its melting point. In such a way the physical arrangement inside the chamber can be varied since the vapour particles are produced from the solid cathode material and, thus, there are not the restrictions deriving from the formation of a liquid phase. Once the arc has been fired, it focuses in one spot where heat and electronic flow suffice to sustain it. The currents into play are in the order of 100 A, about 10% of which is attributable to the ionic flow. The deposition rate that can be reached with the arc technique varies from 20 µm/h to 100 µm/h, depending on which process is selected according to the desired quality of coating. In addition to the typical parameters of the vacuum deposition processes, the arc deposition allows to control the energy at which the ions hit the substrate. In case of conductive or semi-conductive coatings it can be applied a bias potential by means of a D.C. generator. The limit of the bias voltage is dictated by thermal considerations, since the coated part is heated by the ions condensation.

3.2.2 Ion Beam Deposition

This process is distinguished from glow discharge methods in that ions are derived not from a glow discharge plasma, but from an ion source and the pressure can be maintained at ultra-high vacuum. In primary ion beam deposition, the ions from an ion source are themselves deposited at low energy (about 100 eV) to form the thin film. In secondary ion beam deposition, the ion beam is accelerated at 100 to 1000 keV toward a target material that will be sputtered and deposited on the substrate. The ion beam is usually an inert gas; however, reactive ions can be used to deposit compounds of oxides and nitrides.

The attraction of ion beam deposition is that the energy, rate, and angle of the ions striking the target can be controlled independently and thus the ion generation process can be decoupled from the target voltage and the phenomena at the substrate. Therefore, it is possible to have more separate control of the key fundamental phenomena occurring at the film/substrate surface, such as energy, rate, and direction of incident ion bombardment, rate of incident, inert or reactive, gas particles, and substrate/surface temperatures (to promote epitaxy).

3.2.3 Ion Implantation

This technique is usually dealt with separately, since it is a direct ion implantation and no deposition takes place.

The method consists in bombarding the surface of a substrate with a focused high-energy ion beam (typically in the range 50-200 keV). The ions penetrate the substrate surface and dissipate their energy in a series of atomic collisions. After losing their kinetic energy, \which is dissipated as heat, the ions become an integral part of the substrate near surface layer; this method allows in principle the implantation of any atomic species into any surface to produce novel alloys, the composition of which are not constrained by thermodynamic considerations regarding solubility. This is a major advantage of ion implantation over other coating techniques since there are no adhesion problems: the modified surface region is not susceptible to delamination under the influence of thermal or mechanical stresses. The implant layer thicknesses may be up to several hundred nanometers. Conventional ion implantation equipment operates at relatively low current density, typically 10 $\mu A/cm^2$, but by using a higher current density, the time to reach the required total dose can be reduced. Although ion implantation causes localised heating of the surface of the substrate the bulk properties are retained; the changes in dimensions and distortions encountered with some surface coating technologies are avoided.

The preferred angle of incidence of the ion beam with the substrate surface is 90°: as the angle of incidence with respect to the normal increases, the depth of penetration decreases. Since ion implantation involves the generation of an ion beam the process is necessarily a line of sight technology and therefore to achieve a uniform flux density over complex shaped substrates the components to be treated must be rotated.

The single ion, after penetration into the substrate, does not follow a straight path until the rest point, since it undergoes inelastic collisions with the atoms of the substrate.

These last ones are themselves on turn undermined and they may initiate a cascade of collisions which upsets the original lattice. The distance travelled over by the ion is defined as range (R). This is a random process and gives generally an impurity/depth profile of the Gaussian type; the average of such a distribution is referred to as average range. The energy of the ion beam influences directly both the range and distribution of implanted ions. At higher energies the distribution shows a greater scattering around the average (keeping equal the number of implanted ions per unity area, expressed as ions/cm^2).

As soon an ion penetrates into the surface of the material, there is a certain probability that an atom of such a surface is sputtered out of its lattice site. The ratio of substrate sputtered atoms to incident ions is defined as sputtering coefficient (S). As a general rule, S increases by increasing the mass of the incident ion and the incidence angle of the ion beam.

There is a particular dosing level according to which the number of atoms removed from the substrate equals that of the implanted ions. As a consequence, it is established a steady condition and the distribution profile of the implanted species presents a maximum concentration on the outermost surface of the substrate.

Ion implantation may be used to obtain improvements in such properties as hardness, wear resistance, corrosion resistance and fracture and fatigue behaviour.

The main advantages of this technology are:

- implanted near surface layer is integral part of substrate - no adhesion problems
- low temperature process avoids problems of substrate distortion with negligible dimensional variations
- high versatility
- unique alloy formation is feasible
- environmental friendly technology

Some disadvantages are:

- line of sight process, requires component manipulation
- limited to small component sizes
- high cost process

Because of the high capital cost of ion implantation, the selection of appropriate applications requires careful analysis.

The technique is commonly used to implant carbon, nitrogen, and nitrogen-oxygen mixtures on titanium alloys to form compounds such as TiC, TiN, Ti_2N, and Ti-O-N.

In such a way it is obtained a noticeable increase in wear resistance, as pointed out in a specific paper (Oliver et al., 1984, pp. 699-704), that reports the results of wear tests, carried out by the pin-on-disk method, on Ti 6-4 alloy samples in the as received condition and on samples of the same alloy which had been modified on the surface by nitrogen implantation. It can be observed that the implanted samples on the average undergo a material loss by volume which is twice smaller than that of the non implanted samples.

The modified surface composition of the implanted sample is given not only by the presence of nitrogen, but also by the presence of oxygen and carbon which become imbedded in the surface layer, during both the implantation and wear processes, as it has been observed on worn out samples. This surface layer with complex composition is responsible for the alloy fiction coefficient reduction (Pons et al., 1987, pp. 580-587).

Nitrogen or carbon implantations on pure titanium give similar results in terms of breakage under load of the implanted zone, whereas on the Ti 6-4 alloy nitrogen implantation is much more efficient than carbon. However, it has been pointed out that a thermal treatment between 400 and 470°C improves the performance of the carbon implanted alloy, owing to the formation of TiC particles with a diameter equal to 60 nm (Vardiman, 1984, pp. 705-710).

Carbon implantation on the Ti 6-4 alloy increases the life of the material with respect to fretting fatigue, slowing down the formation of debris which causes surface damage and subsequent crack initiation (Vardiman et al., 1983, pp. 165-177).

A nitrogen implantation method at high temperature has been suggested for increasing the nitrogen penetration depth inside the Ti 6-4 substrate. It has been demonstrated that the major benefits, as far as tribological properties are concerned, are obtained by implanting at high temperature, with a concentration of 10^{18} N_2^+-N^+/cm^2 at 60 keV. The increase of penetration depth, when compared to the depth at room temperature, is higher than 750 nm, and TiN and Ti_2N are formed (Kustas et al., 1992).

These samples have shown the lowest values of friction coefficient (down to $\mu = 0.12$) in absence of lubrication with μ decreasing while the applied load is increased up to the critical value of 98 N at which the implanted layer breaks.

3.2.4 Thermal Spraying

Thermal spraying processes allow the obtainment of coatings starting from powders, wires or rods, made up of metallic, ceramic or cermet (ceramic phases dispersed into a metallic matrix) materials. The material to be deposited is melted in the interior of an energetic source and then accelerated toward the substrate, where it quickly solidifies, giving place to overlapped lamellar structures.

When melted particles reach the surface to be coated have a high kinetic energy and, at the moment of impact, they flatten forming thin layers called splats. Thus, the coating structure consists of overlapped, solidified and tied one to each other splats.

Pores, unmelted particles, and oxide inclusions, in addition to the splats, are generally observable in typical thermal sprayed coating cross-sections.

Porosity is due generally to gases absorbed by the coating during its formation to shadowing phenomena.

Oxide inclusions are caused by the interactions of melted particles with the spraying environment and because of the coating surface heating up during the deposition process. At the moment of impact the oxide film, covering each particle, breaks and it becomes trapped within the splats.

The thermal spraying technology, according to the type of thermal source utilised, can be divided into three categories, namely *Combustion, Electric/Wire-Arc,* and *Plasma.* Each one of these categories encompasses several variants.

In the *Combustion* spray processes the powders are melted by the chemical energy derived from the oxidation of a combustible material.

The *Electric/Wire-Arc and* the *Plasma* processes utilise, as thermal sources for melting and accelerating the particles, an electric arc and a gaseous plasma environment, respectively.

The plasma state is generated by an electric arc, established in the interior of a torch. The plasma gases are generally Ar, H_2, N_2, He or mixtures of them. Diatomic gases have a higher enthalpy, due to the double dissociation (from molecule to atom and then to ion) process. The plasma gas flows through the annular duct, where the arc strikes at high frequency between the electrodes. It propagates through the interior of the gas jet, going out through the nozzle as a flame (**Figure 21**).
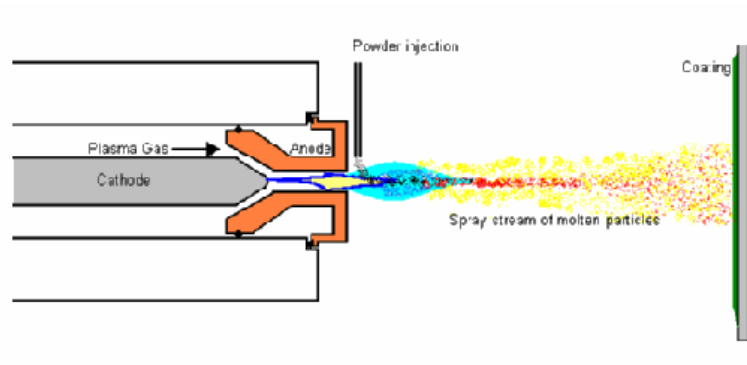
Fig.21 - General layout of the plasma spray process

Temperatures between 10,000 and 15,000 °C are reached inside the plasma; and, for this reason, the torch is water force-cooled.

Speed and temperature of particles depend on the flow and flame inlet distance of the powders which are injected by means of a gas carrier. The speed of particles, at ambient pressure, is in the range of 120-350 m/s; at low pressure such a speed reaches 400-500 m/s.

Characteristic parameters of plasma spray processes are:

- Powder sizes must be optimised for obtaining the desired coatings. Generally, grain size distributions with 5-45 µm or 30-80 µm diameters are utilised. Fine powders produce more dense coatings with less surface roughness.

- Particle shape must be such as to maximize the powder flow ability. Shape irregularity may cause agglomeration problems in the feeders and jeopardize coating uniformity.

- The distance between nozzle and substrate must be reckoned according to the type of powder to be deposited. Short distances allow an elevated coating density and increase cohesion; however, if they are too low they may induce too high temperatures of the substrate and cause the formation of coatings with a high percentage of unmelted particles.

- The deposition angle must be as much as possible near 90° and not less than 60° to avoid shading phenomena that cause an increase in the coating porosity.

- The powders flow allows, keeping constant the power, to modify the degree of melting of the particles, the cohesion force, the effectiveness of deposition, the levels of porosity and oxide inclusions in the coating.

- The relative speed between torch and substrate must be such as to warrant, at every run, a layer with a substantial thickness (10-30 µm) without an excessive overheating of the coating.

- The substrate temperature must not be too low to avoid that the cooling of particles on its surface is too quick and not too high to avoid excessive thermal stresses within the coating and at the substrate-coating interface.

The main technological variants of the plasma spray are:

- Air Plasma Spray (APS)
- Vacuum Plasma Spray (VPS)
- Inert Plasma Spray (IPS)
- Reactive Plasma Spray (RPS)
- High Pressure Plasma Spray (HPA)

Air Plasma Spray

Such a technique is carried out in air at atmospheric pressure. The length of the flame is a few centimetres only because of the air restraining action on the plasma particles. The distance between torch and substrate, during deposition, ranges around 12-16 cm.

The powders employed have large grain sizes (40-90 µm) and the resulting coatings have a residual porosity around 5%, because of the low speed of particles. The level of oxide inclusions is elevated generally, due to the work environment. The deposition temperature does not go over 350°C and adhesion with the substrate surface (roughened by sand blasting) is of a mechanical nature.

Vacuum Plasma Spray

Deposition is carried out at pressures ranging between 100 and 400 mbar, which allow to lengthen the torch flame, resulting in an increase of the time particles dwell inside the plasma jet (dwell time). The absence of atmosphere favours overheating (600-900°C) the substrate and the arising of diffusion phenomena between coating and substrate. Adhesion is, thus, of metallurgical type.

VPS coatings are very dense, almost without any porosity and oxide inclusions; layers with thickness ranging between 100 µm and 1 mm can be obtained.

Inert Plasma Spray

An inert gas is introduced into the deposition chamber; generally Ar or He are used to prevent oxidation or other products that might form when highly reactive materials (Cr, W, Mo, Ti) are deposited. Moreover, Ar cools the plasma jet with less effectiveness than air and the hotter is the plasma, the more increases the dwell time.

Reactive Plasma Spray

Such a technique produces coatings which are formed by reacting the sprayed material with reactive gases present in the deposition chamber. In such a way it is possible to obtain ceramic coatings (TiN, CrN, etc) which could be otherwise obtained by sintering or vapour phase deposition technologies only.

High Pressure Plasma Spray

This technique utilises pressures as high as $4*10^5$ Pa to favour the melting of large size (> 100 μm) particles, since the higher pressure promotes a higher heat exchange.

Typical products, which are obtainable by plasma spray, are:

- thermal barriers: ZrO_2 + Y_2O_3 deposited onto M-Cr-Al-X (M = Ni, Co, Co-Ni; X = Y, Hf, Si, Ta etc), ZrO_2 +MgO, ZrO_2 +CeO, ZrO_2 + TiO_2
- corrosion resistant coatings: M-Cr-Al-X
- abradable coatings: BN-Al, metallic dispersions in graphite, etc
- polymeric coatings: polyethylene, Ni + polyethylene, etc
- wear resistant coatings: carbide dispersions in a metallic matrix, Al_2O_3, etc

The feasibility of coating components with complex geometries depends on the availability of multi-controlled axle robots capable to handle torch motion. In such a way, it is possible, for example to obtain layers with uniform thickness even on turbine blade surfaces.

Modern plasma spray plants, due to the availability of automatic multiple powder distributors, make possible fast depositions of multilayer with graded stoichiometry and mechanical properties from the substrate-coating interface up to the top layer.

3.2.5 Thermo-chemical treatments

The thermo-chemical surface treatments allow the modification of materials and they represent an alternative solution to the coating deposition. They consist in promoting the diffusion of suitable chemical elements (carbon and nitrogen) into the surface layer of the material. These elements increase the surface hardness of the material and generate a fine dispersion of carbides and nitrides, combined with the metal or with the alloy elements.

As in the case of steel, the surface hardness is the primary objective of the diffusion treatments of titanium alloys. However, in some cases, it is utilized for developing a chemical barrier on the surface. Oxidation is the main method to form a protective barrier, although aluminizing constitutes a further alternative.

The temperatures required for an adequate diffusion depend on type of alloy, diffusing species and its concentration gradient on the surface. Plasma assisted techniques allow lower diffusion temperatures, whereas saline bath treatments allow a better control of the oxygen with respect to gas diffusion methods.

The available processes utilizing saline baths are numerous, but they are not frequently used in industrial production. One of the most used processes is the *Tiduran* which consists in dipping the components to be treated into a cyanide saline bath at about 800°C. The hardness profiles depend on the exposure time. The *Tiduran* process has been used for process control valves and high performance engine components of motor vehicles and spacecraft.

Although oxygen is usually considered as an undesired impurity, its ability to harden the titanium surface trough the formation of a solid solution is often exploited. Oxygen surface diffusion produces within the hardened layer three distinct zones:

- A brittle TiO_2 top layer which is afterwards removed
- A several microns thick TiO_2-TiO layer
- A hardened region containing dissolved oxygen

The "useful" zones for the wear resistance are constituted by the one rich in oxygen and by the intermediate (TiO_2-TiO) layer.

The extent of surface hardening and the depth of the oxygen rich layer depend on the exposure time to air and on the temperature.

76

The nitriding process produces a gold coloured surface layer of TiN (δ) above a thicker layer of Ti$_2$N (ε). Below these two layers there is another hardened layer with a thickness varying between 10 and 100 μm (according to the exposure time and treatment temperature) and containing dissolved nitrogen. The surface hardness can be increased more than 500 HV.

3.2.5.1 Ionic nitriding and carburising

The plasma diffusion treatments aim at introducing species such as nitrogen, carbon, boron etc. into a material surface. This, while kept at high temperature, is brought into contact with a carrier gas containing the activated species of nitrogen, carbon or boron.

In particular, nitriding and carburising with positive ions, which derive from the plasma generated by an electric glow discharge, are efficient treatments for producing hard surfaces, resistant to wear, fatigue, and corrosion.

Carburising is a diffusion treatment which allows enriching the surface layer of a material with carbon. In the case of a steel component, this process causes an elevated surface hardness combined with good characteristics of bulk toughness.

The plasma technology, when compared to the conventional gaseous carburising technique, allows a better control of the composition and uniformity of the carburised layer, offering at the same time less risks of deformation.

There are two types of industrial plasma carburising processes: one utilizes a mixture of propane gas, hydrogen, and argon; the other one uses pure methane or diluted with hydrogen only. The advantage of utilizing the plasma carburising process consists in the penetration uniformity of the treatment (including complex geometries), guaranteed by the possibility of activating and stopping the carbon transfer from the atmosphere to the specimen very quickly (a few seconds).

The plasma nitriding (known also as ionic or glow discharge nitriding), similarly to carburising, is a surface treatment which gives small deformations only. It is also a very advantageous technique since the sputtering action generated by the plasma cleans and activates the surface and removes any oxide film that may be present or it is formed during the process. Another advantage is that the nitriding process may be carried out at lower temperatures. However, it is possible a nitrogen migration across the grain boundaries which is responsible for brittleness.

In this process the energy of a glow discharge plasma is used to form a plasma trough which the nitrogen ions are accelerated toward the surface of the piece to be hardened.

The ionic bombardment heats up the piece, cleans its surface and provides activated nitrogen. Plasma nitriding is the preferred nitriding method whenever a selective treatment is required and it is often used to improve the properties of the material before the PVD coating process.

The ionic nitriding and carburising have the advantage of producing layers of nitrides and carbides with higher thickness when compared to the conventional thermo-chemical treatments.

The compounds often utilized in the nitriding processes may constitute a source of hydrogen, that, due also to the process high temperature, can diffuse into the alloy and cause its brittleness (hydrogen damage).

A very important part is played, in this case, by the alloy microstructure because, as it was pointed out, the α alloys tend to form hydride (brittle) which depresses their mechanical characteristics, whereas the β alloys keep hydrogen in solid solution, minimizing brittleness, but, at the same time, reducing the tendency to hardening.

It must be pointed out that the titanium containing alloying elements such as Al, Cr, Mo, V, and W is particularly suitable for ionic nitriding (Gicquel et al., 1990, pp. 1743-1750; Huang et al., 1992, pp. 97-101) since these elements have a strong affinity for nitrogen, which plays a fundamental role in surface hardening (Ignatiev, Kovalev, Melekhin, 1993, pp. 233-236). The tribological properties of plasma nitrated titanium alloys are definitely better than those of untreated alloys, in terms of both wear rate and friction coefficient (Lanagan, 1988, pp. 1957-1962).

The fatigue performance of the nitrated alloy depend strongly on the substrate conditions prior to treatment: the Ti 6-4 alloy in the annealed condition shows, after nitriding, a marked life reduction (more than 21%) with respect to the untreated alloy. That may be due to the increase of the α grains and production of a continuous α matrix. On the contrary, by using as a starting material the alloy obtained by the solution treatment and aging (STA), the fatigue deterioration of the nitrated product decreases to a maximum of 4%.

3.2.5.2 Laser nitriding and borating

Thick surface layers of nitrides and borides have been produced by various methods such as laser surface heating and introducing into the surface hard particles, generated from reaction with gas (nitrogen or methane) or heating surface deposits (graphite or boron nitride).

The erosion resistance (mass loss) of the laser nitrated Ti 6-4 alloy is elevated when compared to the untreated alloy: the nitride layer delays the beginning of the erosion process that is characteristic of the type of alloy.

At beginning the treated layer maintains itself unbroken for a few impacts; after it breaks down it is removed gradually, exposing the uncoated surface of the alloy that initiates the characteristic (steady state) erosion process. A comparison with a TiN coating on Ti 6-4 alloy obtained by PVD showed a lower resistance: it was removed after a few impacts (Lanagan, 1988, pp. 1957-1962).

Boride coatings on titanium alloy have shown a good resistance to impact of high velocity particles.

Very thick (up to 80 µm) and dense coatings have been produced on Ti 6-4 alloy by laser boriding and the erosion rate has decreased because the material removal mechanism is converted in a breakage process of the coating rather than an erosion process of the surface material.

3.2.6 Chemical and electrochemical depositions

Titanium and its alloys are difficult to plate since the presence of surface oxides may prevent a good adhesion between plating and substrate. Thus, it is necessary a careful preparation of the surface.

The properties that are improved (wear resistance, lubrication, corrosion resistance) vary according to the type of plating process that generally includes methods of electroplating, electroless plating and coatings by chemical conversion.

The term electroplating refers usually to the bath electroplating process, where the piece to be plated constitutes the cathode of an electrochemical cell.

The ASTM B 481 specification describes three separate processes for the surface preparation and the electroplating of titanium and its alloys. Hard chromium is the most common plating for wear resistance, whereas copper and some precious metals are used for different applications.

The hard chromium plating requires a surface pre-treatment to remove the oxide for promoting a good adhesion of the coating. This pre-treatment may consist in a electro less nickel plating or a high-chloride nickel strike bath.

The copper electroplating of titanium and its alloys may be a first step prior to subsequent plating. After cleaning and prior to plating, the titanium surface must be

activated chemically by an acid dip followed by a dichromate dip to promote a good adhesion of the plated coating.

The purity of water and other reactants to prepare the activating solutions is a critical parameter, as it is the hydrofluoric acid content in the acid and dichromate baths which must be controlled carefully.

After an appropriate activation, titanium may be plated in a standard acid bath of copper sulphate.

The typical thickness of the deposits is about 25 μm. The most interesting and peculiar feature of a copper plated surface is the capability of lubricating.

Copper plated titanium wires are available commercially and they have been used in applications requiring electrically conductive surfaces. Currently, titanium wires are plated in a continuous process at a speed of 60 m/min in acid baths of copper flu borate at a current density varying between 7.5 and 12.5 A/dm^2. The copper deposit is a thin coating or a flash; by using higher current density, the copper thickness is increased at the expense of adhesion.

The electro less plating baths have been developed for elements such as copper, Silver, and nickel, however, the most used one is the nickel/phosphorus system for antiwear coatings.

The deposit is obtained by catalytic reduction of ions of the plating metal without utilizing electric current.

The electro less nickel coatings are used for their corrosion and wear resistance. The deposition rates (10 μm/h on the average) are low when compared with those of the electro deposition methods; however the electro less deposits, typically 50 μm thick, are definitely more uniform.

Chemical conversion coatings form whenever a substrate surface reacts with the surrounding environment. Simple examples of conversion coatings include the anodized surfaces and the formation of surface oxides due to exposure to air. The conversion coatings may be applied also by dipping the material into a tank containing the coating solution.

Generally, conversion coatings are thin (2.5 μm) and not hard enough to be used successfully in antiwear applications. However, these types of coatings (in particular the potassium titanate) are used on titanium for improving lubrication since they act as bases for retaining lubricants.

The phosphate-fluoride coatings are used because they increase the adhesion of paints on titanium (although the sand-blasting pre-treatment gives a good surface preparation for the same type of adhesion). Results of drilling experiments illustrate the effectiveness of the conversion coatings when used with various lubricants. Tribological tests at high speed have indicated a marked improvement in the wear characteristics of the metal after the coating and lubricating with a mixture consisting of one part of molybdenum disulfide and two parts of thermosetting phenolic resin.

Wear tests with alternate motion have shown that conversion coatings and oxidized surfaces improve wear characteristics, but if the coated samples were also oxidized, the improvement was noticeable.

Conversion coatings increase the titanium oxidation rate at a temperature of about 425°C and up to 595°C. The original coating is retained above the titanium oxide layer.

The baths used for these coatings employ variable amounts of reactants, dipping times, and temperatures. The resulting coatings consist mainly of potassium and titanium fluorides and phosphates.

The well known anodizing treatments may be carried out on titanium and its alloys, although the resulting coatings are much thinner and softer than those produced on aluminium by the same treatment. The process produces a smooth TiO_2 coating, with uniform appearance and texture, having also a uniform colouration which may change from blue to violet. The dioxide layers that form have a limited thickness ranging between 0.1 e 0.2 μm and they may be obtained utilizing a wide gamut of acid, neutral and alkaline electrolytes. In an acid environment at higher temperatures (60-80°C), the oxide layers are about 10 μm thick. The titanium anodizing generally gives to the less noble metals a limited protection only against galvanic corrosion. If it is used in combination with solid lubricants helps to prevent seizure. The variety of colourations which can be obtained on titanium, due to the light interference with thin layers of oxide, have allowed the use of this metal in decorative applications and the development of original fields of research and art.

Advanced surface treatments called "electro ceramic", which produce thick and hard, compact and adherent coatings, have been developed for increasing wear resistance of titanium and its alloys (and other light alloys such as aluminium and magnesium). The process producing such coatings modifies deeply the metal surface that is polarized negatively (by applying a high bias) and is dipped into a liquid electrolyte (constituted by an oxidizing solution), utilizing a plasma glow discharge. This generates at the same

time the oxidation of the alloy surface and the formation of a compact layer of ceramic material.

Unlike the processes where the coating is deposited by other techniques (e.g. thermal spraying), in this case the ceramic layer forms by the conversion of the metal itself and, therefore, it is not subject to the lack of adhesion problems which are typical of conventional coatings. Another advantage of this technique is that, unlike anodizing, it is not sensitive to the presence of alloying elements, such as copper, in the material to be treated.

The hard deposits that are obtained have thickness ranging between 50 and 100 µm, whereas deposits possessing optimal thermal and electric insulation may reach a thickness of 200-600 µm.

The disadvantages of this technique may be summarised by the fact that the material to be treated must contain a high percentage of aluminium in order to obtain an efficient modification.

3.2.6.1 TiN electrochemical depositions

Available processes for TiN deposition require high temperatures (800°C) and/or high vacuum. This is due to the reaction speed between metallic titanium and gaseous nitrogen or compounds containing nitrogen being usually low at room temperature. The TiN coating can be produced also by an electro chemical nitriding of titanium. One of the available methods utilizes liquid ammonia as a solvent, an appropriate electrolyte (potassium amide), and temperatures ranging between - 78 ÷ + 25°C.The process is similar to the metal anodizing in aqueous solutions which is responsible for the formation of dioxide coatings. Many researchers have attempted to develop electro chemical methods for nitriding titanium, utilizing also the same liquid ammonia; however the use of high temperatures as a necessary step for treating the film and obtaining the TiN, often causes the imbedding in the TiN itself of impurities containing oxygen, carbon, and halogens. The electro chemical technique described by Griffiths et al. (2001, pp. 579-580) causes the breakage and the removal of the original TiO_2 layer, always present on all titanium surfaces exposed to air. Furthermore, the use of potassium amide as an electrolyte permits a clean reaction from an electro chemical point of view and it guarantees an exclusive migration of nitrogen containing anions toward the titanium anode. Thus, the problem due to the embedding of impurities in the coating and post deposition treatments, previously mentioned, are eliminated. It has

been observed also that the utilization of low-density currents during the electro chemical process allows controlling the film thickness through the whole amount of charges passing across the system, whereas high density currents produce nanostructured titanium.

3.3 TiN coatings deposited by vapour phase technologies

TiN coatings are used widely because of their hardness characteristics, high melting point, good corrosion and wear resistance and good conductivity. Some TiN properties, as compound and as coating, are reported in **Table 17** which summarizes data reported in different papers.

Tab. 17 - Properties of TiN coatings deposited by PVD

Physical properties of titanium nitride (TiN) coatings	
Composition	TiN, purity >99%
Process	PVD
Appearance	Metallic golden colouration
Thickness	Ranging between 0.25 and 12 μm. Typical thickness in various applications ranging between 1 and 5 μm
Uniformity	Coating conforms uniformly to the substrate. No build-up occurs on corners (unlike plating operations). Coating "throws" well into features. In deep holes, coating tapers off from 1 to 7 diameters of depth
Hardness	Hardness > 2000 kg/mm^2 Knoop or Microhardness Vickers. Values of 2500-3000 are typical. They are equal to about 85 Rc. Coatings harder than the hard chrome or carbides
Adhesion	(The coating forms a metallurgical bond to the substrate that will not flake, blister, chip or peel. In fact, the coating is actually implanted [has actually reacted with the substrate] slightly into the surface layer of the substrate)
Friction coefficient	TiN generally gives low friction coefficients with counter parts such as steels, carbides, TiN, ceramics, and platings. Friction coefficient is a property of the system and not of the material only. It depends on many factors among which the material itself, the counter part, the lubricant, the temperature, the speed, the load, the surface finish of the counter part, and the type of motion (reciprocating, rotating). The published values

	may have wide variations. They oscillate between 0.05 and 0.90. A typical value for TiN against steel is 0.65
Non-stick	TiN forms an anti-sticking surface, excellent when compared to most of the other materials
Toxicity	Non-toxic. According to the FDA's (Food and Drug Administration) and USDA(United States Department of Agriculture) requirements, it has been approved for use in numerous medical devices, including implants and for food contact.
Thermal resistance	Stars to oxidize at 600° C in air. More resistant under an inert atmosphere
Melting point	2930° C
Deposition temperature	Varies between 200 and 450° C. The standard process is carried out at 400°C and produces one of the most tough coatings
Electric resistivity	25 µOhm-cm.
Chemical resistance	Inert to acids, alkaline compounds, and solvents
Thermal expansion coefficient	9.4×10^{-6} /°C
Thermal conductivity	0.046 Cal/sec.-cm-°C
Density	5.22 g/cm^3
Crystalline structure	Cubic centred faces.
Young' s module	600 Gpa.
Poisson ratio	0.25
Heat of formation	80.750 kCal/mole. (3.5 eV/mole)
Band Gap	3.35 - 3.45 eV

Film deposited by PVD or CVD show a texture that varies according to the conditions of production.

Je et al. (1966) have investigated the texture of TiN coatings grown on Si (0 0 1) substrates, kept at 375 K, by radio frequency (RF) magnetron sputtering, inside a chamber where the TiN target was located at a distance of 10 cm from the substrate.

The source was operating in RF with a power density ranging between 6 and 12 W/cm^2. Both Ar at a pressure of 5×10^{-3} Torr and a mixture of Ar (5×10^{-3} Torr) and N_2 (1.5×10^{-3} Torr) were used as carrier gases.

During the initial phase (< 23 nm) of the film growth, it was obtained a casual distribution of the orientation, indicating that nucleation was taking place at random.

In a random orientation growth, the peak (0 0 2) intensity increases rapidly until the film thickness reaches 100 nm. After this phase, it is the intensity of the peak (1 1 1) that starts to grow rapidly.

It would be necessary to know the surface energies relevant to the TiN reticular planes to be able to explain the results based on the model of preferential growth. Unfortunately it is not even known the plane with a minimum surface energy. On this regard there are two different views: some researchers think that the minimum energy belongs to the planes (1 1 1), while others believe the minimum energy to be a property of the planes (1 0 0). The first ones base themselves upon the fact that TiN may have a good conductivity similar to that of metals. On the other hand, Pelleg (1991, p. 117) calculated the lattice energies basing himself on the fact that TiN has the same structure of NaCl. According to his calculations, the surface energy increases in the order (1 0 0), (1 1 0) and (1 1 1). Chemical bonds in TiN, however, have metallic, covalent, and ionic characteristics (Toth, 1971, p. 248).

The experimental results obtained by Je et al. (1966) can be explained according to the model of preferential growth, if one assumes that the planes (1 0 0) have the minimum surface energy. The random orientation in the initial phase of film growth is due to the substrate temperature (373 K) being too low (TiN melting point = 3203 K) to allow atoms to reorganize in a stable position. While the film grows, the temperature of the deposit increases because of the heat released during condensation with consequent increase of the atomic mobility. That favours the development of the texture <1 0 0> followed by <1 1 1>.

Ho and Je (1993, p. 1692) ascribe the texture modification to the competition that arises among the surface and deformation energies in the film, basing themselves on the Pelleg et al. suggestions (1991, p. 117) according to which the texture in tin TiN coatings is due to the lowest overall energy of the film that is the sum of surface and deformation energies.

Furthermore, the film would grow in the direction (1 0 0) with the lowest surface energy if this is the predominant factor, and in the direction (1 1 1) with the lowest deformation energy, when this last one is predominating.

The texture variation may be attributed to the build up of the deformation energy which is determined by the increase of the film thickness.

The growth process of the film at low temperatures is, basically, determined by the interaction between the vapour and the surface to coat and, thus, the overall energy of a film cannot be a determinant factor in the texture formation.

3.3.1 Effects due to boron addition in TiN coatings

The coatings constituted by boron and titanium nitride, TiBN, although have attracting properties of high hardness (Gissler, 1994, p. 556), good corrosion (Matthes, Broszeit, Kloos, 1993, p. 97) and wear (Knotek et al., 1990, p. 107) resistance, and have been a subject of scientific interest, until now they have not had a significant commercial role.

The research about TiBN has been focused most of all on the sputtering and electron beam (EB) methods of deposition or direct evaporation of the coating, starting from Ti-B-N heat pressed, available commercially (Ronkainen et al., 1990, p. 888; Matthews et al., 1991, p. 213; Matthes et al., 1991, p. 489).

Regarding this last method of deposition are reported hardness values ranging between 20 and 30 GPa and a wear resistance, in pin-on-disk sliding motion against M50 steel counter part, resulting higher than that obtained with TiAlN coatings.

Tamura and Kubo (1992, p. 255) have evaporated titanium and boron from two crucibles in a Ar/N_2 plasma and have observed an increase in the hardness of the coating from about 5 to 38 GPa by increasing the boron content and an increase in the corrosion resistance with respect to TiN, but, at the same time, an increase in the friction coefficient.

Yang et al. (1996, p. 287) instead have evaporated directly Ti-B alloys, still in Ar/N_2 plasma, and have observed that an increase in the boron content from 3 to 16% (with a constant ratio for TiN=1) determined an increase in the hardness from 35 to 45 GPa.

Addition of boron to TiN causes a grain refining, a strengthening of the boundary grain zone and the formation of super-hard dispersed phases in the film.

Rother el al. (1997, p. 564) have obtained TiBN coatings containing 1% of boron atoms (Ti:N=1) by reactive deposition with cathode arch.

These coatings, unlikely those of TiN and TiAlCN do not show any decrease in the hardness when they are exposed to one hour tempering cycles at 700°C in air, and they offer a better performance in milling and punching tests.

Rebholz et al. (1998, p. 2851) report about hard (40GPa) TiBN coatings containing c-BN which, however, show poor tribological (pin-on-disk) properties due to the brittle nature of the coating, that is caused by the absence of a Ti reach ductile interlayer.

Hard TiAlBN coatings have been deposited for solving this problem. These coatings were produced by EB co-evaporation of Ti and TiAlBN from two twins crucibles. In this case, the aluminium addition to the system gave an additional flexibility, which has

allowed to adjust appropriately the elastic properties of the coating during deposition (Rebholz et al., 1999, p. 242).

The subsequent step (Rebholz et al., 1999, pp. 648-653) consisted in the deposition of TiBN from a single crucible by reactive process in order to generate a ductile intermediate layer with mechanical/elastic properties similar to those of the steel substrate (avoiding the direct evaporation of the brittle refractory alloy).

To this end it was initially developed a Ti(B) alloy material, with about 5% of boron, which was then evaporated under an Ar or Ar/N_2 plasma.

The alloy containing boron behaves, during the evaporation phase, likely pure Ti and it forms a molten pool rather than giving a reaction of apparent sublimation, as it is observed instead for TiB_2 and for the mixtures Ti/TiB_2 or TiBN/TiAlBN.

According to this methodology it has been obtained the three following types of coatings, the colouration of which varies as a function of their nitrogen content: in particular, $Ti_{0.98}B_{0.02}$ has a metallic colouration, $Ti_{0.52}B_{0.02}N_{0.46}$ pale gold and $Ti_{0.44}B_{0.02}N_{0.54}$ clear gold (reference is TiN yellow gold).

The SEM analysis of these coatings has pointed out a fine columnar structure for the Ti(B) type and an extremely compact morphology for both types containing nitrogen: this second case is consistent with what was found by other researchers for the TiBN coatings (Rother, Kappl, 1997, p. 163) and it would show a grains refining effect due to small additions of B.

Another encouraging datum is that related to the roughness values after deposition of the coatings which resulted similar to those measured prior to deposition, with the exception of what was found for the TiBN/TiAlBN coatings (obtained by direct EBPVD deposition of the refractory alloys) in which it was observed a surface roughening.

The tribological properties of the boride coatings have been evaluated utilizing a reciprocating-sliding ball-on-plate apparatus with a fixed spherical counter part made of SAE52100 steel (750 HV) and WC/6%Co.

The Ti(B) interlayer coatings only were worn out , showing a wear behaviour similar to that of the bare AISI 316 in sliding against a steel spherical counter part. Both the Ti(B)N and TiN coatings, instead, did not show damage signs.

In the experiments carried out with the tungsten carbide counter part both the Ti(B) and TiN were worn out quickly with rates similar to those observed for the bare AISI 316.

The Ti(B)N containing 46% nitrogen showed a lower wear rate, but eventually it failed; only the coating containing 54% nitrogen did not show any failure sign, but, even more important, it had a wear rate at least two orders of magnitude smaller than those of the commercial TiN coatings, produced by EBPVD.

3.4 MoS$_2$ deposition assisted by ionic bombardment

MoS$_2$ deposited by IBAD (Ion Beam Assisted Deposition) can protect efficiently titanium and the Ti-6-4 alloy (Seitzman, Bolster, Singer, 1996, pp. 10-13), giving long life coatings with very low friction coefficients like for steel and ceramic materials (Seitzman, Bolster, Singer, 1992, p. 93; Bolster et al., 1991, p. 207).

Comparing the friction coefficients of bare and MoS$_2$ coated (thickness less than 300 nm) titanium based substrates (Ti and Ti-6-4), it is observed a marked decrement in the coefficients of the coated samples. This is due to the efficient lubrication of the sulphide: $0.3 < \mu < 0.4$ for the uncoated samples and $0.01 < \mu < 0.06$ for the coated ones.

The life tests (defined as the number of slid revolutions until the friction coefficient μ reaches the value of 0.2) carried out on samples (substrates) of Ti, Ti-6-4 alloy, and steel coated with MoS$_2$, deposited at two different temperatures (323 K for the coating labelled AT and 473 K for the coating labelled HT) gave the results shown in **Figure 22**. It is observed that the life of the coating on titanium based substrates depends slightly on the temperature deposition (samples AT slightly better than HT). It is also pointed out that life does not depend on the presence of an intermediate TiN layer 50 nm thick between substrate and coating.
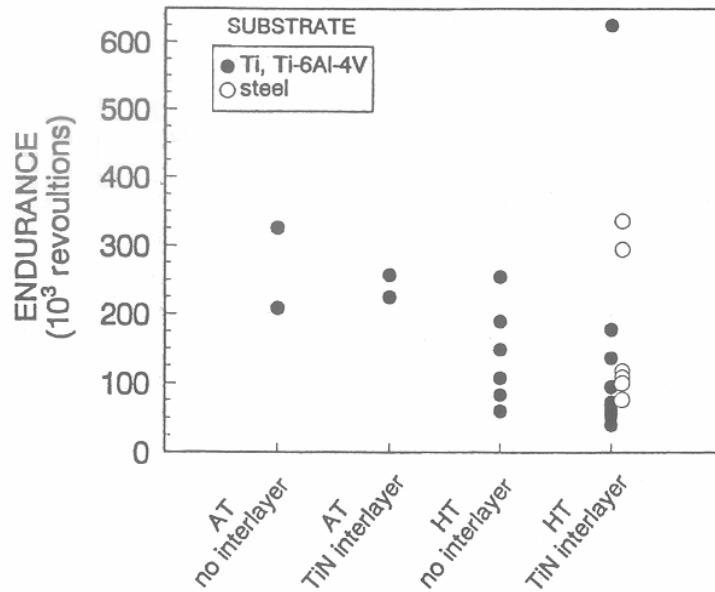
Fig. 22 - Tribological testing results (lifecycle) for MoS$_2$ coatings deposited by IBAD (AT = coating deposited at 323 K; HT = coating deposited at 473 K) (Seitzman, Bolster, Singer, 1992, p. 232).

This behaviour is in contrast with that obtained with MoS$_2$ IBAD coatings on steel, where the TiN layer was necessary for getting a good performance of the HT coatings and to prevent the degradation of the annealed AT coatings (Seitzman, Bolster, Singer, 1992, p. 232). In fact, on the steel, the nitride layer acts as a diffusion barrier for elements coming from the substrate and which would poison the coating. It seems that up to 473 K such a barrier is not needed for titanium.

The results (in terms of friction coefficient, of the pin-on-disk, sliding against a same material counter part) of the tests carried out at a variable load (increasing and decreasing) on samples of Ti-6-4 alloy, coated with 295 nm of MoS$_2$/TiN, are shown in **Figure 23**.
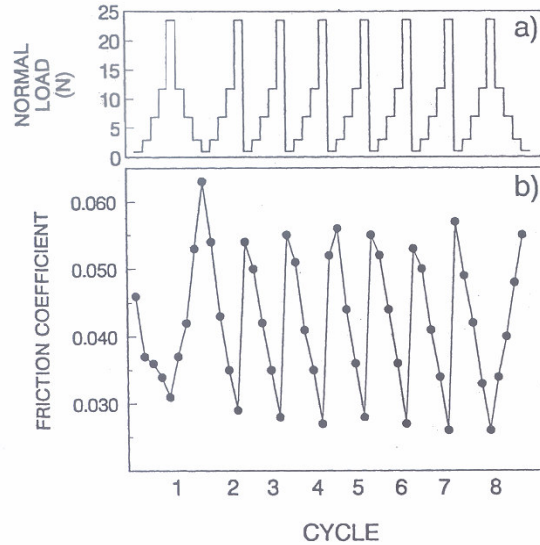
Fig. 23 - Results of Pin-on-Disk tests at a variable load (increasing and decreasing), on samples of Ti-6-4 alloy, coated with 295 nm of MoS_2/TiN (Seitzman, Bolster, Singer, 1992, p. 232)

It can be observed that friction coefficient varies in an inversely proportional way to the load variation; it was furthermore verified that, like steel, the MoS_2 IBAD coatings on titanium based materials maintain a low friction coefficient even at high loads, complying in such a way with models of Hertzian contact. This suggests that such coatings could protect the surface of titanium alloys up to loads equal, or even higher, to the elastic limit.

3.5 DLC coatings

DLC (Diamond Like Carbon) coatings are deposited by techniques such as CVD, PE (Plasma Enhanced) CVD, IBAD, magnetron sputtering and, more recently, laser ablation (Davanloo, Park, Collins, 1996, pp. 2042-2050) and PSIII (Plasma Source Immersion Ion Implantation).

Although DLC film do not possess all the properties of the diamond single crystal, they show some characteristics which are comparable to those of natural diamond. This makes them promising for antiwear applications, cutting tools and biomedical implants, bearings, and gears, lubricating layers for kinematical systems.

The deposition of DLC film on Ti-6-4 alloy has been considered as an alternative solution to the Cu-Ni-In coating obtained by plasma spraying and which is currently

utilized for improving fretting and wear properties of Ti-6-4 in turbine engine applications (Wu et al., 2000, pp. 207-217).

The worn out surfaces show variable signs - from moderate to severe - of delamination of the Cu-Ni-In coating, detachment of scale and tribo-oxidation.

It is thought that the failure takes place because of the defects in the interior of the coating and surface brittleness due to oxidation. In fact, generally this type of coatings obtained by thermal spraying present a high surface roughness, elevated porosity, low thermal stability and low reproducibility: that may degrade their performance.

Investigations about the adhesion problems of DLC film on the Ti-6-4 alloy substrate have pointed out that the implantation of ions determines the best adhesion with respect to other coating processes, due to the lack of sharp interfaces. Utilization of intermediate layers, as for example, a thin (500 Å) film of silicon which acts as binder between the nitrated alloy and the DLC film (Meletis, Erdemir, Fenske, 1995, pp. 39-45) or SiC between substrate and DLC (Kustas et al., 1993, pp. 113-119) overcome the delaminating problem that is observed in the case of DLC coatings deposited directly on the alloy.

The RFICPECVD (Radio Frequency Inductively-Coupled Plasma-Enhanced Chemical Vapour Deposition) technique, compared with those of the IBAD type results more advantageous since it does not require surface pre-treatments or steps for the formation of binding layers, producing, in any case, film with excellent adhesion.

Adhesion is determined by the type of bond that is established between the DLC film and the substrate. The DLC coatings deposited on transition metals such as Ni, Fe, and Co usually determine the formation of graphite interposed layers, generating a poor adhesion.

It is thought that the excellent adhesion of the DLC film directly deposited on Ti-6-4 may be attributed to the high hydrogen concentration (95%) in the RFICP, which favours nucleation and growth and reduces the surface oxides, allowing carbon to react with the metal. It was also found that the formation of carbides helps diamond growth.

The investigation by means of non destructive optical methods (ellipsometry) of the DLC film has allowed to obtain information about the sp^3 carbon and an accurate measurement of the film thickness.

The DLC film deposited on Ti-6-4 alloy by PECVD have a very smooth and uniform appearance when compared to the Ti/MoS_2 obtained by sputtering or Cu-Ni-In by thermal spraying, deposited on the same substrate.

Traction tests indicate that there is a good adhesion between the DLC coating and the substrate (breaking point is 1.1×10^2 MPa for the DLC coating, 2.7×10^1 MPa for Cu-Ni-In, 7.7×10^1 MPa for 25% Ti/75%MoS$_2$, all deposited on an identical Ti-6-4 alloy substrate. This can certainly increase the operation life of the coating (Bucholtz, Kustas, 1996, pp. 330-337). It must be pointed out that by the titanium addition, the Ti/MoS$_2$ coating retains the good lubricating properties and the load bearing capability, deriving from the MoS$_2$ and, simultaneously, improves adhesion. The results of block-on-ring tests carried out on bare Ti-6-4 alloy and same alloy coated with DLC, 25%Ti/75%MoS$_2$, or Cu-Ni-In film are reported in **Figures 24** and **25** which indicate clearly that the DLC coating has a better performance than the uncoated substrate.
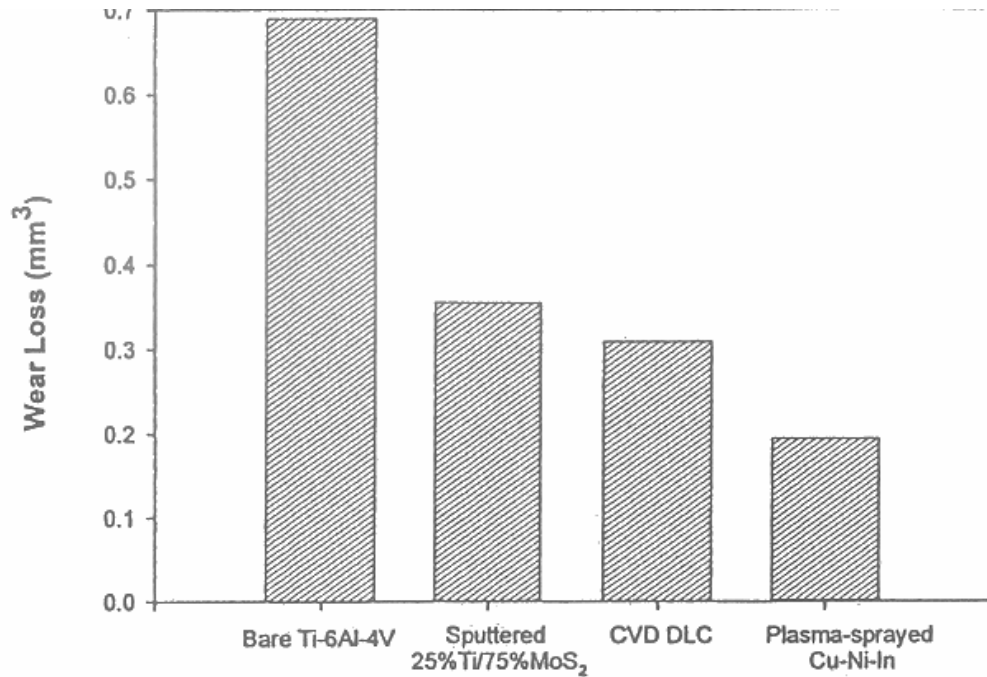
Fig. 24 - Results of block-on-ring tests carried out on bare Ti-6-4 alloy and same alloy coated with DLC, 25%Ti/75%MoS$_2$, and Cu-Ni-In film (Bucholtz, Kustas, 1996, pp. 330-337)
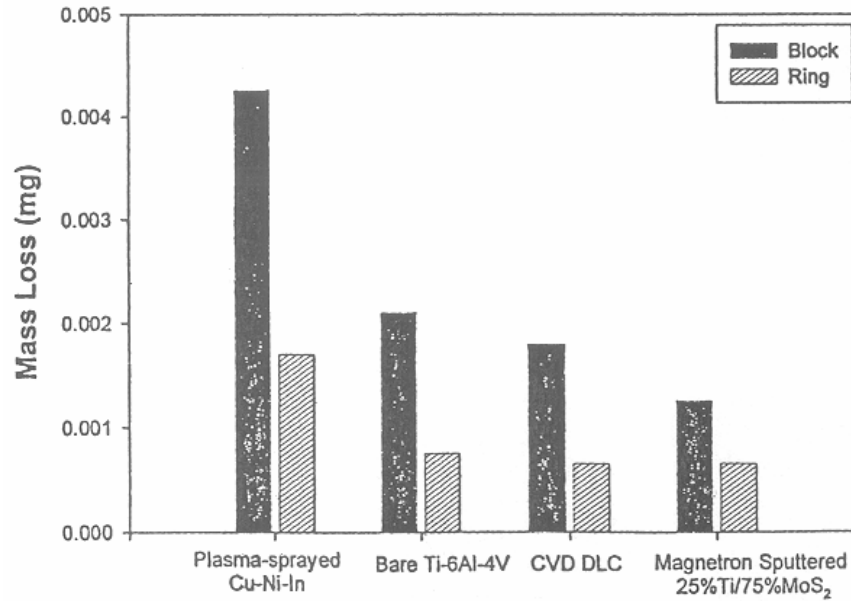
Fig. 25 - Results of block-on-ring tests carried out on bare Ti-6-4 alloy and same alloy coated with DLC, 25%Ti/75%MoS$_2$, and Cu-Ni-In film (Bucholtz, Kustas, 1996, pp. 330-337)

The same above figures and a comparison of the wear bands, suggest that the wear loss is not a good criterion for evaluating this property, and, as a consequence, the quality of the coating. This last one results softer and less adhering than DLC or Ti/MoS$_2$; moreover, it breaks off under load and, because it is lacking uniformity, it delaminates near the wear band, generating abrasive particles.

3.6 Duplex Surface Engineering

Thin coatings such as PVD-TiN can provide a surface with improved tribological properties in terms of low friction and high resistance to wear, but premature failure will occur if the substrate deforms under a high applied load. On the other hand, deep hardened layers produced by different processes/technologies (as thermo-chemical treatments) can sustain high contact stresses but still exhibit higher friction coefficients and wear rates when compared with most ceramic coatings. The involvement of the sequential application of two (or more) established surface technologies to produce a surface composite with combined properties constitutes the *duplex surface engineering* (Bell, Dong, Sun, 1998, p. 127-137).

Duplex processes are not simply mixing two surface technologies; the resultant performance of a multilayer system is the result of the synergetic effect of the individual

93

processes. Duplex processes should be designed so as to produce composite layers that constitute a multi-layer system in which the properties of the individual layers are complementary to one another (Wierzchon, 2004, p. 458-464).

3.6.1 Mechanical aspects

Contact mechanics is concerned with the stresses and deformations which arise when the surfaces of two solid bodies are into contact. The classic work of Heinrich Hertz (1882, p. 156) formed the basis of the present theoretical knowledge of static and rolling contact mechanics. Hertzian theory shows that the maximum stress does not occur at the surface, but at certain distance below the surface. Thus, under Hertzian contact conditions, failure of materials is initiated below the surface.

Several more recent mathematical models demonstrated also that:

- if sliding is present and the coefficient of friction is not negligible, than a tangential traction is also present on the surface, in addition to the normal loading. This tangential traction induces subsurface stresses in addition to those due to the normal load (Smith, Liu, 1953, p.157).
- The surface topography has a significant effect on the pressure distribution. Depending on the topographic parameters, the maximum pressure in rough contact can be many times higher than that in smooth contact, and the pressure peaks arise from the highest asperities (Webster, Sayles, 1986, p. 314).

Whereas it is possible to make bulk mechanical tests on substrate materials to determine their stress-strain curves and full constitutive equations are therefore possible to determine, it is almost impossible to do the same for coatings. For these reason there has been some interest in using indentation tests to determine the constitutive equations for the coatings. Bull, Berasetegui, and Page (2004, 857-866) developed a predictive hardness model to explain the evolution of hardness and Young's modulus with plastic depth for a coated system. The predictions can be improved considering the effects of fracture during the indentation. This model is sufficiently flexible to combine realistic descriptions of operating deformation mechanism with coatings architectures that lead to varying properties as a function of depth.

Based on mathematical modelling and FEM analyses, it has been found that in most coating systems plastic deformation initiates in the substrate, near the interface, when subject to relatively high intensity loading. Plastic deformation does not initiate in the coating until a large plastic zone has been developed in the substrate. It is clear that deep case hardening can significantly enhance the load bearing capacity of the substrate-coating system.

To this end, Mao, Sun, and Bell (2007, pp. 5796-5803) demonstrated that, considering a steel treated with a duplex plasma nitriding + PVD-TiN, the iron nitride layer (Fe_4N) formed during nitriding has high elastic modulus and helps to reduce the stress level into the duplex system. It has been observed that in this case the subsurface iron nitride layer behaves as a 'stress barrier'.

Considering a layered system produced with a duplex process, mathematical models and FEM analyses demonstrated that an interface crack or adhesive failure may initiate in the layered media if the plastic shear strain at the interface is beyond a critical value. The magnitudes of the shear stress and strain along interfaces vary significantly with the friction coefficient. Thus, low friction coatings such as nitrides and oxides used as top layers for duplex systems not only increase the wear resistance but also decrease interfacial shear stress, reducing the probability of debonding.

The effect of the film thickness, surface roughness, hardness and yielding, have been well summarized by Podgornik and Vizintin (2003, pp. 39-47). "The function of the hard film is to separate the substrate from the counter-face and to reduce wear by hardening the top layer of the surface. However, if the substrate is not hard enough to carry the load and to support the film, film will lose its function. When loaded, the film will deflect in accordance with the deformation of the substrate and the increased stresses within the film or at the interface between the film and the substrate may be higher than the strength of the material, which will result in crack initiation and propagation, and finally in film failure…... When a rough surface is covered by a hard film the surface roughness may remain or be altered to some extent, depending on the deposition method. During sliding, scratching of the hard asperities in the counter-face often occurs and this has the effect of increasing friction and wear. For a certain film thickness minimum surface roughness has to be obtained to avoid film spallation under load and sliding…… Failure of a coated surface under many tribological situations is

seldom caused by conventional wear but by the debonding of the film from the substrate (adhesive failure), by fracture of the film (cohesive failure), or even by subsurface fracture (substrate failure). In all cases the failure is mainly caused by crack initiation and propagation in or near the film….However it is imperative to determine the spatial distribution of the plastic stresses and the initiation and development of the plastic zone, which are highly dependent on the film thick and strength of the substrate".

3.6.2 Metallurgical aspects and examples of general applications

From the metallurgical point of view, it is essential the identification of the metallurgical reactions resulting from the interaction among the different layers (substrate/interlayer, interlayer/top coating). These interactions generally affect the tribological performances, the corrosion resistance and the adhesion of the multilayer system.

Although many surface treatment combinations are possible, only a few duplex technologies have been developed and the combinations have been such as:

- glow discharge assisted nitriding combined with the formation of surface titanium nitrides or chromium nitrides layers.

  Unlubricated, self-matched gear test results have demonstrated the great potential of such duplex treatments for high performance gear applications (Bell, Dong, Sun, 1998, pp. 127-137).

  The AISI 316L austenitic stainless steel is very attractive for biomedical application, due to its excellent biocompatibility properties, as well as its superior corrosion resistance. However, the practical use of this material is limited in many cases by the need for specific tribological and mechanical properties since wear debris can cause a harmful biological reaction with the tissue inside the body and can ultimately breakdown the implant system. Solid lubricant based hard diamond-like-carbon (DLC) coatings, thanks to their specific properties (high hardness, low friction coefficient, high smoothness), can be successfully applied to overcome the surface problems of the AISI 316L. But in many cases, due to the very thin nature of the DLC coatings, the soft substrate carries the applied load, which can lead to a catastrophic failure of the thin film, when subjected to a concentrated load, through the collapse of the layer on the plastically deformed soft biomedical substrate.

96

Rhaman et al. (2006, pp.5310-5317) successfully carried out a continuous duplex process on AISI 316L steel for biomedical application, consisting of plasma nitriding followed by in situ deposition of a DLC coating. This duplex treatment significantly increased the composite hardness and reduced the plastic deformation of the substrate. Results of the tribological testing showed the overall properties of this coating compared to the a non-duplex one.

De Las Heras et al. (2008, pp. 2945-2954) demonstrated the successful application of a duplex process (plasma nitriding + PVD-TiN) on the AISI 316L steel, studying the tribological behaviour of the system depending on the applied load. At low applied loads, the duplex treatment improved the wear resistance during the sliding/rolling contact (only abrasion is visible). However, upon increasing the applied loads fatigue and delamination wear mechanism appeared. In the case of the highest applied load, delamination is the main wear mechanism observed.

Kwietniewski et al. (2004, pp. 27-32), studying a duplex process (plasma nitriding + PVD-TiN) on M2 steel cutting tools, found that careful attention must be taken when comparing flat coupons to complex shaped substrates. In plasma nitriding systems without auxiliary heating, nitrogen incorporation depends on the plasma current density and, therefore, temperature, which can be significantly higher at the tool edges, forming an excessive deep and brittle diffusion case, reducing the service life of the duplex treated tools. Another study (Lee, Kim, Hong, 2005, pp. 266-271) demonstrated the superior wear resistance of EHA (Electro Hydrostatic actuator) pump parts made of AISI 4340 steel, when subjected to a duplex process (plasma nitriding + UMS/PVD-TiN).

Much research was paid to the comprehension of the process parameters influence on the duplex systems performances. He, Chen, and Davison (2005, pp. 1464-1471) studied different duplex treatments on SKH51 and SKH2 alloys, by changing the nitriding atmosphere and the TiN deposition temperature. The conclusions evidenced that an important factor in achieving successful duplex treatments is through avoiding substrate softening of the steel. The Arc Ion Plating (AIP) process is thus suggested as an excellent method for hard coating/nitrided duplex treatments, particularly for the plain carbon and low alloyed steels, prone to softening, as high quality hard coatings can be produced at low deposition temperatures.

Relating the industrial applications, Podgornik (2001, pp. 318-323) investigated the possibility to treat with e duplex process some machine elements subjected to

complex stresses. The results showed that duplex surface engineering, consisting on plasma nitriding and hard coating deposition has a great potential for improving the tribological properties of contact surfaces, not only under sliding but also under rolling conditions.

A micro scale abrasive wear test has been used to evaluate the wear resistance of duplex and non duplex (Ti, Al)N, TiN and CrN coatings on AISI H13 steel (Batista, Godoy, Matthews, 2002, pp. 363-372). All duplex coatings showed higher micro-abrasive wear resistance than their single-layered counter-parts, with the duplex (Ti, Al)N achieving the best performance.

- The combination of the electrochemical/chemical deposition technologies (i.e. hard Cr, electroless Ni) with glow discharge assisted diffusion processes.

  For example, $Cr_2N+Cr+(Cr,Fe)_7C_3$ composite layers on AISI 1045 steel demonstrated higher corrosion and wear resistance than those of the galvanic Cr coatings or of the Cr nitride coatings produced by vacuum arc evaporation (Wierzchon et al., 2000, pp. 31-35).

In the field of die coatings for Al die casting, a research group of the Colorado School of Mines (Lin et al., 2006, pp. 2930-2941) presented an optimized design methodology that is based on a multi-layered and graded coating system that first identifies the most appropriate working layer that has minimal chemical interaction with the material being formed; an intermediate layer that accommodate the residual thermal stresses induced by the forming cycles; and an engineered adhesion layer that provides strong adhesion of the coating system on the substrate. In addition, the substrate can also be subjected to a surface modification treatment that will provide an improvement in the mechanical properties of the substrate surface to better support the coating system. An example of an optimized die coating architecture is: Cr_2N (working layer) + graded Cr_2N/CrN (intermediate layer) + Cr (adhesion layer) + ion nitrided H13 steel (treated substrate).

Another study on complex surface engineering system was carried out by Rhaman et al. (2005, pp. 1451-1457) utilising a AISI 316L steel as substrate. In this work the effect of duplex treatments consisting of plasma nitriding and $TiN+MoS_x$ coatings with and without graded interlayer on the mechanical and tribological properties of the stainless steel substrate were investigated. TiN based coating on plasma nitrided substrate showed lower wear rate than the coating on non nitrided steel. Among all the systems, coating with graded interlayer on plasma nitrided surface showed lowest wear rate due

to the presence of well-adhered graded interlayer and hard load supporting nitrided surface underneath the coating than the other systems.

3.6.3 Titanium applications

Thin hard coatings generated by PVD deposition can provide a titanium alloy surface with greatly improved tribological properties in terms of low friction and high resistance to wear. However, premature failure will occur if the substrate deforms under high loads. Repeated deflections of the coatings can cause fractures of fatigue cracks that eventually destroy the film. Stress filed analysis on sliding contacts under loading has established that when the friction coefficient is reduced the maximum shear stress moves gradually into the substrate away from the substrate/coating interface. Under these conditions the Ti6Al4V alloy may not be able to provide adequate support for the hard coatings, adversely affecting their tribological performances. Hardening of the substrate layers can inhibit deformation and reduce the abrupt change in properties at the substrate/coating interface, thus minimizing effects due to the mechanical response.

The load bearing capacity of a hydrogen-free Cr-DLC coating deposited on untreated and BDO-treated (BDO = Boost Diffusion Oxidation) Ti6Al4V alloy has been investigated to explore the application of titanium alloys in some tribological conditions such as titanium gears (Dong, Bell, 1998, 282-289; Zhang, Dong, Bell, 2006, 5237-5244). In this case, duplex treatments result in a dramatic improvement in the load bearing capacity of the Ti6Al4V alloy, as determined by scratch test and pin-on-disc sliding wear testing.

Duplex treatments on Ti6Al4V alloy obtained with the combination of plasma nitriding and the deposition of carbon nitride CN_x films by PVD were studied in detail (Yongqing et al., 2000, pp. 12-19; Yongqing et al., 2000, pp. 2215-2227). Compared with a CN_x film directly deposited on Ti6Al4V substrate, the load bearing capacity of a CN_x film deposited on plasma nitrided layer was improved dramatically. Furthermore, smooth CN_x films could effectively reduce both the interfacial stresses and the stresses near the surface thus providing a good tribological behaviour. Considering different materials as counterparts during the tribological ball-on-disk testing (Yongqing, Hejun, 2001, pp. 16-15): with the steel, the material transferring from the ball is the main wear phenomenon. With alumina ball a graphitization phenomenon of wear debris takes place, contributing to the lubrication of the system. Finally, utilising polyethylene pins an abrasion of both substrate and counterpart is observed.

Another duplex treatment obtained by combining nickel diffusion (ND) deep case hardening with low friction wear resistant TiN and DLC coatings have been designed and applied to high strength Timetal 550 titanium alloy (Kwietniewski et al. 2001, pp. 284-292). Experimental results showed that load bearing capacity of the thin films can be dramatically improved when deposited on ND-treated Ti alloy substrate relative to material coated with TiN and DLC alone. It was also found that DLC/ND duplex system possessed superior load bearing capacity to the TiN/ND.

The effects on steel of TiN coatings, deposited by PVD techniques, have been investigated extensively and it has been confirmed that the tribological properties of the substrate are improved strongly (Matthews, Murawa, 1985, p. 31).

However, the same result is not reached if TiN is deposited directly on the Ti-6-4 alloy, because of its poor capability to bear the load. In fact, it is observed at the interface coating-substrate a rapid deterioration of the adhesion that causes a flaking or "peeling" of the coating, in particular under cyclic stress conditions.

TiN, which is utilized extensively as a thin film for controlling the primary wear mechanism, in particular the adhesive wear, actually shows a limited applicability regarding the abrasive or erosive wear.

It was observed, for example, that, since the dimension of the impinging particles into a slurry pump or in airplane engine applications is almost always one order of magnitude higher than the maximum thickness (about 6-7 μm) obtainable for the coating (Leyland, Matthews, 1994, pp. 19-25), spalling of the coating is likely to occur.

The load bearing by the substrate, in this situation, is not sufficient to prevent wide failures of the coating, caused by brittle fracture.

Therefore, it has arisen a twofold requirement:

- to provide a support mechanically suitable for the brittle coating and/or
- to uncouple the surface properties (or close to the surface) of the coating from those of the substrate.

This last point must be taken not only in the sense of optimising the mechanical properties, but also improving corrosion resistance, since, in many cases abrasive wear occurs in water environment.

Indeed, even tool steels and surface modified steels with alloying elements which, theoretically, should furnish the best load support for hard coatings, often result the least suitable from the point of view of corrosion resistance, because the hardening mechanism of the substrate is often based upon the principle of grain boundary precipitation for controlling grains growth and dislocation motions. The segregation of the alloying elements, induced by this phenomenon, is obviously undesirable in terms of electro chemical effects.

Leyland and Matthews (1994, pp. 19-25) describe a deposition methodology which generates a "tough" composite coating with a thickness higher than 60 μm, characterized by TiN layers with interposed Ti layers (multilayer coatings).

The treatments (based on PAPVD techniques for the deposition of thick "multilayer" coatings) allow the utilization of substrates that encompass a wide range of material typologies. This is due to these techniques providing a flexible way of deposition which allows to vary continuously the chemical and mechanical properties from substrate to surface and to realize a tailored product. The galvanic effects which might accelerate the coating breakage, through the anodic dissolution and debonding at the interface substrate-coating, can be suppressed by reducing the density of punctual defects and introducing a composition gradient within the coating. The advantage of multilayer coatings consists in the capability of controlling the rate of brittle fracture, usually associated with TiN deposited on "soft" substrates, and replacing it with a ductile break mechanism giving a better performance in the abrasive wear tests in presence of a third body and in the simulation tests of erosion due to particles in the air.

The EB-PAPVD technique allows a flexible control of the coating thickness, nitrogen content, and interface properties and, in particular, a narrow control of the structure and thickness of the deposited layers simply by controlling the nitrogen flow during the evaporation of titanium. The plasma conditions, in particular the control of thermo-ionic emission of electrons, represent a critical factor for maintaining a high degree of cohesion of the coating.

Abrasive and erosive wear tests in air were carried out on various coatings, deposited on a ASP 23 (tool steel hardened to 62 H_{RC}). It was observed that the multilayer coating 30 μm thick, made up of 12 TiN/Ti double layers and characterized in every layer by a 1:1 TiN:Ti ratio, gave a performance significantly higher than that of the uncoated substrate, with a decrease in the loss of specific weight higher than 40% measured in four hours of test duration. On the contrary, the coating with the same whole thickness,

but characterized by a 2:1 TiN:Ti ratio showed a weight loss of about 10% higher than that of the substrate, even if it was less than that obtained for a standard single layer TiN coating 4 μm thick. Although the wear rate of multilayer coatings was initially high enough, it decreased in time, settling at constant value; instead, an opposite behaviour was given by the substrate in the as received condition (ASP23), for which the wear rate was initially low. The initial wear rate of the uncoated ASP23 was virtually null; however, after a certain incubation time, the weight loss increases suddenly. The course of this erosive process has been interpreted as a consequence of the sample surface initial smoothness. In particular, the roughness increase and the plastic deformation, induced by the impacts with the alumina particles on the smooth surface, cause the acceleration of the wear process. Once the fatigue limit of the layers close to the surface is reached, it would seem that the crack propagation across the grain boundary is responsible for the chipping of wide areas of the material, determining, thus, the observed rapid increase of weight loss. Similarly to what occurs in the abrasive wear tests, the multilayer 1:1 TiN:Ti coating shows in the erosion tests, at beginning, a wear rate high enough. It can be observed that the coating 7.5 μm thick (characterized by three 1:1 TiN:Ti double layers) gives a weight loss which is about 20% less than that of the analogous coating 30 μm thick (twelve couples of layers in the same ratio of the previous coating). The reason of such a behaviour is not clear; however, it might be due to a slight reduction in the integrity of the thicker coating because of the melt replenishment process during the deposition cycle.

The unsatisfactory results relative to the 30 μm coating, with a 2:1 TiN:Ti ratio, have been attributed to a brittle behaviour, similar to that of the TiN single layer. Such behaviour is deduced from the analysis of the impact craters, showing signs of scattered cracks and delaminating of the single layers around the impact point. Comparison with analogous craters of coated samples with a 1:1 ratio shows that in the 2:1 stoichiometry the damage is less severe. Furthermore, it has been observed that the density of defects on the surface of the 1:1 coating is much lower than that of the 2:1 equivalent coating, for the same exposure time. This indicates that the increased toughness of the thicker Ti interposed layers, indeed, gives a whole protection against impact damages, caused by a large portion of the impinging particles. It must be pointed out that the experiments were carried out at a normal angle of incidence. For such a condition it is expected that a hard and brittle coating has the worst behaviour and that a tough material substrate shows a satisfactory behaviour.

When interpreting the data relevant to the erosion phenomenon, it is necessary to keep in mind both the angular distribution of the impacting particles (ideally it should be investigated a range of incidence angles variable between 0° and 90°), since this parameter plays a main role in determining the wear rate and the mechanical properties of the different materials. The authors reached the conclusion that both abrasive and erosive wear resistances benefit even when thickness of the coating is less than 10 μm; however, in erosive wear, the substrate load bearing capability becomes a very important factor in case the coating is thin.

In practice, the thickest coatings are important in all those applications that require extending "in-service" life of the material, both in terms of mechanical and corrosion resistance properties. In such a case the coating toughness is of primary importance, especially for controlling erosive wear, because the hardness increase, obtainable, for example, by increasing the TiN content above 60-65%, causes the undesired result of making brittle the coating itself and shortening its life.

The idea of an intermediate layer between the hard coating and the substrate was developed aiming at generating a support for the load, when the substrate was not able to bear it, as it was pointed out for the Ti-6-4 alloy. Such an idea became reality with the development of the treatments called "Duplex".

Wilson et al. (1993, pp. 600-607) have compared the wear resistance and fatigue properties of coatings deposited on Ti-6-4 alloy by Thermoionic triode PA-EB-PVD, in particular TiN, CrN, and Nitron, commercial name of the coating obtained by plasma duplex nitriding followed by a process of TiN deposition.

The results of microhardness tests show for the Nitron (thickness about 2 μm) the best performance, equal to 1400 HK at a load of 100 gf, when compared to TiN (thickness about 2 μm) equal to 550 HK and CrN (thickness about 1.5 μm) equal to 650 HK at the same load. It is interesting to note that the hardness of CrN is higher than that of TiN, although the thickness of CrN is lower. The increase in the load bearing capability for TiN and CrN becomes very obvious when the applied thrust load is decreased.

The results of abrasive wear tests underline, once more, the poor characteristics of the substrate in the as received condition and at the same time a slight improvement in the resistance of the single PVD layers of the two nitrides that, however, falls down after about 200 revolutions (tests carried out with dry rubber wheel apparatus). On the contrary, after an identical test, Nitron remains intact and it does not indicate significant

weight loss. It was also pointed out the ability of Nitron to resist breaking and chipping when compared to single layer coatings.

All the coatings improved fatigue resistance of Ti-6-4 alloy; the most significant result (10% improvement), in terms of life, was given by TiN, followed close by Nitron (6% improvement). CrN gave a more marginal result (3% improvement).

The results of pin-on-disk tests, shown in **Figure 26**, indicate that the substrate load bearing capability is improved by both TiN and CrN; in fact the wear of the disc is minimal. The Nitron coated disc exhibits a weight increase caused by the material transfer coming from the AISI 52100 steel pin.

Optical micrographs of the discs show a severe adhesive wear with redeposition of debris into the as received substrate, whereas the TiN and CrN coatings remain essentially intact; areas of the pin material, indicating a material transfer between the two coupled systems, appear in the Nitron.

In conclusion, the deposition of a TiN coating on a nitrated surface improves the load bearing capability, wear resistance, and adhesion properties of the Ti-6-4 alloy more than the single layer coating of the same material deposited on the same substrate by the same PAPVD technique.
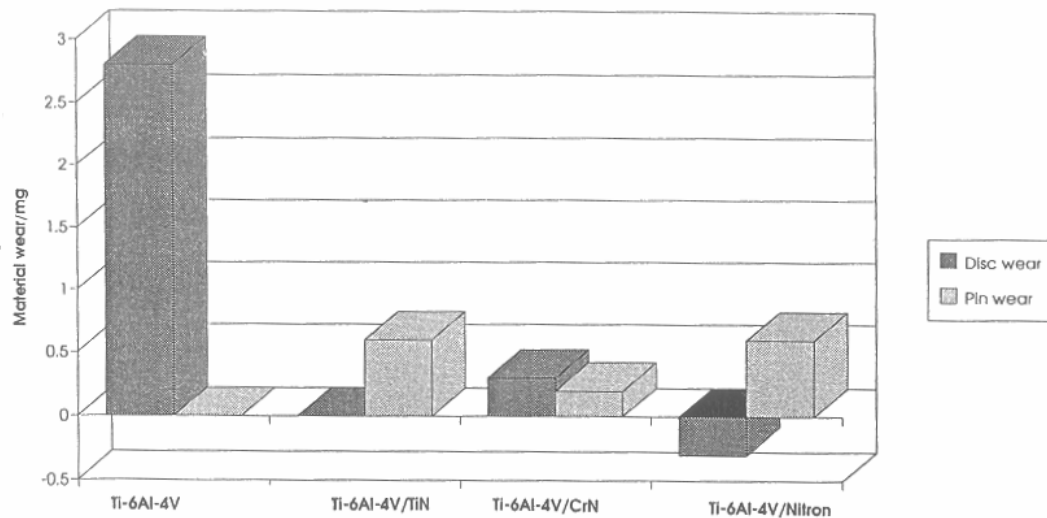
Fig. 26 - Results of pin-on-disk tests (Wilson et al., 1993, pp. 600-607)

III - RATIONALE

According to the stress field analysis of coated systems with thin and brittle coatings deposited on relatively soft substrates such as Titanium alloys, deformation initiated in the substrate at the coating/substrate interface would be the most common failure in presence of high concentrated loads. By increasing the thickness of the coating or the strength of the substrate material, deformation of the substrate can be considerably reduced and the load bearing capacity of the system significantly increased.

Two types of technological solutions are currently being pursued:

- chemical diffusion treatments of the titanium alloy substrate followed by deposition of hard thin coatings (duplex treatments)
- Multilayer thin coatings, made up of various materials (TiN, TiC, TiCN, CrN, CrC, DLC) or different microstructures

Both approaches aim at realising layers with graded mechanical properties, going from the bulk toward the outermost surface, without significant discontinuities. The main limiting factors consist in the exiguity of the thickness of such layers, in the inherent slowness (tens of hours) of the processes and in their unfavourable economy.

The present work aims at overcoming the above-mentioned limitations by stimulating and catalysing the introduction of state-of-the-art surface engineering technology into key industrial applications for titanium alloy components. The focus of this research is in developing an innovative surface treatment, consisting of two consecutive phases:

- deposition by Reactive Plasma Spraying (RPS) of a thick (hundred of micrometers) composite Ti/TiN coating on the titanium based substrate;
- deposition by Physical Vapour Deposition (PVD) of a thin (a few micrometers) hard, TiN based coating, single or multilayer, on the already deposited thick coating.

The selection of the Reactive Plasma Spray technology to realize the thick interlayer is based on the following considerations:

- the possibility to deposit Ti/TiN composite coatings (Ti nitrides dispersed in a Ti alloy) having a good chemical compatibility with both the substrate (Ti6Al4V alloy) and the top layer (TiN deposited by PVD-arc).

- The possibility to modify the mechanical characteristics of the coating by controlling the process parameters (i.e. plasma gases, deposition temperature and chamber pressure directly influence the coating hardness).

- The possibility to obtain a hardness of the interlayer in an intermediate range between the substrate (200-300 HV) and the top layer (2000-2500 HV).

- The possibility to obtain an elastic modulus of the interlayer in an intermediate range between the substrate (100-110 GPa) and the top layer (580-600 GPa).

- The RPS technology looks competitive with other deposition processes from an economical point of view, especially because of the relatively duration of the process (few minutes for the deposition of hundreds microns).

Thus, with the proposed coating system:

the deposition of the Ti/TiN interlayer can **limit the deformation of the system**, reducing the abrupt change in properties at the substrate/coating interface, minimizing effects due to the mechanical response.

The low friction TiN coating used as top layer not only **increases the wear resistance** but also decreases interfacial shear stress, **reducing the probability of debonding**.

The combination of the proposed technologies (RPS and PVD) could lead to **favourable cost/benefit ratios**, especially considering the limited duration of the whole process, when compared to other duplex systems.

IV - EXPERIMENTAL

1. Deposition apparatus

1.1 Controlled Atmosphere Plasma Spray (CAPS)

Reactive Plasma Spray (RPS) depositions were carried out utilising a Controlled Atmosphere Plasma Spraying (CAPS) equipment made by Sulzer-Metco. This apparatus, described in detail elsewhere (Carassiti et al., 1995), includes a 80 kW plasma torch, installed in a vessel that can work in air, argon or nitrogen atmospheres, with a pressure ranging from 10^3 to 4×10^5 Pa. CAPS apparatus and details of a typical torch are shown in **Figures 27** and **28** respectively.
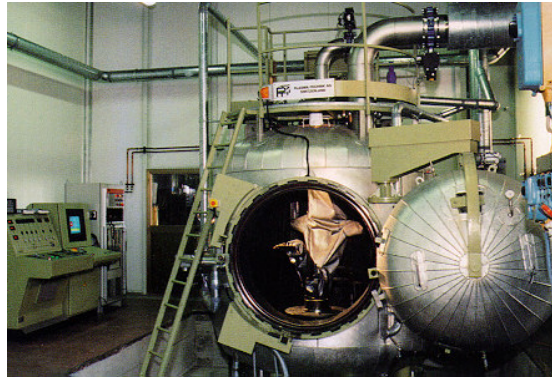
Fig. 27- Controlled Atmosphere Plasma Spray Apparatus – CAPS (Centro Sviluppo Materiali S.p.A.)
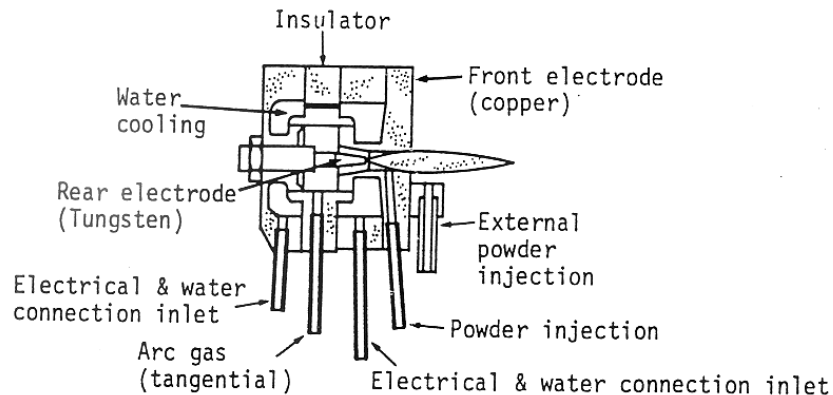
Fig. 28 - Scheme of a typical plasma spray torch (Arthur ed., 1985)

1.2 Physical Vapour Deposition (PVD)

The TiN depositions were carried out utilising a Physical Vapour Deposition (PVD), batch type coating machine, MA 1100, manufactured by Microcoat S.p.A. and consisting of a 1000 mm × 1150 mm chamber equipped with 4 arc sources located at a distance of about 170 mm from the substrate samples disposed on a rotating turntable. **Figure 29** shows the Microcoat PVD apparatus.

Fig. 29 - Microcoat MA 1100 PVD apparatus (Centro Sviluppo Materiali S.p.A.)

2. Deposition processes

2.1 Ti/TiN by Reactive Plasma Spray (RPS)

In this work, a gas atomised Ti-4,5Al-3V-2Mo-2Fe powder, consisting of particles with a spherical morphology and ranging between 40 and 80 µm, was sprayed on Ti-6Al-4V alloy substrate, while nitrogen was present in both the deposition chamber and the plasma stream. This powder was characterized, before spraying, by Scanning Electron Microscopy – Energy Dispersive Analysis of X-ray (SEM-EDAX), X-Ray Diffraction (XRD), and laser light grain size distribution. The parameters utilised in the RPS deposition process are listed in **Table 18**. They were developed on the basis of previous work (Tului et al., 2002) and by investigating the influence of different process conditions on coating characteristics, namely residual porosity, hardness profile, nitriding level, friction and wear. The substrate samples (rectangular 30 mm x 50 mm x 3 mm specimens), before spraying, were exposed to ultrasonic cleaning in acetone or trichloroethane for 60 s. After RPS deposition, sample surfaces were mechanically polished to reach a roughness of 0.3 µm Ra.

Tab. 18 - Parameters of the RPS deposition process

Deposition temperature, °C	390-470
Pressure inside deposition chamber, Pa (x 10^2)	1180
Torch distance from substrate, mm	120
Torch motion: translatory speed, mm/s	400
distance between each pass, mm	5
Plasma gas 1, Ar, slpm	20
Plasma gas 2, N_2, slpm	31
Power of plasma generating DC arc, kW	20-28
Substrate negative bias, crossing current, A	15
Powder gas carrier flow rate, slpm	5

Two spraying campaigns were carried out to select the optimized process parameters. In the first one, all the deposition runs were carried out on the basis of the experimental matrix reported in **Table 19**, designed accordingly to a Design Of Experiments (DOE), following a reduced central composite design with coded values which are necessary for the statistical analysis of the experimental results (Breyfogle, 1992, P. 176). The following parameters were chosen as independent variables:

- N_2 concentration in the plasma gas mixture. It ranged from 3 to 50% by volume of the 65 SLPM (Standard Litres Per Minute) total flow.
- Substrate temperature during spraying. It ranged, among the experiments, between 150 and 600°C. The substrate was cooled by an N_2 gas flow and temperature was monitored by means of a K-type thermocouple fixed on the back of each sample.
- N_2 pressure into the spraying chamber, ranging from 35 to 180 kPa.

Tab. 19 - Experimental matrix for RPS runs (DOE methodology)

Sample code and order			Factor A: Pressure (mbar)		Factor B: N$_2$ in plasma gas (% on a total of 65 SLPM of Ar-N$_2$ mixture)		Factor C: Substrate temperature (°C)	
Sample code	Standard order	Run order	coded value	real value	coded value	real value	coded value	real value
122_1	15	1	0.00	1075	0.00	27	0.00	375
122_2	10	2	0.00	1075	0.00	27	1.41	600
122_3	8	3	0.00	1075	1.41	50	0.00	375
122_4	12	4	0.00	1075	0.00	27	0.00	375
122_5	5	5	-1.41	350	0.00	27	0.00	375
123_1	3	6	-1.00	560	1.00	43	1.00	535
123_2	4	7	-1.00	560	-1.00	10	-1.00	215
123_3	9	8	0.00	1075	0.00	27	-1.41	150
123_4	6	9	1.41	1800	0.00	27	0.00	375
123_5	7	10	0.00	1075	-1.41	3	0.00	375
124_1	1	11	1.00	1590	1.00	43	-1.00	215
124_2	11	12	0.00	1075	0.00	27	0.00	375
124_3	14	13	0.00	1075	0.00	27	0.00	375
124_4	13	14	0.00	1075	0.00	27	0.00	375
124_5	2	15	1.00	1590	-1.00	10	1.00	535

Power of the DC arc, which the plasma was generated from, was maintained in the range of 20-28kW. Its value was derived from the nominal power, taking into account (subtracting) that dispersed in the cooling water.

Coatings with an average thickness of 350 µm were deposited onto Ti6Al4V rectangular specimens (30mm x 50mm x 3mm).

The following characteristics of the coatings were considered for the optimisation of the RPS process parameters: residual porosity, nitriding level and hardness.

The results of the DOE experimentation allowed to select the best RPS process parameters (Table 1). These were utilised in the second campaign experimentation which utilised the same CAPS apparatus. However, a negative polarity was applied to the substrate during the deposition. Samples without and with bias were identified as RPS1 and RPS2, respectively.

2.2 TiN by PVD

In this work the TiN film was deposited by a PVD-arc technique. This, along with electron beam gun evaporation, constitutes one of the two principal evaporative processes. The arc technique is favoured to produce TiN hard coatings. In this method an arc is initiated on one or more titanium cathodes (arranged around the walls of the reaction chamber). The arc source creates dense plasma of high kinetic energy ions which in this case permitted a deposition rate of about 0.8 μm/h.

Such a technique was chosen mainly for the following reasons:

1. The arc obtained under vacuum is a kind of glow discharge which sustains itself by means of the electrons and ions originating from the electrodes producing the same arc. The utilisation of such a technique is based on the capability of producing coatings exploiting the charged species which constitute the electric arc. It is possible to control the path of the coating material from the source to the substrate and its energy at the moment of impact. Controlling the energy of the impinging beam allows the formation of coatings with higher density, purity and adhesion. Controlling the path is also done to alleviate the problem due to the micro and macro particles (*droplets*) that, detaching themselves from the electrodes, may remain entrapped within the deposit, deteriorating its mechanical and adhesion characteristics.

2. The higher reactivity of the vapour produced by the electric arc, due to the species being ionised, allows the formation of stoichiometric coatings with better results with respect to the techniques based on the evaporation by electron beam or magnetron sputtering.

Table 20 reports the process parameters used for the TiN depositions. Particular attention was paid in evaluating the effects of deposition temperature and substrate bias during the coating process.

Tab. 20 - Deposition process parameters for TiN by PVD-arc

Batch n°	Deposition time (min)	Substrate bias (V)	Temperature (°C)
1	120	165	400
2	120	150	400
3	120	135	400
4	120	165	520
5	120	150	520
6	120	135	520

The TiN production process, starting from polished (0.3 µm Ra surface roughness) RPS-coated substrates, consisted of the following eight sequential steps:

1. Argon pressure at 3×10^5 Pa for 5 s for cleaning the samples from dust.
2. Ultrasonic cleaning with acetone or trichloroethane for 120 s.
3. Three sequential glow discharges with argon, each one for 2 minutes, with negative substrate biases of 450 V, 550 V, and 650 V, respectively; at a chamber pressure of 2 Pa.
4. Metal ion bombardment (MIB) with titanium ions in argon at a constant negative substrate bias of 700 V for 1 min, with 55 A sources and at a chamber pressure of 3 Pa.
5. MIB with titanium ions in argon at a decreasing negative substrate bias from 700 V to 100 V for 1.5 minutes, with 50 A sources and at a chamber pressure of 0.8 Pa.
6. Titanium flash deposition for 0.6 minutes with a substrate bias of 100 V, with 50 A sources and at a chamber pressure of 0.8 Pa.
7. MIB with titanium ions in nitrogen at a decreasing negative substrate bias from 500 to 135 V for 1 min, with 50 A sources and at a chamber pressure of 1.5 Pa.
8. TiN deposition for 4 hours with a constant substrate bias of 135 V, 50 A sources, and at a chamber pressure of 1.5 Pa.

3. Coatings characterization

Coating samples, some after the fabrication process and some others in between steps, were characterized by XRD, Optical Microscopy (OM), SEM-EDAX, Glow Discharge Optical Emission Spectrometry (GDOES), X-ray Photoelectron Spectroscopy (XPS),

porosity, hardness, and tribological tests. In particular, *structure, composition, nitriding* level, and *nitride phases* were assessed by XRD, GDOES and XPS. The *residual porosity* was determined by an image method analysis. Adhesion was assessed by scratch testing.

3.1 Apparatus and procedures

3.1.1 X-Ray Diffraction (XRD)

For the coating characterizations relative to this work the following diffractometers (Bragg-Brentano geometry) were employed:

- Siemens D-500
- Italstructures
- Seifert PAD VI (Cu kα radiation)

The acquisition time of a diffraction diagram ranges, depending on the investigation requirements, from about 100 minutes to 24 hours.

The study of the stoichiometry, very important for investigating the formation of solid solutions of different compounds, requires the calibration of the equipment by a blank sample, generally zinc oxide.

The primary elaboration of data and the qualitative determination of the phases present are carried out utilising the calculation codes furnished by the equipment manufacturers; while, own calculation codes or those developed by research centres are utilised for further analysis.

The validity of the utilised methods is periodically controlled by means of reference samples, prepared on purpose.

In our case a particular methodology was adopted in analysing the XRD results relative to the RPS coatings, to have a comparison among the different DOE samples. The following factors were calculated for each pattern:

α_{TiN} = (height of the most significant TiN peak)/(eight of the most significant Ti peak)

α_{Ti2N} = (eight of the most significant Ti_2N peak)/(height of the most significant Ti peak)

Considering all the DOE samples:

$$\alpha_{TiN,MAX} = MAX \; [\alpha_{TiN}] \quad\quad \alpha_{Ti2N,MAX} = MAX \; [\alpha_{Ti2N}]$$

Then, for each sample, the following normalised parameters were calculated:

$$\alpha_{TiN,N} = \alpha_{TiN} / \alpha_{TiN,MAX} \quad\quad \alpha_{Ti2N,N} = \alpha_{Ti2N} / \alpha_{Ti2N,MAX} \quad\quad \alpha_{TOT,N} = (\alpha_{TiN,N} + \alpha_{Ti2N,N})/2$$

with $\quad\quad \alpha_{TiN,N} \, , \, \alpha_{Ti2N,N,} \, \alpha_{TOT,N} \in [0,1]$

3.1.2 Optical Microscopy (OM)

The same equipment for the image analysis was also used for characterizing the various coatings by optical microscopy.

3.1.3 Scanning Electron Microscopy/Energy Dispersive Spectroscopy (SEM-EDAX)

SEM (ASTM E 3-01, ASTM E 766-98, ASTM E 986-97) consists in scanning the surface of a specimen to be examined with an electron beam; the secondary electrons emitted from the surface are captured, obtaining a surface topography image, representative of the surface features of the specimen. The topographic image is generated by variations in contrast (intensity) in analogy to light microscopy.

Back scattering of on-coming electrons is a function of the atomic number of the solid. This phenomenon is utilized in phase detection by mass-differentiation. Consequently, topographic information is obtained from about 200 Å deep layer, whereas atomic number information is obtained from about three times the above depth.

EDAX (ASTM E 1508-98) permits qualitative analysis of rough surfaces and quantitative analysis of the elemental composition of very localised areas of smooth surfaces, with a resolution of about 0.5% and accuracy of about 10%.

A Cambridge 240 SEM equipped with EDAX was used for examining the coating surfaces at various steps of the deposition process. Also, fractured zones of the coatings were examined, to relate microstructure with the mode of mechanical fracture, to predict

the mechanical properties of the coated alloy samples, to verify the correctness of their heat treatment, and finally, to design coatings with new property graded combinations.

Fractures were caused by soaking the coated samples in liquid nitrogen. After enough time to allow the coatings to reach the liquid nitrogen temperature, samples were bent to induce brittle breakage. In such a way the detachment of small fragments of coating from the RPS substrate was attained. These fragments were placed on special sample holders for the SEM observation. The low temperature of liquid nitrogen allowed to avoid plastic deformation of the TiN coating before its breakage. Furthermore, the small dimensions of the fragments avoided polarization inside the SEM chamber, since TiN is not a good electrical conductor.

Coatings thickness (ASTM B 748-90) was determined by utilising SEM images derived from samples prepared by lapping their cross-sections, because smooth surfaces were needed for carrying out the measurements (100 in different points, for each sample).

3.1.4 *Glow Discharge Optical Emission Spectrometry (GDOES)*

GDOES (Broekaert, 1987, p. 537) can be used to measure the optical emission spectra of any element in the periodic table. A ionised gas causes a rapid and relatively uniform sputtering of the sample surface that constitutes the cathode, and, further, the plasma excites the atoms giving rise to the characteristic optical emissions.

In the glow discharge, the electrical power is supplied between the sample (cathode) and the hollow anode by a power supply operated at 0.5 ~ 2 kV and 5 ~200 mA. The gas, usually Ar, is introduced, and the pressure near the cathode surface is regulated to a few hundred Pa. The voltage between the cathode and the anode extracts electrons from the cathode, causing ionization of the gas and the creation of a plasma.

GDOES analysis allows the concentration profiles of the elements constituting the material to be analysed, starting from the surface down to a maximum depth of 100 µm. Coatings were analysed with an ISA Jobin-Yvon JY50S spectrometer. It consists of the following three groups of components:

a) a glow discharge source, where atoms in samples are sputtered and excited to emit characteristic spectral lines
b) an optical unit including spectrometer with photoelectric detector
c) systems for spectrometric control, signal recording and computation

The technical features of this apparatus are the following:

- depth resolution: 10 nm
- analysed area: 12 mm^2
- detectable elements: all in the periodic table
- possibility of analysing up to 13 (polychromator) + 1 (monochromator) elements at one time
- erosion rate: 30 – 100 mm/s, depending on the material
- sensitivity: 50 – 100 ppm
- minimum sample size: 20 mm diameter or 400 mm^2

GDOES was employed to determine the chemical composition and thickness of the PVD coatings. These data were elaborated from the GDOES profiles. The elaboration was carried out utilising the following formula:

$$\sum_i C(x)i\Delta SiDi = q(x) \text{ g/m}^2$$

where C(x)i is the concentration of the element x at the interval i, ΔSi is the depth of the sputtered layer at the same interval i and Di is a density of the material with the interval i, and q(x) is the amount of the element x in the coating.

3.1.5 X-ray Photoelectron Spectroscopy (XPS)

XPS is a powerful analytical tool for surface chemical analysis. This technique involves analysis of low-energy electrons emitted by the specimen and typically provides compositional information in the 5-20 Å region near the surface.

In XPS analysis, photoelectrons are ejected from the surface as a result of the interaction with an incident x-ray beam from an aluminium or magnesium source. Consequently, XPS analysis is the perfect tool for determining surface chemistry, the ionization states of surface atoms, and general studies of thin film. With the provision of in-situ sputtering, depth profiles in thin film can be obtained.

The XPS spectra were measured on a Leybold Heraeus LHS10 spectrometer equipped with an EA11 electron energy analyzer using Mgkα radiation ($h\nu = 1253.6eV$) as the excitation source. The analyzer operated in the fixed analyzer transmission (FAT) mode with a constant pass energy of 50 eV. Under such conditions the full width at half

116

maximum (FWHM) of the Ag $3d_{5/2}$ peak on an Ar-ion sputter-cleaned silver surface was 0.98 eV, and the resolution was about ±0.2 eV. The binding energy (BE) was referred to the Fermi level of the electron energy analyzer, and the linearity in the BE scale was calibrated by the measurements of the Au $4f_{7/2}$, Ag $3d_{5/2}$, and Cu $2p_{3/2}$ peaks at 83.8, 367.9, and 932.4 eV, respectively. The spectra were recorded and handled by a HP 2113E data system. The data analysis included smoothing, nonlinear background subtraction, and a curve-fitting procedure using the Gaussian functions. The quantitative data of the chemical composition were obtained by measuring the peak areas and using the known elemental sensitivity factors found in the literature (Wagner et al., 1981). The quantification results of chemical composition under these conditions were accurate to about ±10%. The depth profile information was obtained by sputtering the samples with a scanning argon-ion gun operated at 2.0 keV. The sputtering rate was estimated at about 1.0 nm/min as calibrated by reference materials of known thickness.

3.1.6 Porosity

Porosity is usually defined as the ratio of voids to the total (bulk) volume of a solid.

Regarding the thermal-sprayed coatings, the image analysis technique of the sample cross-section permits to measure quantitatively its porosity. It is a very important microstructure characteristic since it is directly related with mechanical resistance and toughness of the coating. In case of functional materials, porosity often is a property which can control the transport phenomena of solid phases, liquid or gaseous, or it may be utilized for controlling the dielectric characteristics of the materials.

Furthermore, the image analysis is capable of evaluating different phases with micrometric dimensions, and, thus, it may be utilized widely for investigating micro particle composites or self lubricating materials.

The porosity of a coating can be calculated by the following formula:

$$\text{Porosity \%} = \frac{pores\ surface}{selected\ surface} \times 100$$

Where the respective surfaces are estimated directly by the software connected with the microscope.

There is no specific apparatus to determine the porosity of a coating by image analysis techniques. What is needed is a microscope connected with a digital image acquisition

device and a personal computer equipped with a devoted software. An illustration of such an assembly is given in **Figure 30** which constitutes the set-up utilized in this work, consisting of a Nikon Eclipse L 150 A optical microscope coupled with an image analysis and process system, LUCIA 4.80 manufactured by Laboratory Imaging Ltd.

The microscope used may be optical or an SEM: it depends on the type of investigation; in fact for pores or phases with dimensions down to 10 microns, it is possible to employ optical systems, whereas for smaller dimensions the SEM is needed.

The porosity measurements were carried out, for each sample, on 20 different areas, representative of the coating morphology.

Fig. 30 - Image analysis equipment: optical microscope + devoted software (Centro Sviluppo Materiali S.p.A.)

3.1.7 Hardness

Hardness measurements for the RPS coatings were carried out on their sections and surfaces: high loads (HV300g and HV500g) were used to obtain large indentation marks, including very different sampling areas in terms of mechanical properties, i.e. lamellae borders, unmelted particles, oxides and porosity (30 measurements for each sample). In the case of PVD samples, due to the low film thickness (2-3 µm) measurements were carried out directly on the surface. Lasage's model (Chicot, Lesage, 1995, pp. 123-130) was employed which allows to determine the absolute hardness value, by eliminating the influence of the substrate (RPS under-layer). The model uses the following equation:

$$C = \frac{3}{2} \cdot (\tan(74°))^{1/3} \cdot \frac{T \cdot F^{3/2}}{D \cdot G^{1/2}} + 1 - \frac{3}{2} \cdot (\tan(74°))^{1/3} \cdot \frac{T \cdot S^{1/2}}{D \cdot R^{1/2}} \cdot S + \frac{3}{2} \cdot \tan(74°)^{1/3} \cdot \frac{T}{D} \cdot \frac{S^{1/2}}{R^{1/2}} \cdot F - \frac{F^{1/2}}{G^{1/2}} \cdot S$$

Where:

C = whole (substrate + top layer) hardness

D = indentation diagonal, μm

F = absolute coating hardness

G = coating elastic modulus, MPa

R = substrate elastic modulus, MPa

S = substrate hardness, MPa

T = coating thickness, μm

RPS coating elastic modulus was measured according to ASTM E855-90(2000) Standard Test Methods for Bend Testing of Metallic Flat Materials for Spring Applications Involving Static Loading. In particular Test Method C, a four-point loaded beam, was utilised and 5 samples were characterised. A value of 590 GPa was selected for the elastic modulus of PVD coating, according to literature data (Ohring, 1992, p. 552).

3.1.8 Scratch test

Adhesion of TiN coating to the RPS substrate was assessed by scratch test. In such a test a spherical diamond point with a radius of 200 μm moves forward along the coating surface at a controlled speed and with an applied vertical load. The scratch apparatus is capable to measure the force needed for the point advancing in a direction perpendicular to the load. Increase in the tangential load causes detachment of the coating at the interface and, thus, it is possible to obtain a quantitative evaluation of the coating adhesion. Detachment of the coating from the substrate is recorded by a piezoelectric sensor which converts the acoustic emission caused by the detachment into a potential gradient.

Results depend generally on test parameters. In fact, the equipment, of the Revetest type by CSEM, allows to regulate the application rate of the vertical load and the advancement speed of the diamond point expressed as N/mm and mm/min, respectively. Furthermore, it is possible to regulate the detection sensitivity of the acoustic emission that can be expressed in arbitrary units.

Figure 31 shows the most important details of the scratch test apparatus; **Figure 32** gives an example of a graphic typically obtained by a scratch test.

Fig. 31 - Detail of scratch tester (Centro Sviluppo Materiali S.p.A.)
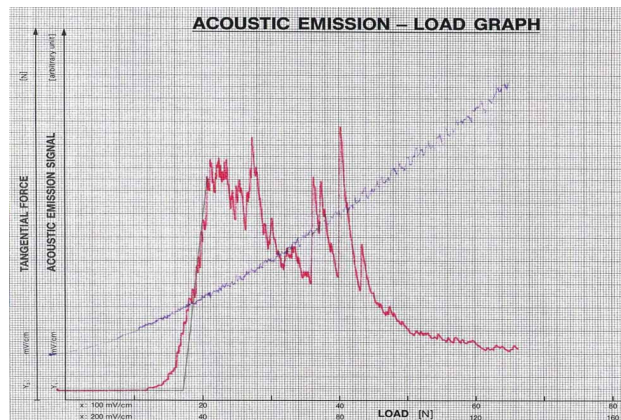
Fig. 32 - Example of acoustic emission graph in a scratch test experiment (Centro Sviluppo Materiali S.p.A.)

4. Tribological testing

4.1 Pin-on-disk

Figure 33 shows a picture of the pin-on-disk apparatus, made by RTM (Torino, Italy). The pin was replaced by a Si_3N_4 ball. Such a contact geometry was selected, to simulate severe wear conditions. The disk specimens were prepared from three different

materials: bare Ti6Al4V alloy, Ti6Al4V + RPS coating, and Ti6Al4V + TiN-PVD coating. The sample surfaces were polished to a 0.3 μm Ra.

Bare Ti6Al4V alloy substrates and samples obtained by RPS, PVD-arc, and RPS + PVD-arc, respectively, were characterized.

Fig. 33 – RTM pin-on-disk apparatus (Centro Sviluppo Materiali S.p.A.)

4.1.1 Ti6Al4V alloy

A first series of tests were carried out on sample pairs of Ti6Al4V alloy flat substrates (disk), in the as received condition, sliding against silicone nitride (Si_3N_4) balls (pin), having Young's moduli equal to 117 and 290 GPa, respectively.

Either sliding speed or load was the variable parameter, while the total sliding distance was kept constant.

Keeping constant the speed at 2 m/s, tests were carried out at 10 N, 15 N, 20 N, and 30 N. Keeping constant the load at 15 N, sliding speeds of 0.4 m/s, 0.8 m/s, 1.0 m/s, and 2.0 m/s were utilised.

Further tests, with load and sliding speed varying within ranges of 1-30 N and 0.4-2 m/s, respectively, were carried out.

Friction coefficient, load and speed were continuously monitored. At the end of each test weight loss and wear scar profile were measured. In some cases, wear volume was assessed by considering a representative wear scar section, integrating the area under a suitable interpolation curve and multiplying it by the length of the track.

Sample surfaces after the pin on disk testing, were observed under the SEM to assess the damage and identify the wear mechanism. In particular, the following experimental conditions were selected for investigation:

1) constant sliding speed equal to 2 m/s with variable load from 15 to 30 N
2) constant load equal to 15 N and variable sliding speed from 1 to 2 m/s.

4.1.2 Three coating types

A second series of pin on disk tests for the three typologies of coatings (Ti/TiN by RPS, TiN by PVD-arc, and Ti/TiN by RPS + TiN by PVD-arc) deposited on Ti6Al4V alloy substrates, was carried out to evaluate the tribological characteristics of each coating. The pin on disk test conditions are summarised in **Table 21**.

Tab. 21 - Pin on disk test conditions for the three coating typologies

COATING TYPOLOGY	DEPOSITION TECHNOLOGY	SLIDING SPEED, m/s	SLIDING DISTANCE, m	TEST DURATION, min	LOAD, N
Ti/TiN	RPS	0.4	720	30	10
Ti/TiN	RPS	0.4	720	30	20
Ti/TiN	RPS	0.4	720	30	30
TiN	PVD-arc	0.4	720	30	2
TiN	PVD-arc	0.4	720	30	5
TiN	PVD-arc	0.4	720	30	10
Ti/TiN + TiN	RPS + PVD-arc	0.4	720	30	10
Ti/TiN + TiN	RPS + PVD-arc	0.4	720	30	20
Ti/TiN + TiN	RPS + PVD-arc	0.4	720	30	30

Finally, further pin on disk tests were carried out on TiN coatings for determining the instant of any sharp change in the friction coefficient. This test was suggested by considering the hypothesis that as soon as the TiN layer was damaged across its full thickness, the friction coefficient from the typical contact TiN/Si_3N_4 would change to that of the $Ti6Al4V/ Si_3N_4$ pair.

5. Mechanical component

After the deposition processes development, as a further scaling up, RPS and PVD depositions were carried out for depositing the multilayer Ti/TiN + TiN coating on real

components: two motor-bike transmission chain sprocket made up of Ti6-4 alloy, each one with 42 teeth.

The gear transmits the motion to the wheel by the teeth contacting a case-hardened steel chain. Thus, the multilayer coating was realised on the toothed gear, utilising the same deposition apparatus and the optimized parameters. The following steps were carried out:

1. fabrication of a gear holder for both RPS and PVD depositions.
2. RPS coating: the geometry of the tooth does not allow to obtain a coating on its surface with an uniform thickness, due to the variation of the impact angle of the depositing particles. On the other hand, the coating, depending on the extent of its thickness, might affect detrimentally the geometry of the component. For this reason, specific deposition arrangement and procedure were developed.
3. PVD coating: the sprocket was fixed on a turntable, set out with two rotations, and it was introduced into the PVD deposition chamber.

V - RESULTS

1. Coatings characterization

The experimental results encompass the following coating characteristics for each sample:

- Composition related to deposition parameters
- Thickness
- Porosity
- Hardness
- Microstructure
- Tribological features

1.1   Ti/TiN by RPS

Figure 34 shows the results of some XRD analyses (Cu kα radiation). All RPS coatings exhibited the presence of titanium nitrides with different stoichiometries: TiN, Ti_2N, and TiN_{1-x}. TiN and Ti_2N were predominant while the amount of TiN_{1-x} was negligible in all the cases.

[1] Sample 122_3   [3] Sample 123_4
[2] Sample 123_5   [4] Sample 122_5

5-0682 I Ti Titanium *
6-0642 D TiN Osbornite, syn ♦
41-1352 I TiN0.30 Titanium Nitride ∇
23-1455 I Ti2N Titanium Nitride
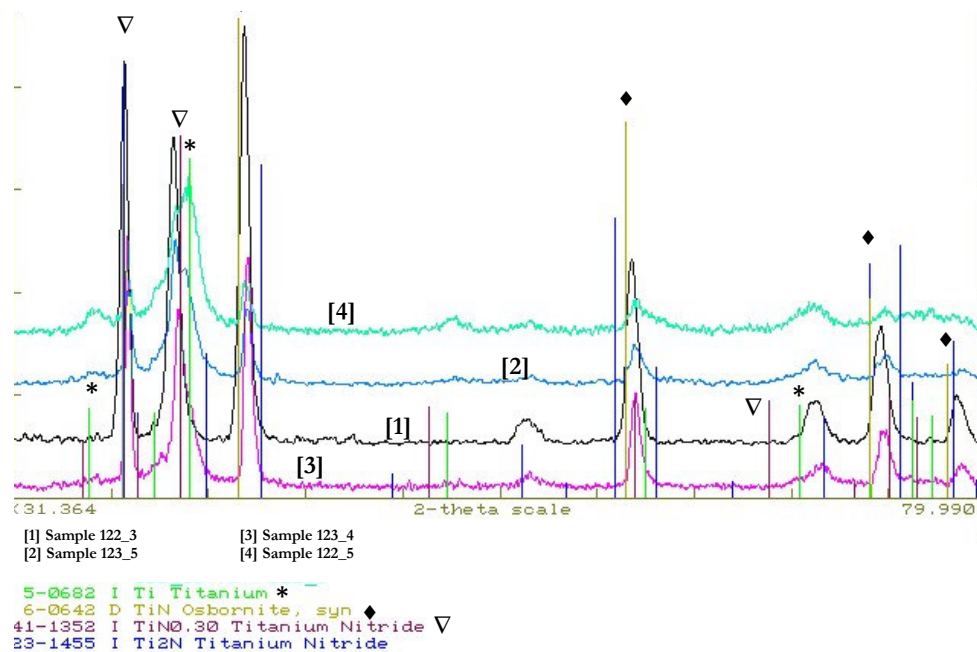
Fig. 34 - XRD Spectra of samples 122-5 [1], 123-5 [2], 124-1 [3] and 124-4 [4]

The GDOES results indicated that the weight percentage of nitrogen retained in the coatings ranged from 2 to 8%. **Table 22** reports sample porosity, hardness (HV_{300} measured on the cross section), and thickness values which were in the ranges of 2 – 16.5 % and 450 – 1100 HV, and 120-425 μm, respectively.

Tab. 22 - Coating porosity, hardness and thickness

Sample Code	Coating porosity (%) (st. dev.)	Coating hardness (HV_{300}) (st. dev)	Coating Thickness (μm) (st. dev.)
122_1	3.1 (0.17)	694 (112)	380 (30)
122_2	5.2 (0.15)	737 (130)	355 (32)
122_3	6.6 (0.15)	880 (139)	330 (20)
122_4	3.7 (0.13)	675 (106)	405 (34)
122_5	5.7 (0.12)	515 (93)	420 (15)
123_1	1.9 (0.10)	655 (103)	350 (24)
123_2	8.2 (0.33)	291 (64)	290 (18)
123_3	4.5 (0.10)	497 (82)	415 (22)
123_4	7.0 (0.20)	818 (108)	365 (30)
123_5	16.5 (0.18)	815 (100)	425 (24)
124_1	12.1 (0.29)	860 (116)	400 (15)
124_2	5.9 (0.17)	590 (123)	370 (31)
124_3	5.6 (0.17)	600 (105)	380 (30)
124_4	5.8 (0.23)	547 (94)	370 (28)
124_5	16.5 (0.18)	462 (75)	125 (15)
125_1	3.61 (0.20)	450 (88)	120 (18)
125-3	2.95 (0.16)	1077 (94)	135 (15)

Figure 35 shows a comparison between cross sectional and surface hardness for each sample. The values are quite similar, thus evidencing a good mechanical isotropy of the coating.

Sample Hardness
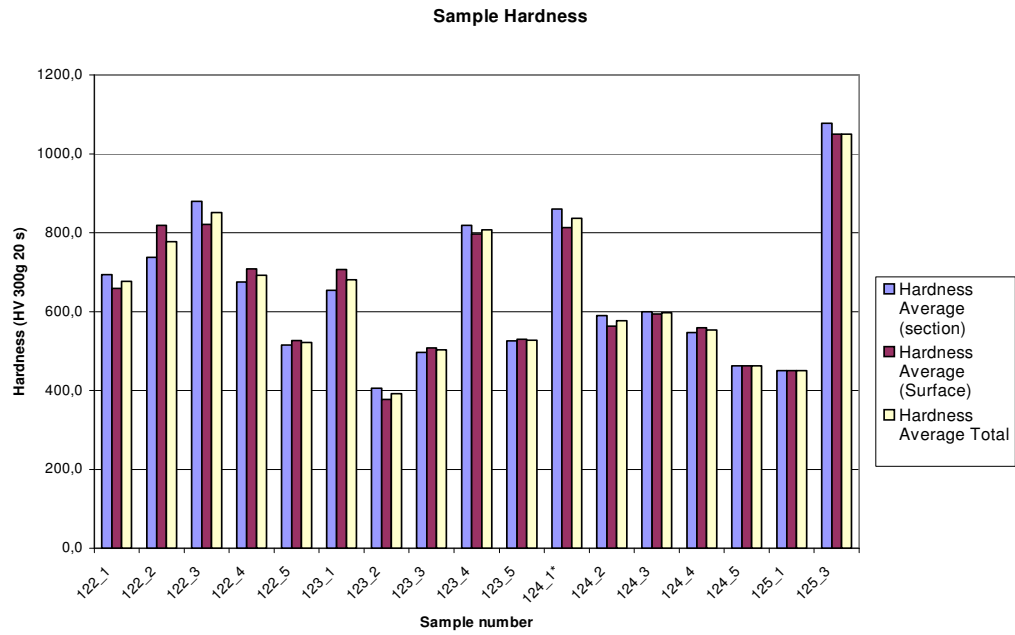
Fig. 35 - Comparison between cross-section hardness and surface hardness

Figure 36 shows $\alpha_{\text{TiN,N}}$, $\alpha_{\text{Ti2N,N}}$ values for each coating. Although these values can not have a quantitative meaning, they have been utilized for comparative considerations among the different coatings.
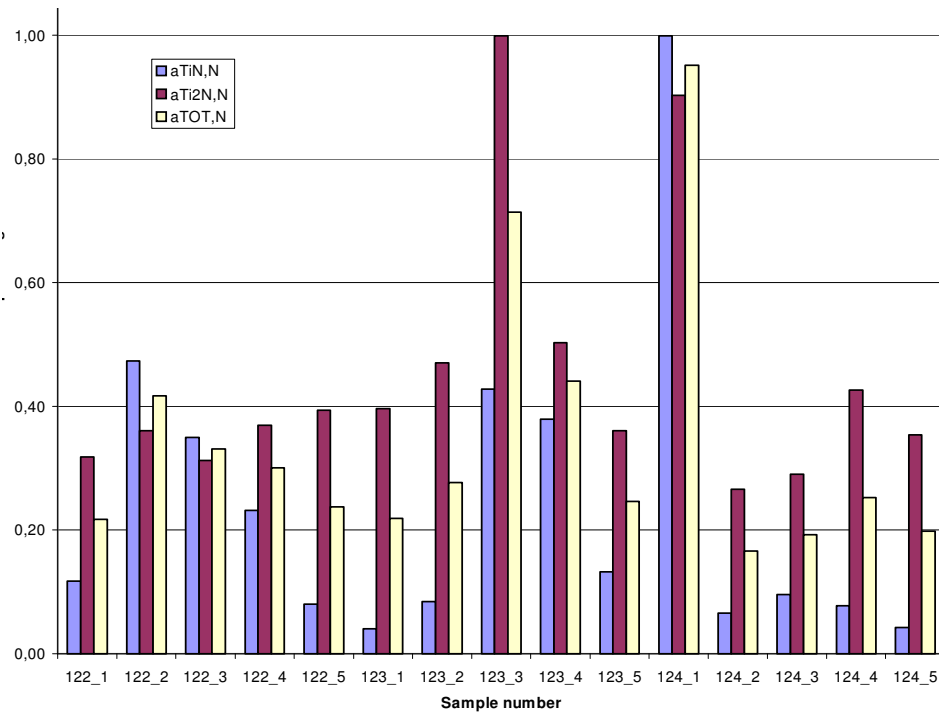
Fig. 36 - $\alpha_{\text{TiN,N}}$, $\alpha_{\text{Ti2N,N}}$, $\alpha_{\text{TOT,N}}$ values for each coating

Figures 37-42 show microstructures of some RPS samples observed by OM.

It is possible to observe the typical plasma spray microstructure:

- lamellar structure;
- unmelted particles (zone A, **Figure 38**);
- Pores (zone B, **Figure 38**);
- Pores due to unmelted particles removed during the polishing of the samples (zone C, **Figure 38**).
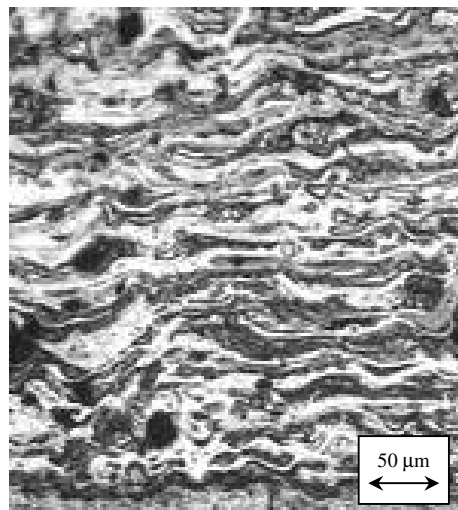
Fig. 37 - Sample 123_4 microstructure (high spraying pressure)
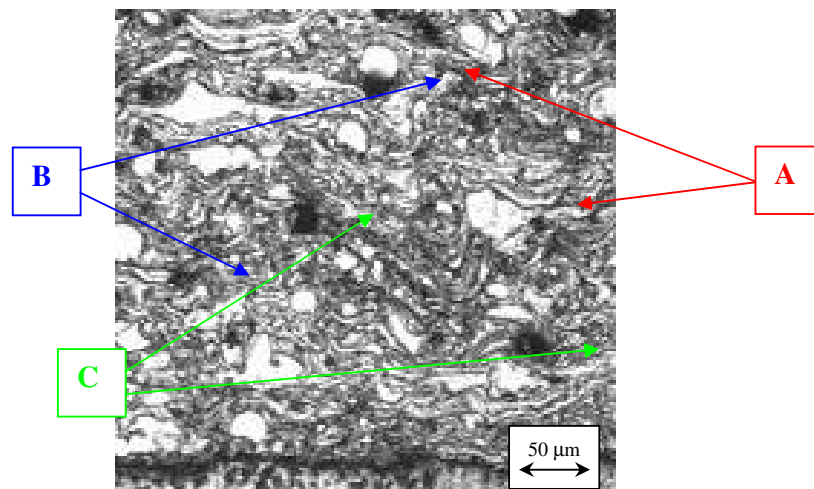
Fig. 38- Sample 122_5 microstructure (low spraying pressure)

127
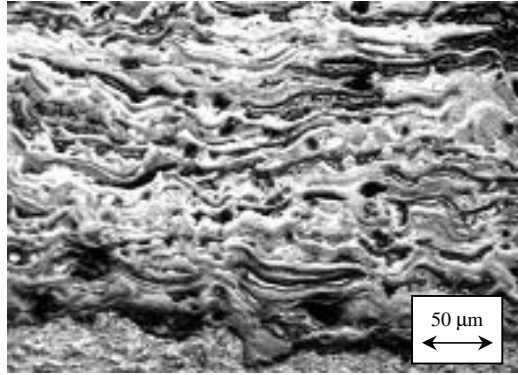
Fig. 39- Sample 122_3 microstructure (high N_2% in plasma gas)
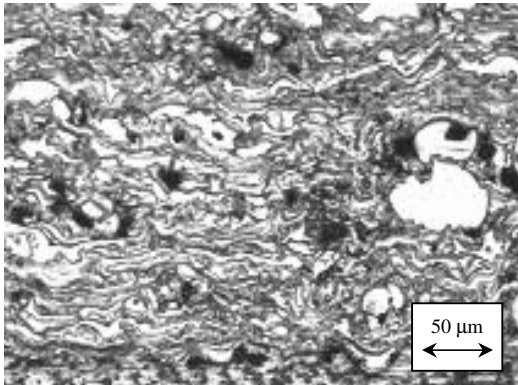
Fig. 40 - Sample 123_5 microstructure (low N_2% in plasma gas)
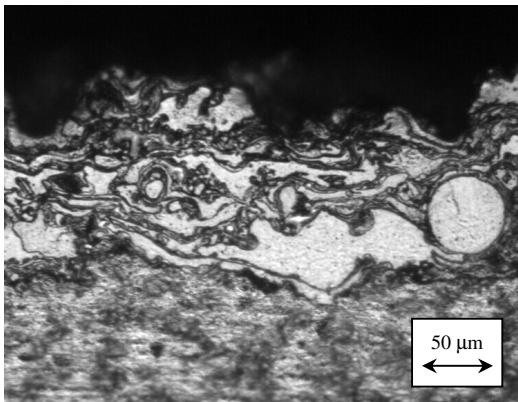
Fig. 41 - Sample 125_1 microstructure (sputtered coating)
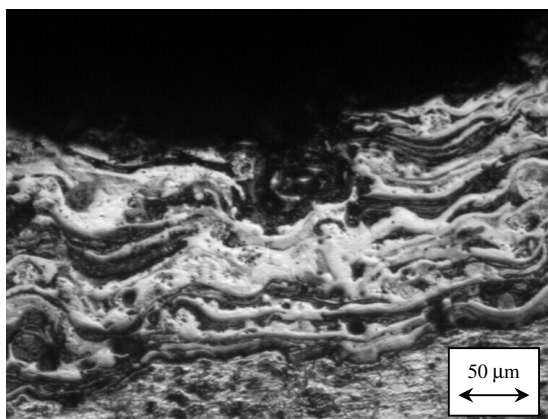
Fig. 42 - Sample 125_3 microstructure (sputtered coating)

Statistical analysis of DOE results led to the following equations, correlating the objective variables (XRD peak heights, porosity and hardness) to the independent ones (N_2 pressure, N_2 percentage in plasma gas, and substrate temperature). Equations with coded values allow a comparison among the different contributions of independent variables on the objective variables, while the equations with the actual factors are quantitative indications of the process parameters effects.

Final equations in terms of coded factors:

$$\alpha_{TiN,N} = 0.23 + 0.16 * \text{Pressure} - 0.11 * \text{Temperature} + 0.14 * N_2\% \text{ in plasma}$$

$$\alpha_{Ti2N,N} = 0.45 - 0.19 * \text{Temperature}$$

$$\alpha_{TOT,N} = 0.36 + 0.11 * \text{Pressure} - 0.16 * \text{Temperature} + 0.073 * N_2\% \text{ in plasma}$$

Hardness = 621.96 + 79.39 * Pressure + 104.60 * Temperature + 119.81 * N_2% in plasma + 91.02 * Pressure * N_2% in plasma

Porosity = 7.05 + 2.5 * Pressure - 2.37 * N_2% in plasma

Final equations in terms of actual factors:

$$\alpha_{TiN,N} = -0.068 + 2.952E\text{-}4 * \text{mbar} - 6.751E\text{-}4 * °C + 0.010 * N_2\% \text{ .}$$

$\alpha_{Ti2N,N} = 0.90 - 1.194E\text{-}3 * °C$

$\alpha_{TOT,N} = 0.38 + 2.151E\text{-}4 * mbar - 9.969E\text{-}4 * °C + 5.126E\text{-}3 * N_2\%.$

Hardness $= 320.49 + 0.14 * mbar + 0.65 * °C - 4.20 * N_2\% + 0.012 * mbar * N_2\%.$

Porosity $= 6.06 + 4.706E\text{-}3 * mbar - 0.17 * N_2\%.$

Only the combined effect (pressure X $N_2\%$) on coating hardness shows some statistical relevance. Other combined effects can be assumed not to be significant for the objective variables.

The DOE statistical analysis and the study of coatings microstructures led to the following observations:

- Nitride formation, coating hardness and particles melting are enhanced by increasing pressure in the spraying chamber. However, brittleness and porosity of the coatings tend to increase too, as illustrated in **Figures 37** and **38**, respectively.
- Particles melting is enhanced by increasing N_2 in the gaseous plasma. This is likely due to the higher enthalpy conferred by N_2 to the plasma, with respect to the contribution of Ar, as shown by **Figures 39** and **40**.
- Extent of nitriding increases by increasing nitrogen content in both spraying atmosphere and plasma gas mixture. This generally results in higher hardness of the coatings.
- The synthesis of TiN takes place mainly in the plasma stream while the nitriding in situ (that's on the substrate, enhanced by its temperature) promotes formation of the Ti_2N phase.

Regarding the samples sprayed with a negative substrate bias, it was found that:

- Sample 125-1 - sprayed at low (300 mbar) N_2 pressure and at low (250°C) substrate temperature - showed low (3.6%) porosity, but an inhomogeneous microstructure, with a large amount of unmelted particles, as illustrated in **Figure 41**; this resulted in low (450 HV) hardness.

- Sample 125-5 - sprayed at higher (1450 mbar) N_2 pressure and at higher (550°C) substrate temperature - showed a good microstructure with well melted lamellae, as illustrated in **Figure 42**. Hardness was the highest (1077 HV) among the sprayed samples.

The above results confirmed that the application of a transferred arc increases the quality of RPS coatings microstructure and their hardness, when the depositions are carried out at high percentages of N_2%, in both plasma gas and spraying chamber, and elevated substrate temperature.

Table 23 shows the characteristics of the optimised thermal spray coatings without transferred arc, identified as RPS1 and with transferred arc, identified as RPS2. DOE methodology led to coatings with good microstructure and high hardness (RPS1). Transferred arc mechanism showed its effectiveness in further increasing the nitriding effect and coating hardness (RPS2).

Tab. 23 - RPS1 and RPS2 coatings characteristics

Coating	Porosity (%)	N2 (wt. %)	Hardness ($HV_{300,20}$)
RPS1	5	8.5-9	1100
RPS2	3	11	1200

Figure 43 shows the microstructure of the RPS2 coating. The melting level of the lamellae and their cohesion are good. The residual porosity is visible. No cracks or macro-defects are evidenced.
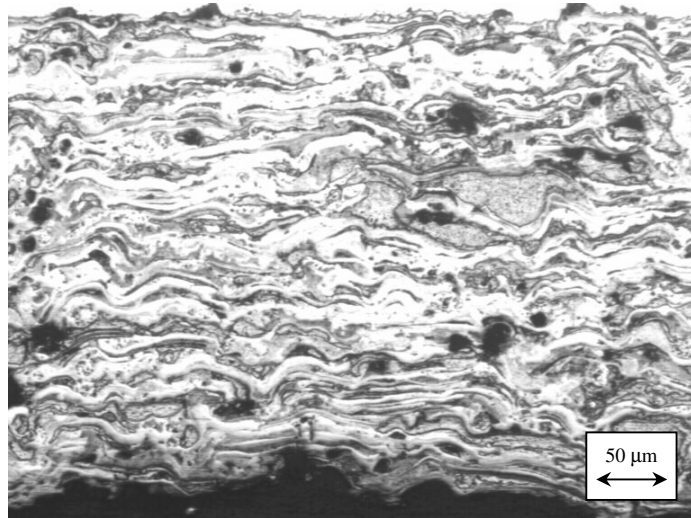
Fig. 43 – RPS2 microstructure

1.2 TiN by PVD-arc

The TiN PVD coating of interest in this investigation was designed for mechanical components made of titanium alloy such as Ti-6Al-4V or composite materials with a titanium matrix. Such components are generally coated after undergoing some kind of thermal treatment. The temperature of 500°C is usually considered as the upper limit to avoid over aging the components during the PVD deposition through the growth of ß precipitates. However, for three PVD batches - namely 4, 5, and 6, which had not been thermally treated - it was decided to increase the deposition temperature up to 520°C, since it was foreseen the possibility of carrying out the aging thermal treatment simultaneously with the TiN deposition.

Figures 44-52 are SEM micrographs showing the morphologies of broken TiN surfaces after soaking them in liquid nitrogen.
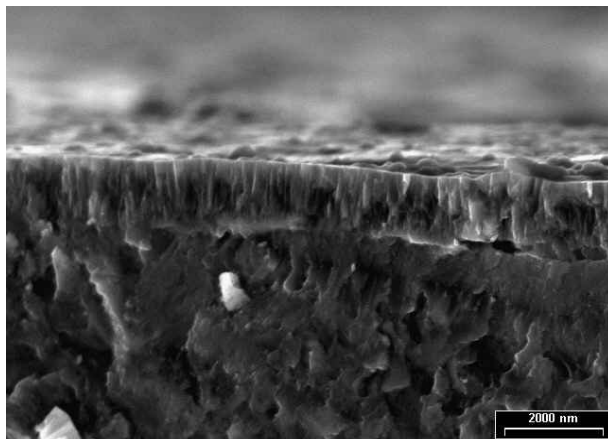
Fig. 44 – Fracture section of TiN coating (Sample 1)
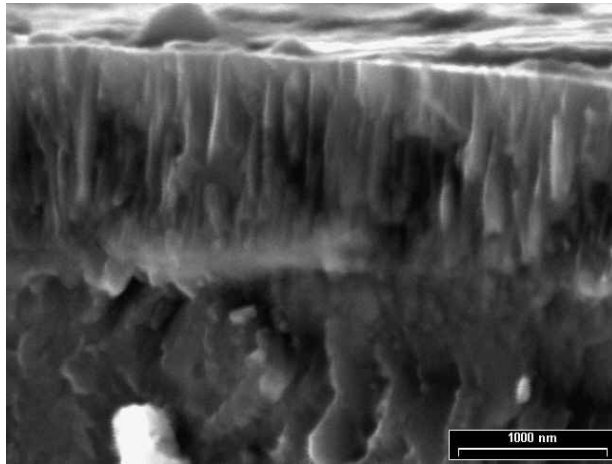
Fig. 45 – Fracture section of TiN coating (Sample 1)
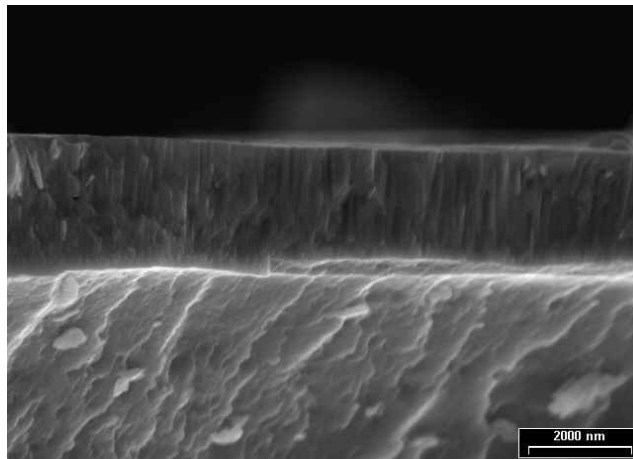
Fig. 46 – Fracture section of TiN coating (Sample 2)
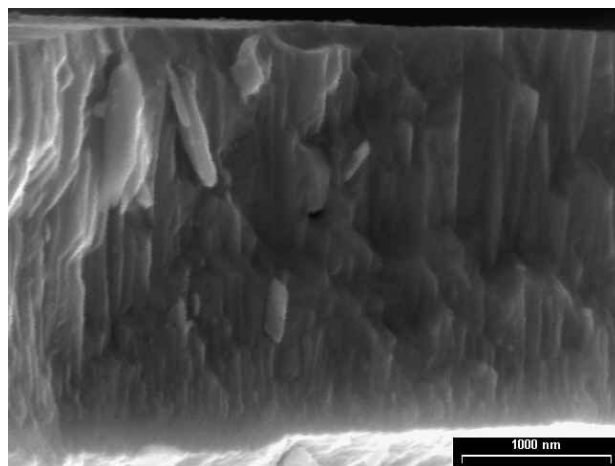
Fig. 47 – Fracture section of TiN coating (Sample 2)

133
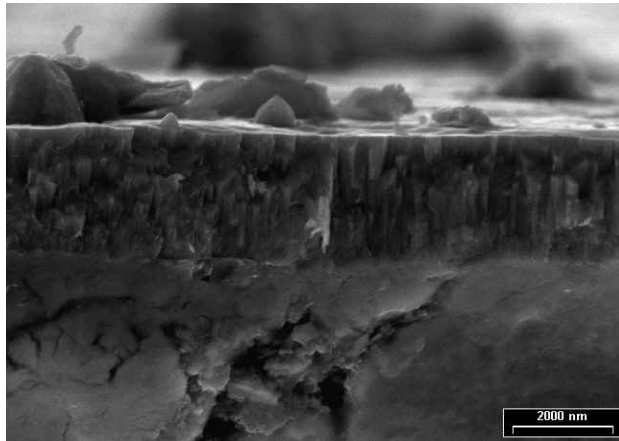
Fig. 48 – Fracture section of TiN coating (Sample 3)
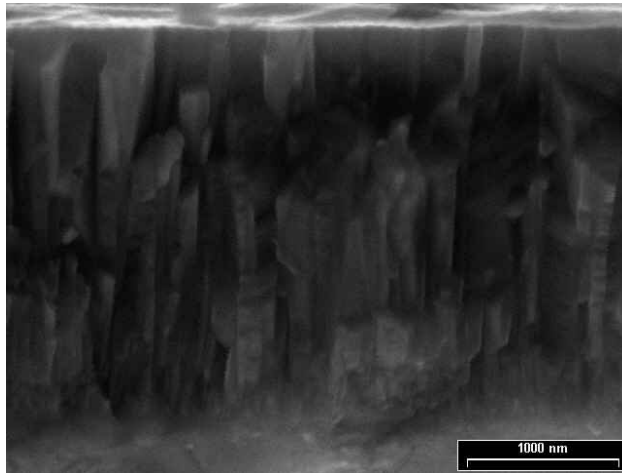
Fig. 49– Fracture section of TiN coating (Sample 3)
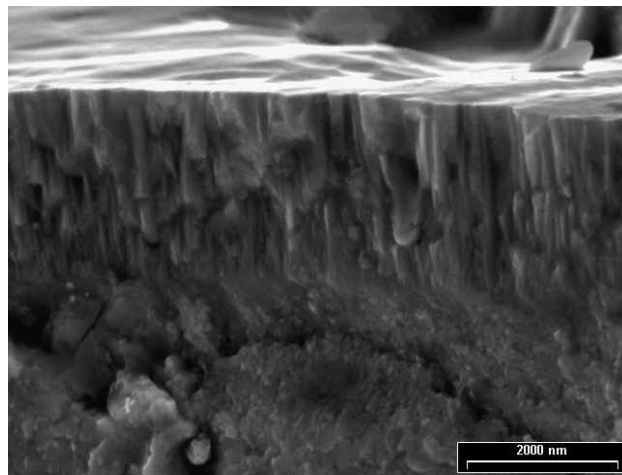
Fig. 50 – Fracture section of TiN coating (Sample 4)

134
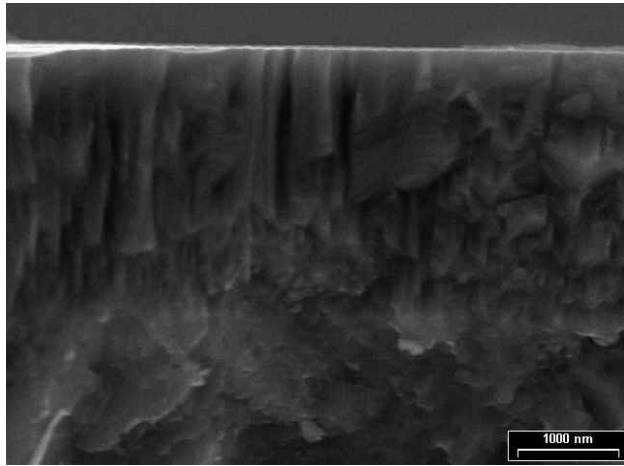
Fig. 51 – Fracture section of TiN coating (Sample 5)
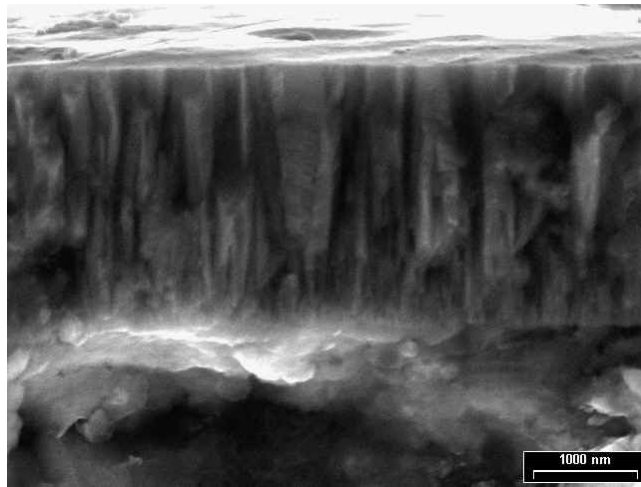
Fig. 52 – Fracture section of TiN coating (Sample 6)

It is possible to observe in these micrographs the columnar structure which is typical of the PVD-arc TiN coatings. All the samples present an outermost layer with a thickness of about 0.5 µm where crystallites have smaller dimensions. Such a layer seems to be thicker in those coatings deposited while utilising a higher bias. In fact, the bias prevents the phenomenon, typical of PVD processes, of crystallites growing again. Thickness values of TiN coatings, measured by SEM, are reported in **Table 24.**

Tab. 24 - Thickness values of TiN coatings determined by SEM

Sample	Thickness (µm)
1	1.8
2	2.4
3	2.5
4	2.5
5	3.2
6	2.7

Hardness values of TiN coatings determined at 300 and 500 g loads are listed in **Tables 25** and **26**, respectively. These tables report hardness values measured by indentation test as well hardness values calculated by utilising the Lesage model. Due to the exiguity of TiN coatings thickness (2-3 µm) their hardness measurement is affected by the substrate hardness and its value changes as a function of the applied load. In particular, in the situation of a coating being harder than the substrate, the coating measured hardness obviously decreases by increasing the applied load. For this reason, hardness of the TiN coatings was calculated utilising the Lesage model, since it allows to derive the absolute hardness value in any case even when high loads lead to substrate deformation.

Tab. 25 – Measured and calculated hardness values for TiN coatings on RPS substrates. Load: 300g

Sample	Measured Hardness		Absolute TiN Hardness	
	kg/mm^2	MPa	kg/mm^2	MPa
1	1022	10016	3297	32309
2	1051	10300	2901	28425
3	924	9055	2053	20122
4	1068	10466	2960	29005
5	1126	11035	2810	27542
6	1097	10751	2947	28878

Tab. 26 - Measured and calculated hardness values for TiN coatings on RPS substrates. Load: 500g

Sample	Measured Hardness		Absolute TiN Hardness	
	kg/mm^2	MPa	kg/mm^2	MPa
1	964	9447	3332	32654
2	971	9516	2753	26985
3	873	8555	1894	18566
4	1032	10114	3243	31785
5	1066	10447	2984	29244
6	1030	10094	3070	30095

It can be seen that for the 6 samples examined the average variation of the calculated (absolute) hardness corresponding to a load increase from 300 to 500 g is around 5.6 % with a maximum variation of 9.5 % only, confirming the validity of the Lesage method. Therefore, it seemed acceptable to estimate the TiN coating absolute hardness final value by averaging the calculated hardness values reported in both **Tables 25** and **26**. The results are synthesised in **Table 27** and **Figure 53**, which consists of a bar graph comparing absolute hardness's between RPS and RPS+TiN.

Tab. 27– Absolute hardness value of TiN coatings

Sample	Hardness (MPa)
1	32482
2	27705
3	19344
4	30395
5	28393
6	29487
RPS	7624

	1	2	3	4	5	6
□ RPS	7624	7624	7624	7624	7624	7624
■ RPS+TiN	32482	27705	19344	30395	28393	29487
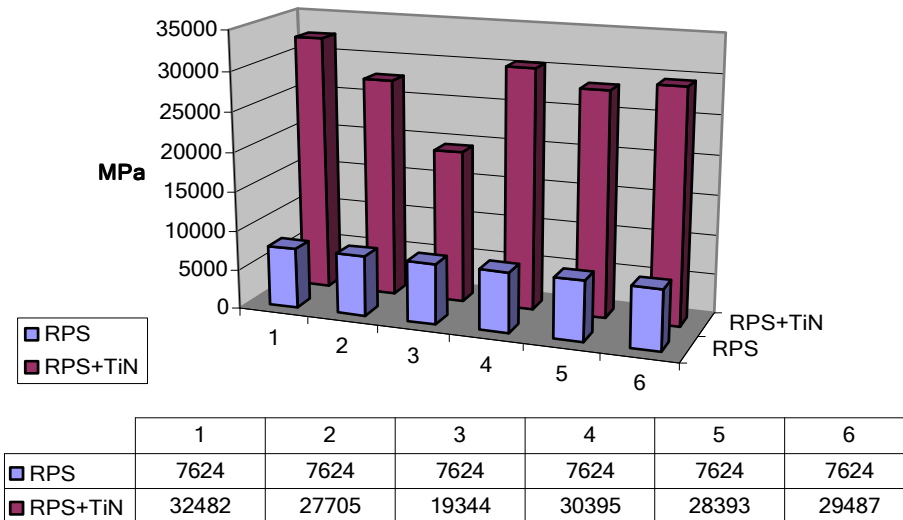
Fig. 53 - Comparison of absolute hardness between RPS and RPS+TiN

1.3 (Ti/TiN RPS +TiN PVD-arc) coating

The development of the multilayer coating was centred on the optimization of the thin TiN coating deposition by PVD-arc technology on the thick RPS substrate consisting of a TiN dispersion within a Ti matrix. A critical feature of a multilayered coating is the TiN adhesion to the Ti/TiN substrate, depending heavily on the morphology and composition of the latter. First experimental results evidenced an unusual phenomenon, consisting in the TiN-PVD film seeming to rapidly fill the surface porosity of the Ti/TiN-RPS coating. This encouraged to study more deeply the nucleation and growth of the TiN films on the thermal sprayed substrate.

To facilitate the analysis, the main steps of the TiN-PVD-arc production process are below reported.

1. Argon flux at 3×10^5 Pa for 5 s.
2. Ultrasonic cleaning with acetone or trichloroethane for 120 s.
3. Three sequential glow discharges with argon, each one for 2 minutes, with negative substrate biases of 450, 550, and 650 V, respectively; at a chamber pressure of 2 Pa.
4. Metal ion bombardment (MIB) with titanium ions in argon at a constant negative substrate bias of 700 V for 1 min, with 55 A sources and at a chamber pressure of 3 Pa.
5. MIB with titanium ions in argon at a decreasing negative substrate bias from 700 to 100 V for 1.5 minutes, with 50 A sources and at a chamber pressure of 0.8 Pa.

6. Titanium flash deposition for 0.6 minutes with a substrate bias of 100 V, with 50 A sources and at a chamber pressure of 0.8 Pa.

7. MIB with titanium ions in nitrogen at a decreasing negative substrate bias from 500 to 135 V for 1 min, with 50 A sources and at a chamber pressure of 1.5 Pa.

8. TiN deposition for 4 hours with a constant negative substrate bias of 135 V, 50 A sources, and at a chamber pressure of 1.5 Pa.

SEM, OM observations and the results of GDOES, XRD and XPS analyses did not show any appreciable differences between RPS samples ultrasonically cleaned with either one of the two solvents, i.e. acetone or trichloroethane.

Figure 54 shows a typical polished surface of an RPS coating, after Ar flux and ultrasonic cleaning. The residual porosity of such a coating was around 3% with an average hardness of about 7.6 GPa.
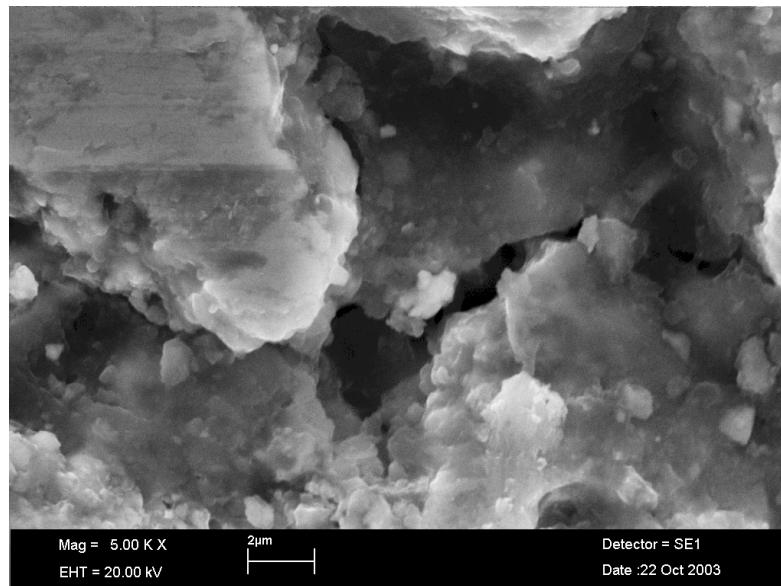
Fig. 54 – SEM micrograph of a typical RPS coating polished surface, after Ar flux and ultrasonic cleaning (production process step 2)

Figures 55-58 show representative surfaces of RPS coatings after glow discharge in Ar, metal ion bombardment in Ar, and Ti flash deposition step, respectively, in each case compared with the surface after the initial solvent cleaning. **Figure 59** shows an RPS surface after the initial solvent cleaning and after the metal ion bombardment in N_2 deposition step.

139
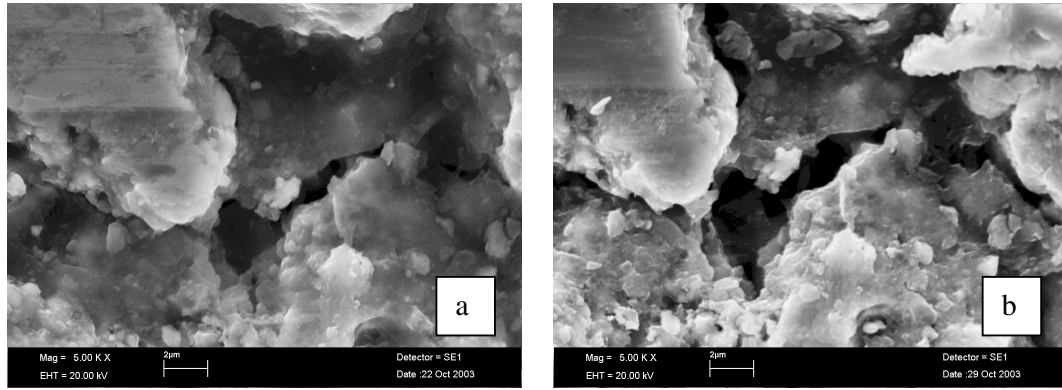
Fig. 55 – SEM micrograph of an RPS coating, after (a) solvent ultrasonic cleaning and (b) three sequential glow discharges with argon (production process step 3)
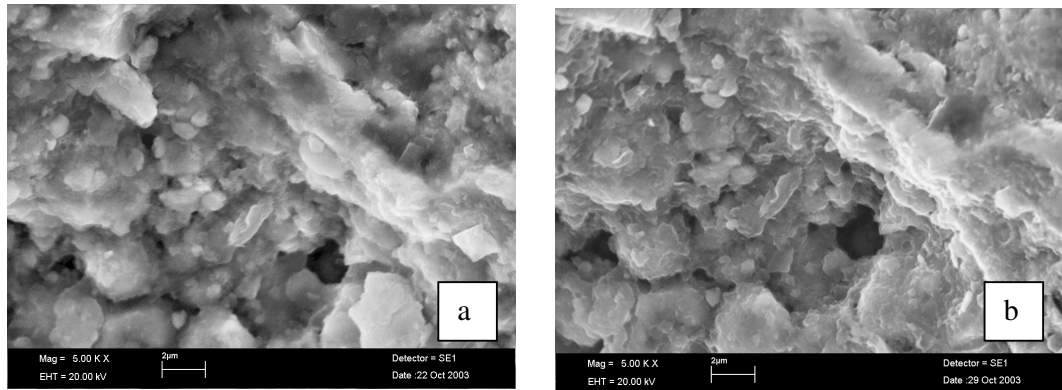
Fig. 56 – SEM micrograph of an RPS coating, after (a) solvent ultrasonic cleaning and (b) metal ion bombardment in Ar (production process step 4)
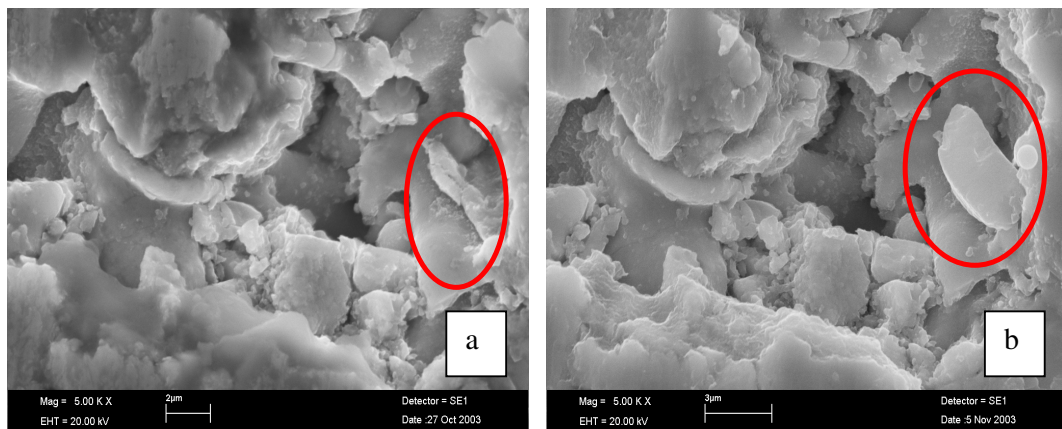
Fig. 57 – SEM micrograph of an RPS coating, (a) after solvent ultrasonic cleaning and (b) Ti flash (production process step 6)
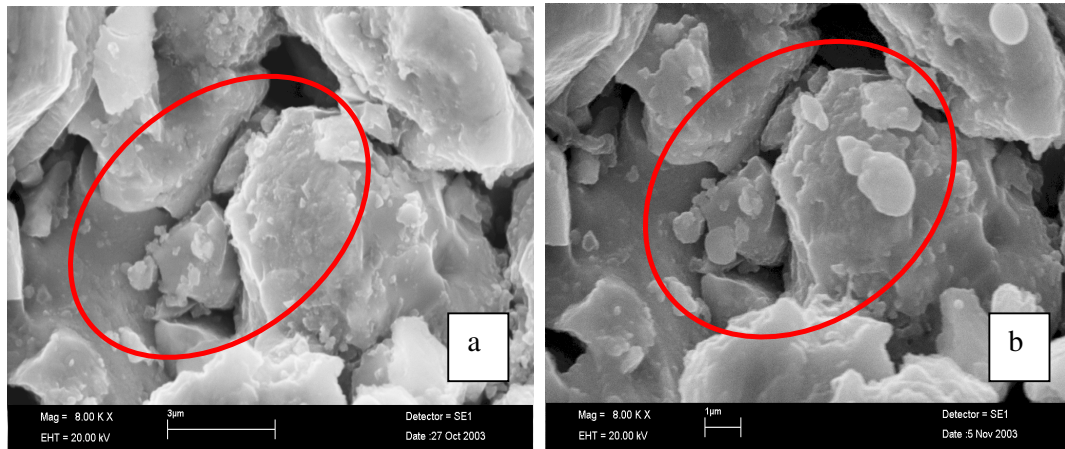
Fig. 58 –SEM micrograph of an RPS coating, after (a) solvent ultrasonic cleaning, and (b) metal ion bombardment in N_2 (production process step 7)

A comparison of these micrographs suggests that the formation of new species, responsible for the filling of the surface voids on the RPS coatings, initiated during the Ti flash deposition (**Figure 57**) and the bombardment with titanium ions in nitrogen (**Figure 58**) steps. **Figures 59** and **60** show a typical RPS surface after a partial (10 minutes) TiN deposition and a cross section of the completed graded system, respectively. Apparently, the filling of the pores went on very quickly during the PVD-arc process.
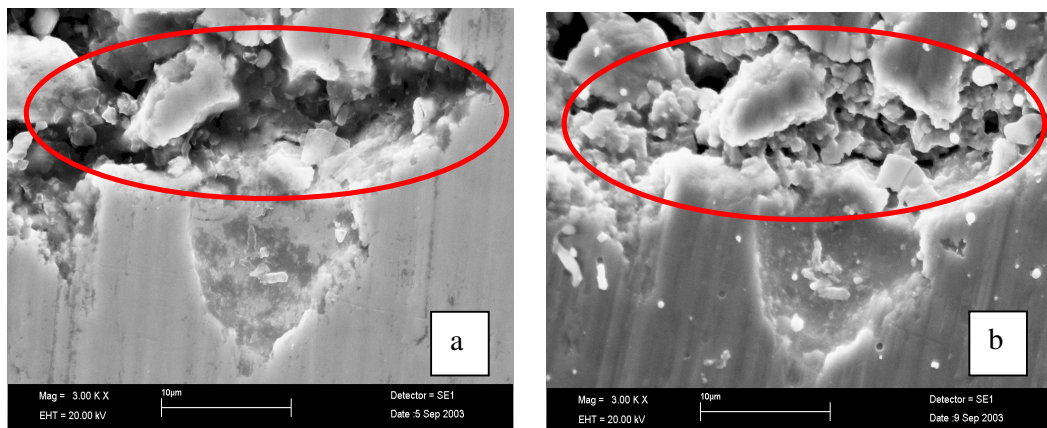
Fig. 59 – SEM micrograph of an RPS coating, (a) after solvent ultrasonic cleaning and (b) after 10 min of TiN deposition
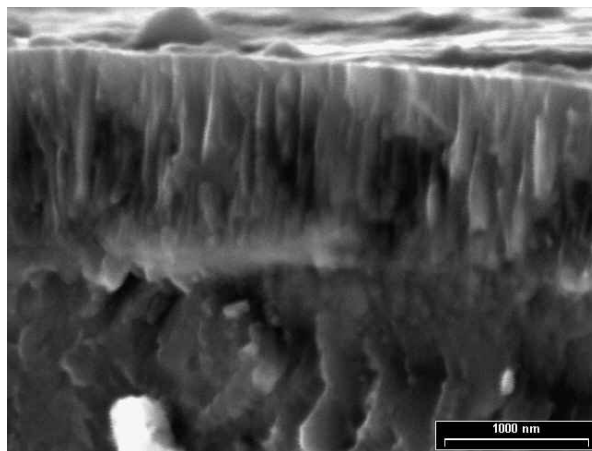
Fig. 60 – SEM micrograph of an RPS coating cross section after 4 h of TiN deposition

XRD analyses (Cu-K$_\alpha$ radiation) confirmed that titanium nitride phases, with different stoichiometries, were present in all thick RPS coatings: TiN and Ti$_2$N were predominant, while the amount of TiN$_{1-x}$ was negligible in all the cases.

The same analysis after the PVD deposition showed the presence of stoichiometric TiN only, exhibiting a (111) preferred orientation.

The GDOES results indicated that the weight percentage of nitrogen in the RPS coatings ranged between 5 and 6%.

The presence of titanium and nitrogen in the RPS coatings, in the as-received condition, was confirmed by the XPS analysis. In addition, XPS showed significant amounts of carbon species contaminants in the form of hydrocarbons (C-C) and carbonyl (C=O) bearing compounds. Moreover some C-N species were also detected, likely due to the reaction between nitrogen and carbon (as a contaminant), during the RPS process.

A typical XPS C$_{1s}$ spectrum of an RPS coating surface in the as-received condition, showing the different carbon bondings, is given in **Figure 61**.
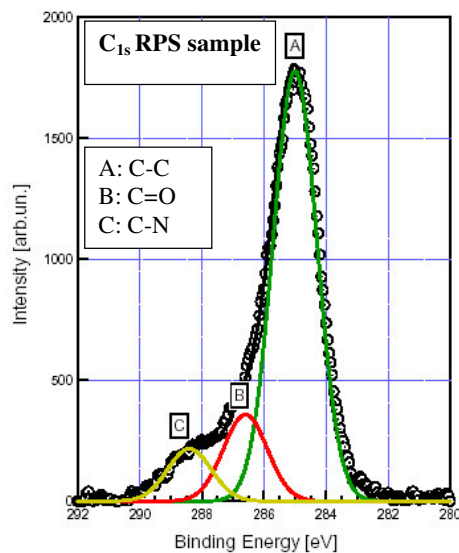
Fig. 61 - XPS C_{1s} spectrum of a typical RPS coating polished surface

In contrast, the typical surface of an RPS coating, after the three sequential glow discharges in Ar (step 3 of the production process) is shown in **Figure 62**. It can be observed, by comparing with **Figure 61**, a drastic reduction of the peak corresponding to the hydrocarbon species which, apparently, were in part converted into three types (3 peaks) of oxygenated species. The CN bond was no longer detected; likely because it was masked by the residual hydrocarbons and the newly formed oxygenated species in the outermost layer.
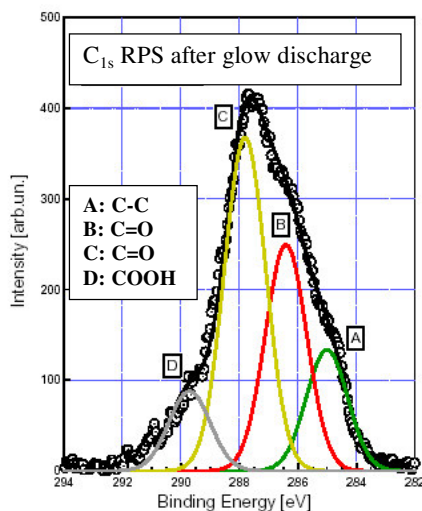
Fig. 62 – XPS C_{1s} spectrum of a typical RPS sample after three sequential glow discharge (production process step 3)

Nitride phases, including the CN species, were detected in the RPS samples after the metal ion bombardment in N_2 (step 7 of production process), as shown in the XPS C_{1s} and N_{1s} spectra, given in **Figures 63** and **64**, respectively.
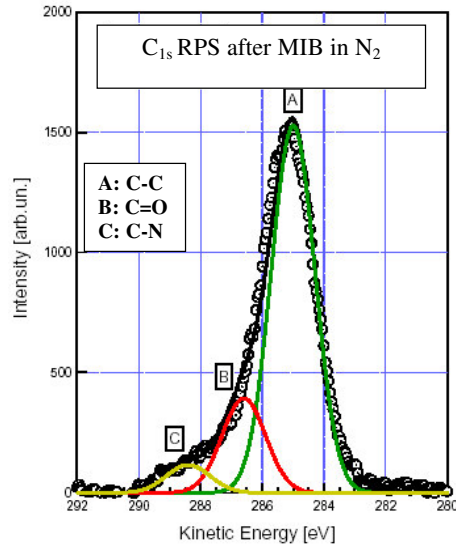
Fig. 63 – XPS C_{1s} spectrum of a typical RPS sample after metal ion bombardment in N_2 (production process step 7)
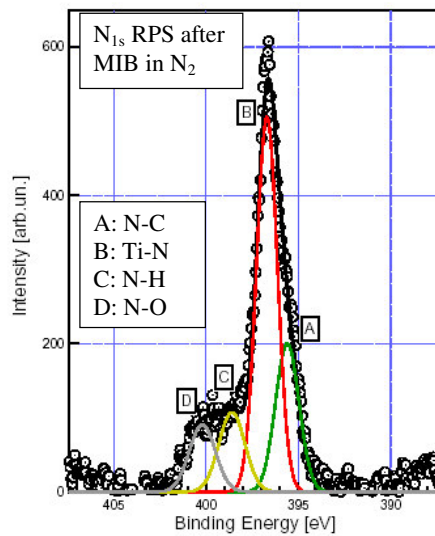
Fig. 64 – XPS N_{1s} spectrum of a typical RPS sample after metal ion bombardment in N_2 (production process step 7)

The average hardness values of the RPS coating and whole coating system samples were 7.6 and 10.1 GPa, respectively. A large scatter, in the order of 15%, among

144

hardness measurements was observed. Likely it was due to the extensive porosity, presence of unmelted particles, and variation in the nitriding level. The absolute hardness value of the TiN top layer, calculated by the Lasage's equation, was about 29.5 GPa.

In the typical surface of a lapped RPS substrate it is possible to observe the lack of uniformity: presence of nitrides, unmelted areas, melted but nitride free areas, pores. It is clear that the adhesion of TiN cannot be the same on the whole surface of the RPS substrate, but it will change drastically according to the different compositions and morphologies of the various zones. For example, it is expected that adhesion to a nitride containing area would be higher than to a nitride free area. Therefore, to assess adhesion it is recommended to consider the weakest possible one, according to composition and morphology of the substrate surface. For this reason, it becomes important the diamond indenter, during the scratch test on such non uniform substrate, to cross those zones which give lower adhesion. Thus, the test parameters were varied in such a way to lower the load application rate. Regulating the indenter speed at 30 mm/min and the loading rate at 60 N/min, it was possible to go from the standard 10 N/mm used for conventional substrates to 2 N/mm. Such a modification allowed to obtain results with lower spread, keeping the same confidence level of 95%. 10 tests carried out on sample n° 6 using the conventional 10mm/min and 100 N/min parameters gave the following results:

- Middle adhesion   =   28.12 N
- Maximum adhesion   =   36.80 N
- Minimum adhesion   =   16.00 N
- Confidence interval ($\alpha = 0.05$) =   4.6

On the contrary, using the 30 mm/min and 60 N/min standard parameters, the following results, after 10 tests on the same sample n° 6, were obtained:

- Middle adhesion   =   22.6 N
- Maximum adhesion   =   24.8 N
- Minimum adhesion   =   20.8 N
- Confidence interval ($\alpha = 0.05$) =   1.3

The results of TiN adhesion to RPS for the six coating samples are listed in **Table 28**.

Tab. 28 –Adhesion of TiN coatings on RPS substrates expressed as critical loads in the scratch test

Sample	Middle adhesion (N)	Confidence interval with $\alpha = 0.05$	Maximum adhesion (N)	Minimum adhesion (N)
1	18.6	1.2	20.4	17.2
2	17.9	2.3	22.4	16.0
3	17.4	0.8	18.8	16.4
4	19.2	1.2	22.4	19.2
5	17.6	0.8	20.0	17.6
6	20.8	1.3	24.8	20.8

Differences among samples didn't seem to be significant, except for sample n° 6 which showed the best performance. Optical microscopy observation of the tracks indicated brittle types of delaminations, since the delaminated zones remained confined to the tracks.

Let's consider a three-dimensional plot of temperature, bias and experimental result. This last one might be, for example, the hardness or the adhesion value measured and so on. It can be sought a curve, described by an equation, having temperature and bias as variables, that nears the experimental points of the tridimensional plot. Utilising a statistical approach known as the method of least squares, it is possible for a given parametric function to determine the parameters that best allow the curve to regress the experimental points. Using a mathematical statistics program such regression curves were sought for the experimental results of hardness, absolute hardness, thickness and scratch test relative to the TiN coating on the RPS substrate.

The curve that mostly neared the experimental points is described by the following type of function:

$$F(\mathbf{x,y}) = a\mathbf{x}^2 + b\mathbf{y}^2 + c\mathbf{x} + d\mathbf{y} + e\mathbf{xy} + f$$

realizing that temperature and bias are equal to **x** and **y**, respectively. By the least squares method, a, b, c, d, e, and f were found.

The curves relative to absolute hardness and thickness of TiN are shown as examples in **Figures 65** and **66**, respectively. In each case, it is shown also the relative regression function. R is a statistical parameter which is indicative of the regression quality; at the most it can be equal to 1, in case the curve includes the experimental points.
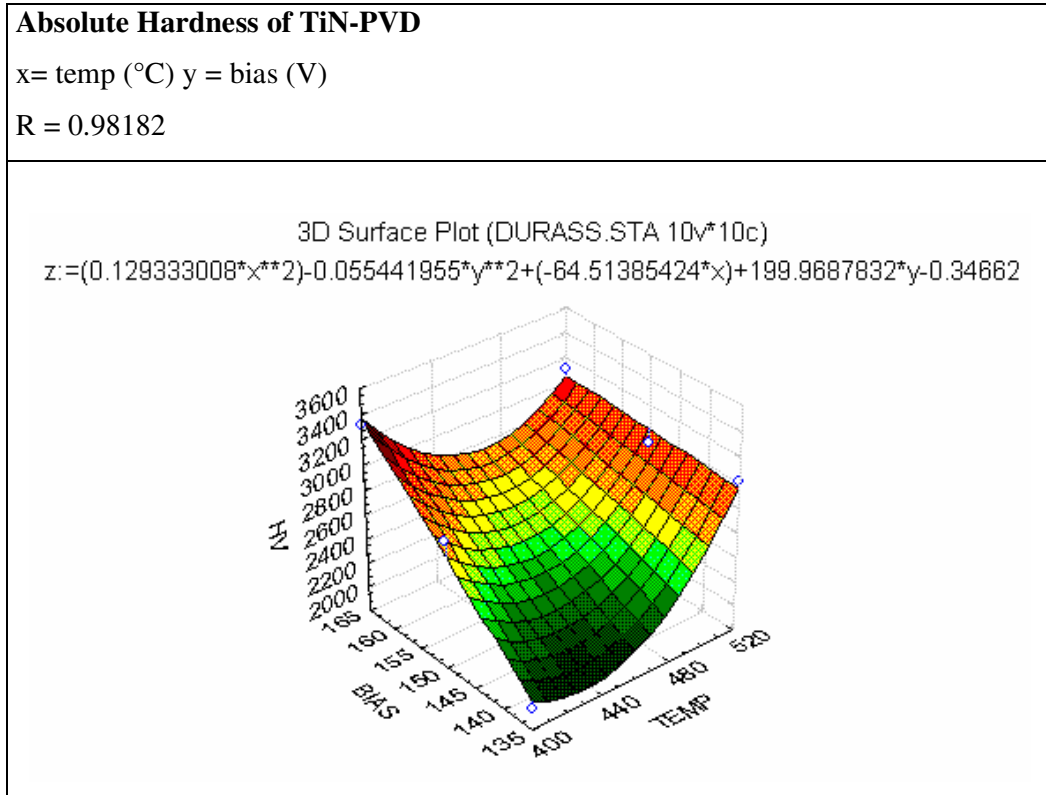

Absolute Hardness of TiN-PVD

x= temp (°C) y = bias (V)

R = 0.98182

3D Surface Plot (DURASS.STA 10v*10c)
z:=(0.129333008*x**2)-0.055441955*y**2+(-64.51385424*x)+199.9687832*y-0.34662

Fig. 65 – 3D Surface plot Hardness = f(bias, temp)

Thickness of TiN-PVD
$X = \text{temp} (°C)$ $y = \text{bias} (V)$
$R = 0.98704$

3D Surface Plot (SPESSORI.STA 10v*10c)

$$z := (-0.000508973 * x^{**}2) - 0.001966667 * y^{**}2 + (0.453227526 * x) + 0.515444489 * y + 0.00013$$
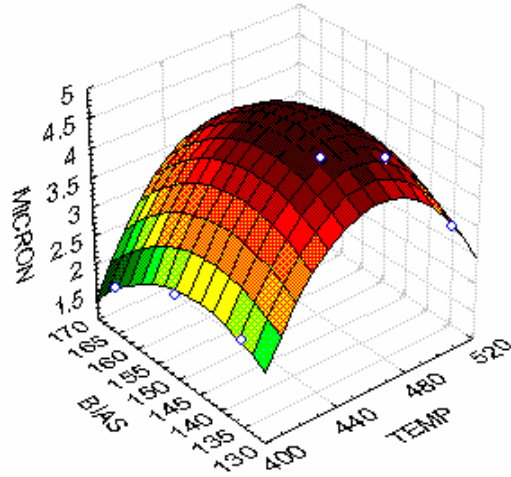
Fig. 66 – 3D Surface plot Thickness = f(bias, temp)

The expected maxima for hardness, adhesion, and thickness of the TiN coating, calculated by the regression curves, are reported in **Table 29**. Each maximum was sought in the ranges of bias between 135 V and 165 V and temperature between 400°C and 520 °C.

Tab. 29 – Expected maxima calculated from regression curves

Coating property	Expected maximum	Bias (V)	Temperature (°C)
TiN hardness (MPa)	33700	165	400
TiN adhesion on RPS (scratch test critical load)	23.1	135	470
TiN thickness (μm)	4.7	146	465

By the analysis relative to the thickness of the TiN coatings, it was observed that the deposition rate reached a maximum corresponding to a certain bias, beyond which the deposition rate started to decrease. During deposition, a higher bias generally leads to an increase of the ions energy towards the growing coating; however, an excessive increase of the bias is detrimental since it causes abnormal (too high) sputtering phenomena.

By the regression curves it was observed that the TiN highest absolute hardness value was obtained at a temperature of 400°C and a negative bias of 165 V. However, taking into account that to such a coating did not correspond the highest thickness, it could be explained why the measured hardness – which was affected by the thickness of the coating and substrate hardness – showed a maximum at a temperature of 520°C and a bias of 147 V.

A very important piece of information is represented by the maximum value of the coating adhesion calculated from the regression curves. Such a maximum, in fact, corresponds to a bias of 135 V. If it is considered that, at least at lower temperatures, a bias increase leads to an increase of the TiN absolute hardness, it is legitimate to conclude that an excessive bias increase (that's a higher intensity of ions bombardment) rises the residual stress within the PVD coating. In other words, this confirms again that: the higher the bias, the higher the coating hardness; however, an excessive increase of the bias leads to a decrease of the coating adhesion.

The samples for the final tribological characterization were realized by utilising the optimized process parameters of both the RPS Ti/TiN coating and the PVD-arc TiN. Such parameters, for sake of clarity are reported again in **Table 30**.

Tab. 30 – Optimized process parameters for the deposition of the graded coating

RPS parameters (Ti/TiN)		PVD parameters (TiN)*	
Deposition temperature (°C)	390-470	BIAS (V)	135
Pressure inside deposition chamber (Pa x 10^2)	1180	Deposition temperature (°C)	450
Torch distance from substrate (mm)	120		
Plasma gas 1, Ar (slpm)	20		
Plasma gas 2, N_2 (slpm)	31		
Power of plasma generating DC arc (kW)	20-28		
Substrate negative bias, crossing current (A)	15		

*For the complete deposition procedure, comprehensive of the cleaning steps, see pag. 130

2. Tribological testing

2.1 Ti6Al4V alloy

Wear rate (expressed in terms of volume of material removed in a unit distance of sliding) plotted versus applied load is shown in **Figure 67**.
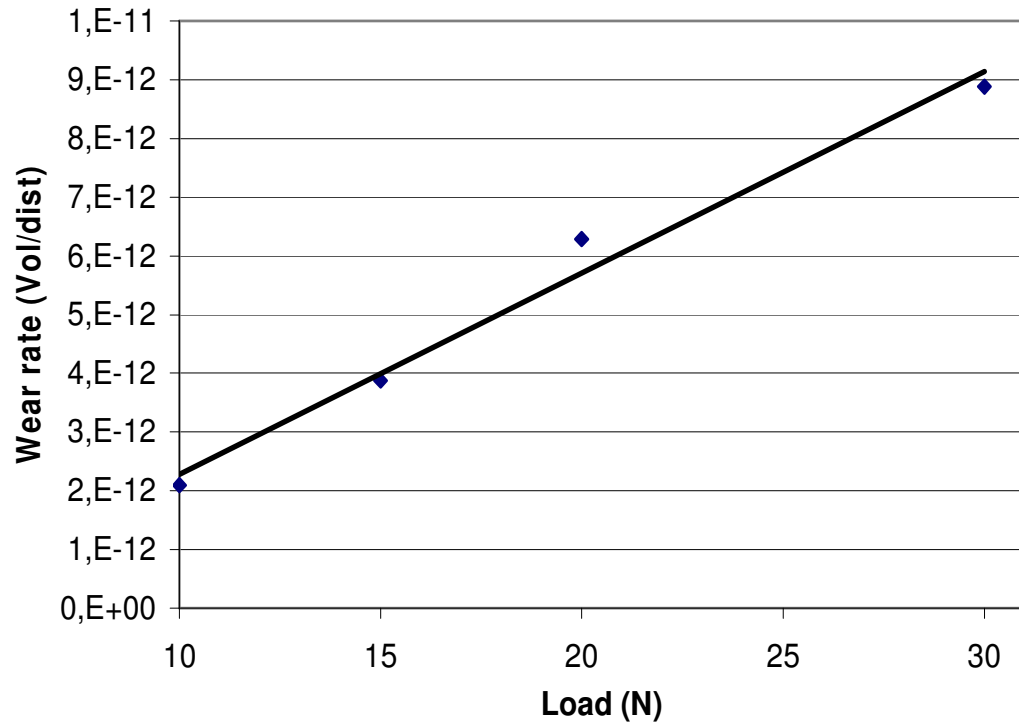
Fig. 67 – Wear rate (V/d) vs. applied load

The linearity of wear rate increasing with load, indicates that wear behaviour can be described by the Archard formula:

$$V(t) = K \times A_r \times d(t)$$

where:

V(t) = volume of material removed

D(t) = distance of sliding at the time t

A_r = real area of contact between the two sliding parts

K = wear coefficient

The real area of contact, A_r, was calculated by the formula $A_r = \dfrac{W}{P}$ where W is the applied load and P is the penetration hardness of the softer material which corresponds also to the largest compressive stress that a junctions region can take without plastic yielding. P depends on the type of relative motion and it was derived by the following formula:

$$P = \frac{P_0}{\sqrt{1 + 3f^2}}$$

where P_0 is the maximum pressure under static conditions, near the yield point (for Ti6Al4V alloy P_0 = 795 MPa) and f is the average friction coefficient which was measured during the pin on disk tests.

Table 31 lists the results of average friction coefficients and weight losses, measured during the pin on disk tests run at a constant speed and variable load. It includes also the values of real areas of contact (calculated by the formula above reported) and of the V/d ratios ("wear rates").

Tab. 31 – Results of pin on disk tests run at a constant speed of 2m/s and various loads for a total sliding distance of 3500 m

LOAD (N)	AVERAGE FRICTION COEFFICIENT	REAL AREA OF CONTACT (m^2)	WEIGHT LOSS (g)	WEAR RATE (V/d) (m^2)
10	1.130	3.28 E-08	3.28 E-02	2.09 E-12
15	0.765	3.13 E-08	6.08 E-02	3.87 E-12
20	0.597	3.62 E-08	9.87 E-02	6.29 E-12
30	0.374	4.50 E-08	1.39 E-01	8.88 E-12

Table 32 lists the results of average friction coefficients and weight losses measured during pin on disk tests run at a constant load and variable sliding speed. Are also included corresponding values of real contact areas and wear rates, calculated by the Archard formula.

Tab. 32– Results of pin on disk tests run at a constant load of 15 N and various sliding speeds for a total sliding distance of 3500 m

SLIDING SPEED (m/s)	AVERAGE FRICTION COEFFICIENT	REAL AREA OF CONTACT (m²)	WEIGHT LOSS (g)	WEAR RATE (V/d) (m²)
2	0.765	3.13 E-08	6.08 E-02	3.87 E-12
1.5	0.770	3.13 E-08	4.26 E-02	2.71 E-12
1	0.860	3.13 E-08	2.83 E-02	1.80 E-12
0.8	0.802	3.13 E-08	4.82 E-02	3.05 E-12
0.4	0.730	3.13 E-08	9.67 E-02	6.13 E-12

Figure 68 shows that the wear decreased by increasing the sliding speed from 0.2 to about 1.1 m/s. The wear rate then increased from a minimum at 1.1 m/s up to a relative maximum at 2 m/s.

Such a behaviour of the wear rate might be due to physical and chemical changes of the sliding surfaces. In fact, at different sliding speeds, friction will fluctuate according to the junction population changes. Sliding speed is also correlated with surface temperature of the materials and it promotes the interactions between sliding materials as well as between them and environment.

Regarding the initial portion of the curve, the increase of speed and, as a consequence, temperature might have favoured the arising of oxidation phenomena which were able to protect the sliding surfaces. The change in the curve slope may be due to a breakdown of the surface oxides, contributing to abrasive wear phenomena.

r
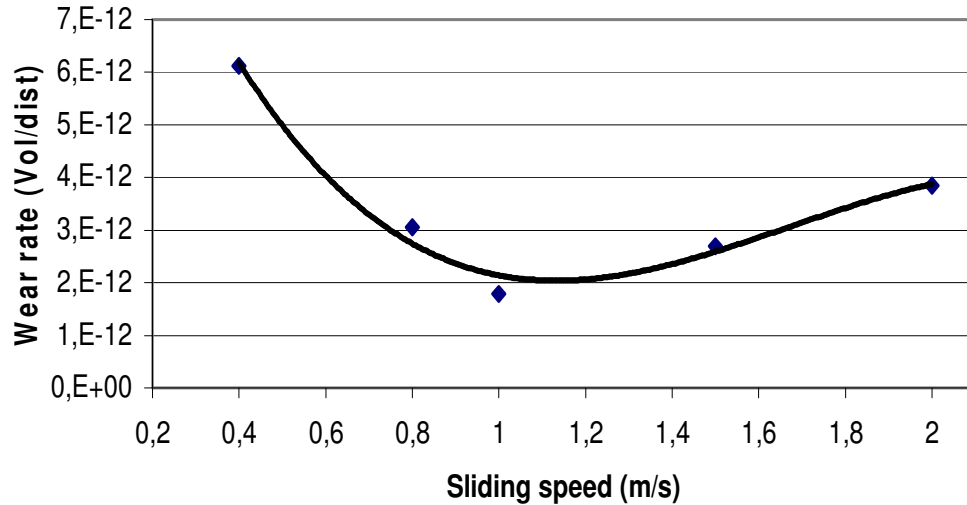
Fig. 68 – Wear rate vs. sliding speed

The test results were manipulated by interpolating them, utilising a devoted software in order to derive a 3-dimensional equation representing weight loss as a function of both load and sliding speed. The results of interpolation are illustrated in **Figure 69**, showing the 3-D area of the weight loss pattern as a function of applied load and sliding speed.

Intepolation: weight loss = f(load, sliding speed)

Interpolazione Perdita peso- Vel. Strisciamento- Carico applicato
Equazione: $z=a+bx+cy+dx^2+ey^2+fxy+gx^3+hy^3+ixy^2+jx^2y$

a=0.2155692 b=-0.012076032 c=-0.2815177 d=0.0010490957 e=0.2013996
f=-0.0059345784 g=-1.6136615e-05 h=-0.052260978 i=0.0040774955 j=-9.9965622e-05
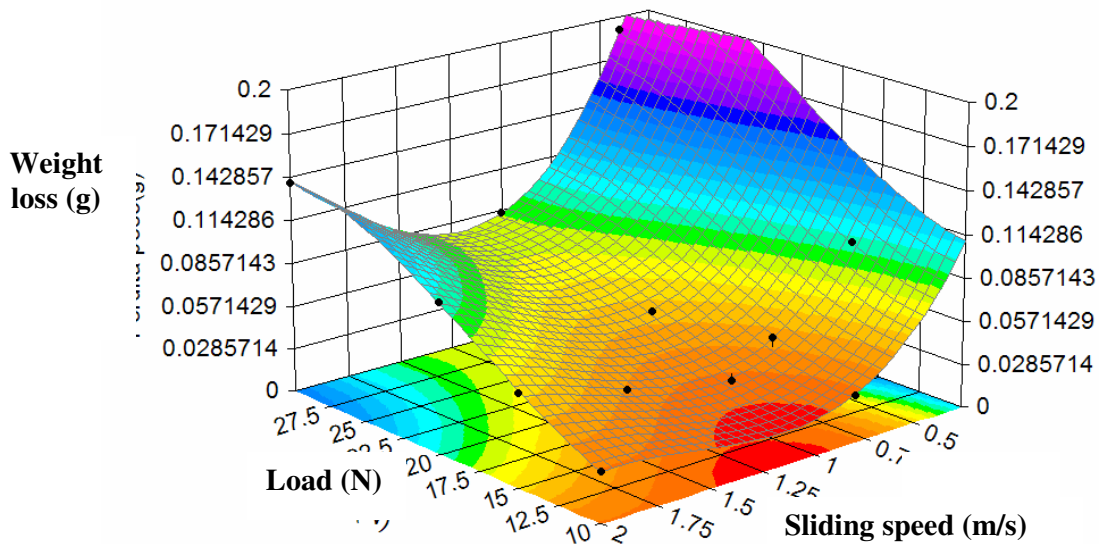
Fig. 69 - Equation and 3-D surface: weight loss = f(load, sliding speed)

153

Figure 70 plots weight loss as a function of sliding speed at different values of load as it was derived by the interpolating equation.
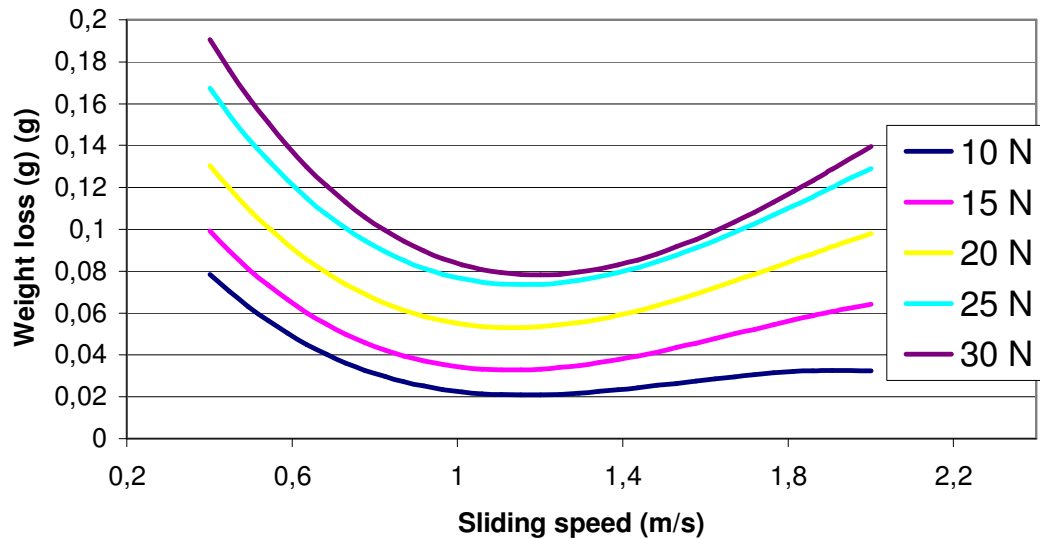
Fig. 70 – Weight loss vs. sliding speed with load as parameter

The behaviour of friction coefficient, as a function of the applied load (at constant sliding speed equal to 2 m/s) and sliding speed (at constant load equal to 15 N), is illustrated in **Figures 71** and **72**, respectively.
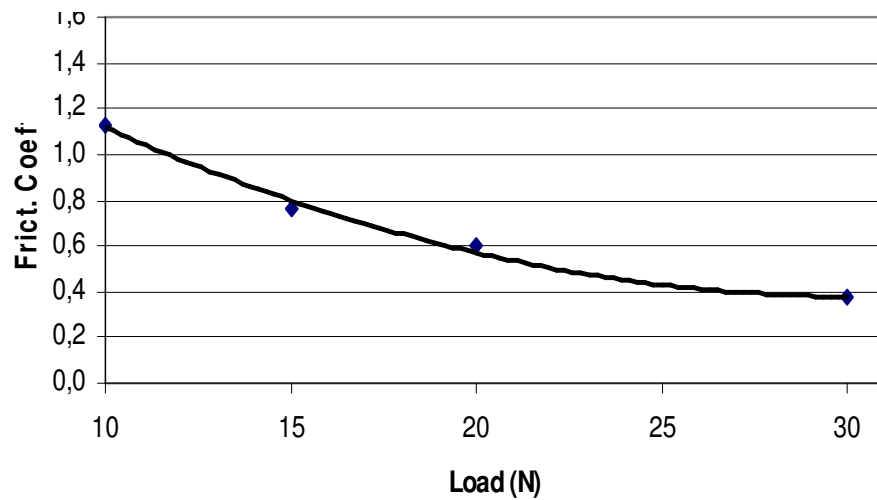
Fig. 71– Friction coefficient vs. load (sliding speed = 2 m/s)
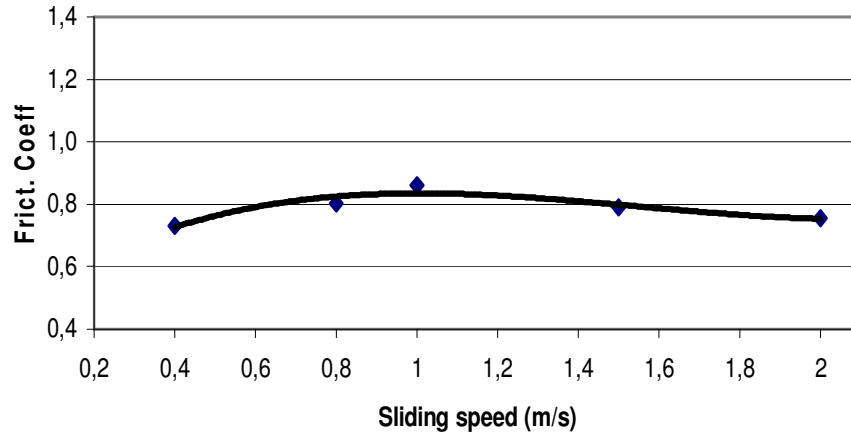
Fig. 72 – Friction coefficient vs. sliding speed (load = 15 N)

Finally, **Figure 73** shows that the wear rate increased linearly by increasing the real area of contact, in perfect agreement with the Archard theory, with correlation coefficient equal to 1. The value of the wear coefficient, K, is in the order of 10^{-4}, in agreement with literature which gives values of K ranging between 10^{-3} and 10^{-8}.

It is worth to remind that wear coefficient will have values at different operating conditions as long as the lubrication mechanism is unchanged. In absence of any lubricant, K represents the probability that a free wear particle forms from a junction.

High values of K ($> 10^{-2}$) are usually considered unacceptable in engineering practice. Lower values of K are usually taken to imply that if rubbing consists of repeated asperity contacts, then the vast majority occurs without wear or surface damage and that only a very small proportion of contacts result in the production of a worn particle. In some cases the wear coefficient may be negative due to transfer of material from one specimen to another and thus can increase the volume.
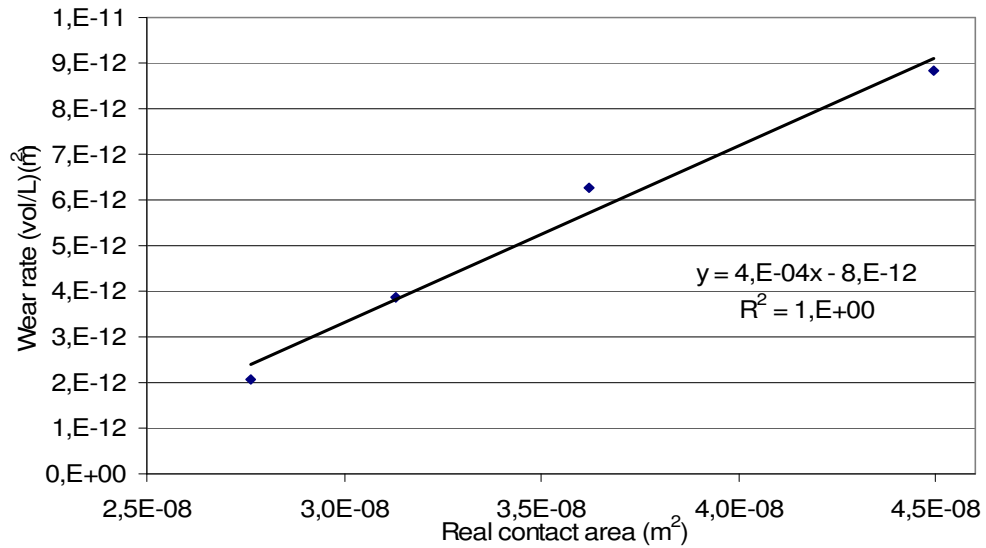
Fig. 73 – Wear rate vs. real contact area

At low loads no surface fatigue could be observed; however, wear mechanism was mainly abrasive, as shown in **Figures 74** and **75**.
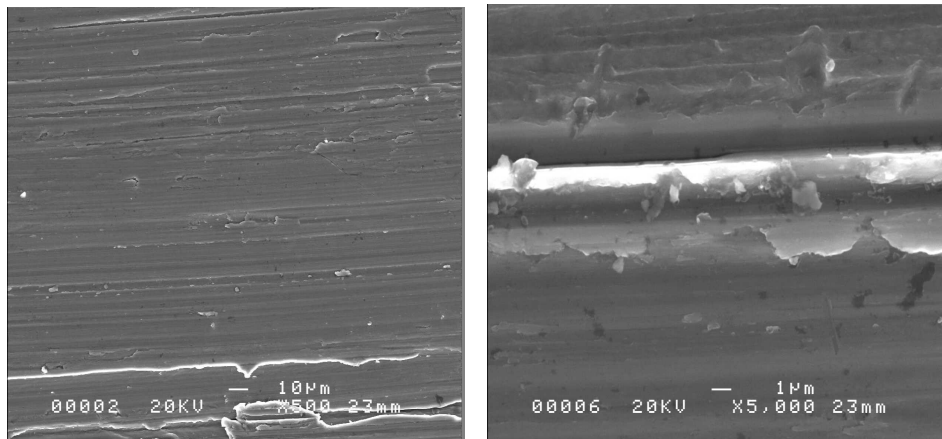
Fig. 74 – Wear track (Load = 15 N; sliding speed = 2 m/s)

Fig. 75 – Wear track (Load = 15 N; sliding speed = 2 m/s)

Keeping constant the sliding speed and increasing the load, the wear remained abrasive in nature, but in some areas of the track it started to form slight delaminations, indicative of adhesive wear, as shown in **Figures 76** and **77**. In this case too there was absence of surface fatigue and the type of wear could be ascribed to two factors: one based on the strong adhesive forces set up whenever atoms of the two sliding materials come into intimate contact according to Bowden and Tabor theory and the other one on

the ploughing by the harder material a series of grooves on the surface of the softer one or breakdown of oxides. The material from the grooves or the oxides was displaced eventually in the form of wear particles, generally loose ones.
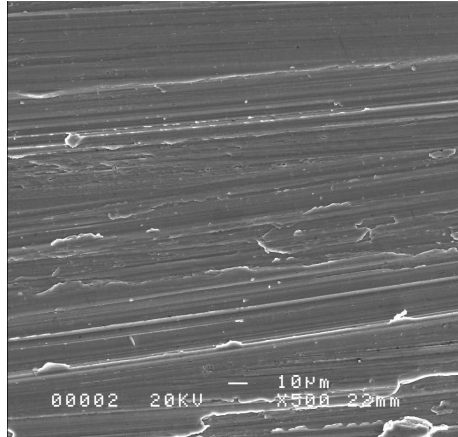
Fig. 76 – Wear track (Load = 20 N; sliding speed = 2 m/s)
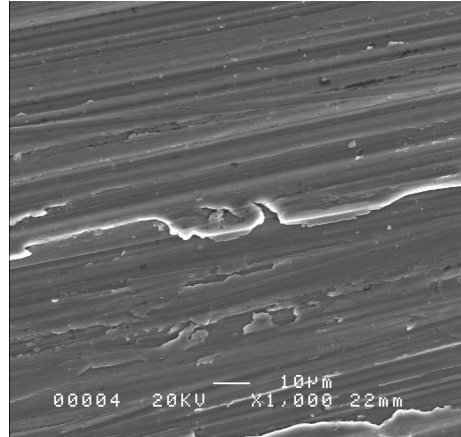
Fig. 77 – Wear track (Load = 20 N; sliding speed = 2 m/s)

At 30 N the grooves due to hard asperities (abrasive wear) had disappeared almost completely, while delaminations (adhesion) and plates detachment (fatigue) could be observed, as shown in **Figures 78** and **79**.
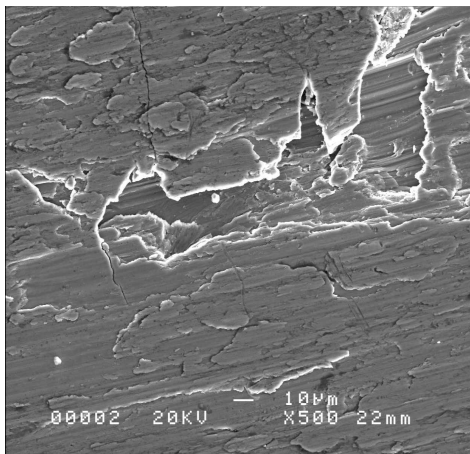
Fig. 78 – Wear track (Load = 30 N sliding speed = 2 m/s)
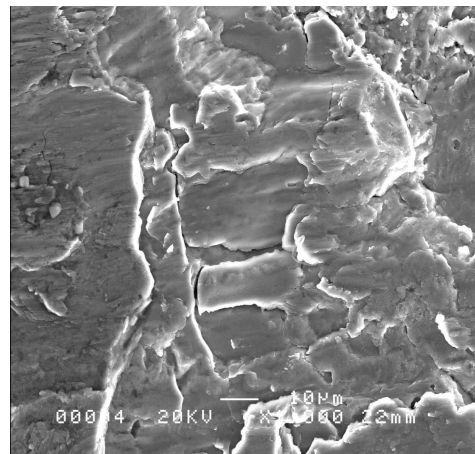
Fig. 79 – Wear track (Load = 30 N; sliding speed = 2 m/s)

2.2 Three coating types

The results of pin on disk tests for the three coating typologies (Ti/TiN by RPS, TiN by PVD-arc, and Ti/TiN by RPS + TiN by PVD-arc] are listed in **Table 33**.

Tab. 33 – Pin on disk test results for the three coating typologies

COATING TYPOLOGY	DEPOSITION TECHNOLOGY	LOAD (N)	FRICTION COEFFICIENT	COATING CONDITION
Ti/TiN	RPS	10	0.717	Slightly damaged
Ti/TiN	RPS	20	0.718	Slightly damaged
Ti/TiN	RPS	30	0.609	Slightly damaged
TiN	PVD-arc	2	0.701	Undamaged
TiN	PVD-arc	5	0.480	Completely damage
TiN	PVD-arc	10	0.507	Completely damaged
Ti/TiN + TiN	RPS + PVD-arc	10	0.702	Undamaged
Ti/TiN + TiN	RPS + PVD-arc	20	0.655	Slightly damaged
Ti/TiN + TiN	RPS + PVD-arc	30	0.660	Completely damaged

It was expected that as soon as the TiN layer became damaged across its full thickness, the friction coefficient from the typical contact TiN/Si_3N_4 would change to that of the $Ti6Al4V/ Si_3N_4$ pair. Such an expectation was confirmed, as illustrated by the graph reported in **Figure 80**. It shows clearly, in fact, that the friction coefficient at both loads of 5 N and 10 N changed sharply around the fifth minute of test and the curves almost overlapped that relative to the Ti6Al4V alloy.
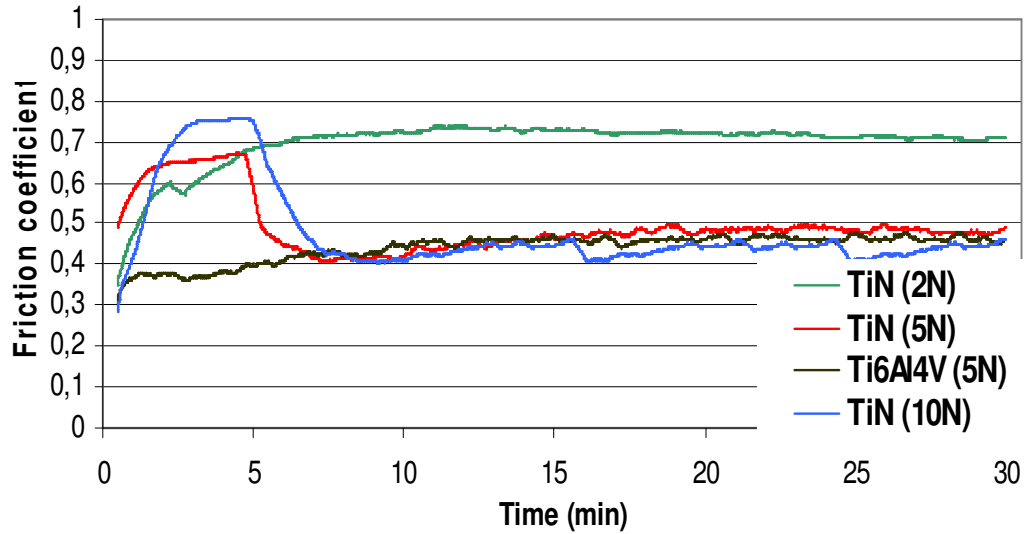
Fig. 80 - Friction coefficient vs. time: assessment of the TiN coating point of fracture

Since the two coatings at the completion of the test resulted to be completely damaged, as shown in **Figure 81**, the sharp change in the friction coefficient indicates the instant the TiN coating was broken down to its interface with the Ti6Al4V alloy. When the same pin on disk test was run at a load of 2 N only, no sharp change in the friction coefficient was observed, as shown by the relative curve in **Figure 80** and by the coating remaining undamaged.
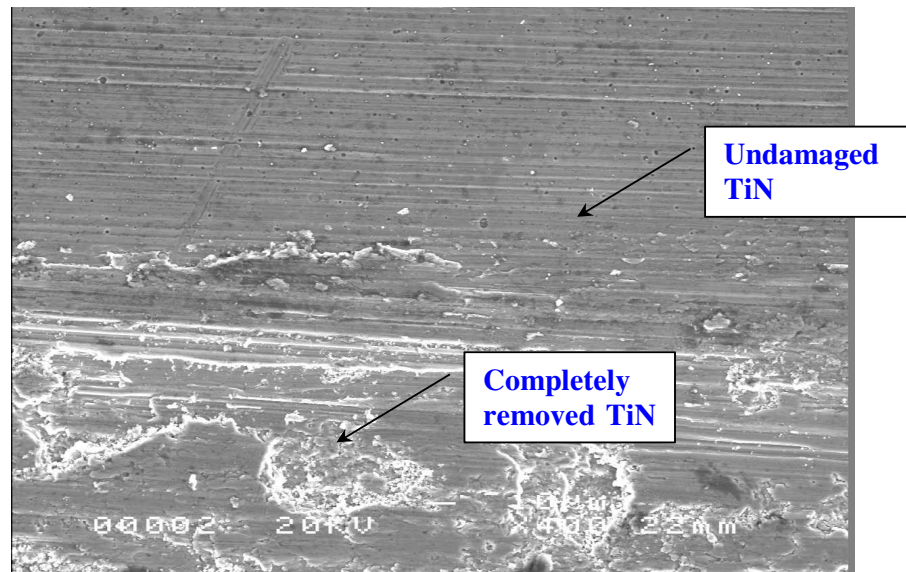
Fig. 81 – Border zone between undamaged and completely removed TiN coating

Performance of the Ti/TiN (RPS) and Ti/TiN + TiN (RPS + PVD-arc) coatings was much better than the PVD-arc TiN coating alone; in fact, for these coatings higher loads were necessary to observe any visible damage.

Damage for the RPS coatings was slight and it increased a little bit by increasing the load with weight losses in the order of a thousandth of gram, close to the limit of the balance precision.

RPS + PVD-arc coatings exhibited a continuous damage by increasing the applied load, but they too had negligible weight losses. These coatings remained undamaged at loads equal to 10 N, while they showed severe damage at 30 N loads.

Figures 82-87 are optical microscopy colour images of the Ti/TiN (RPS) + TiN (PVD-arc) wear track. It can be observed the amount of TiN (yellow) left on the RPS coating (dark grey).
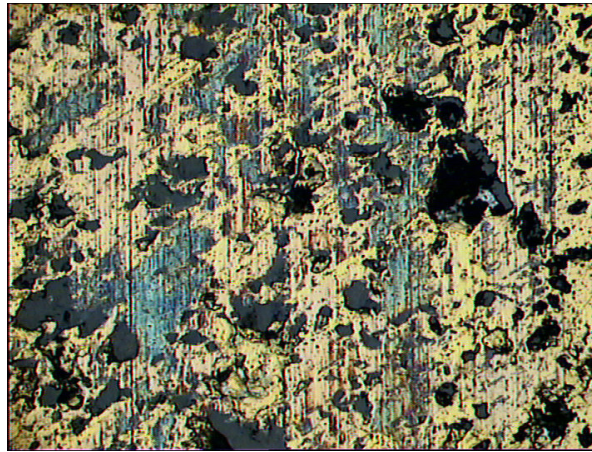

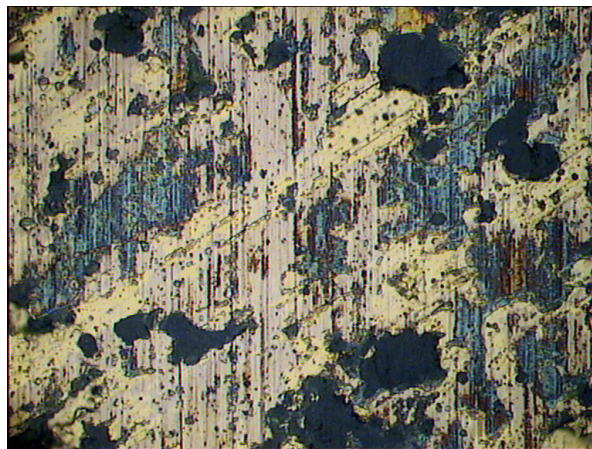
Fig. 82 - (MAG 200X) Load 10 N Speed 0.4 m/s

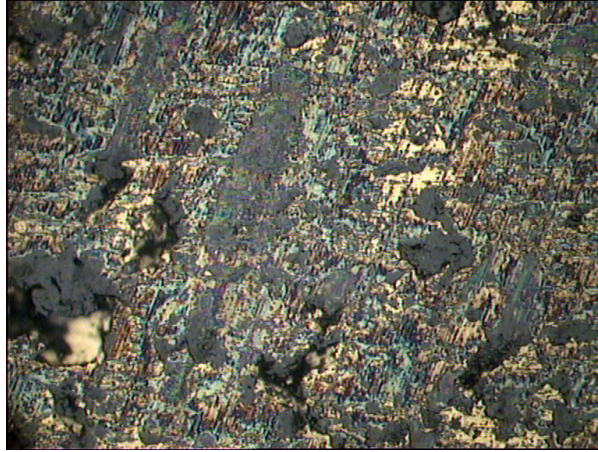**Fig. 83** - (MAG 500X) Load 10 N Speed 0.4 m/s

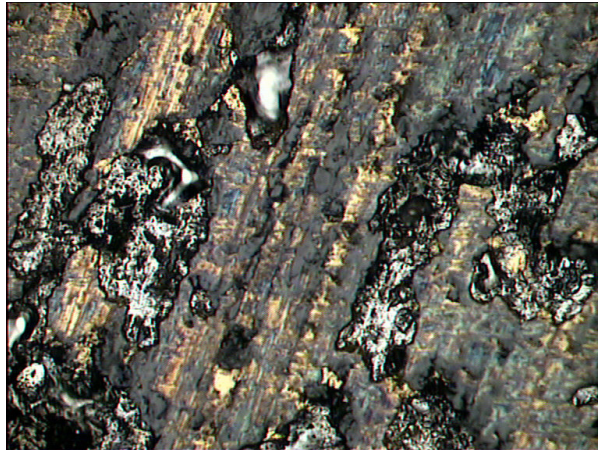**Fig. 84** - (MAG 200X) Load 20 N Speed 0.4 m/s

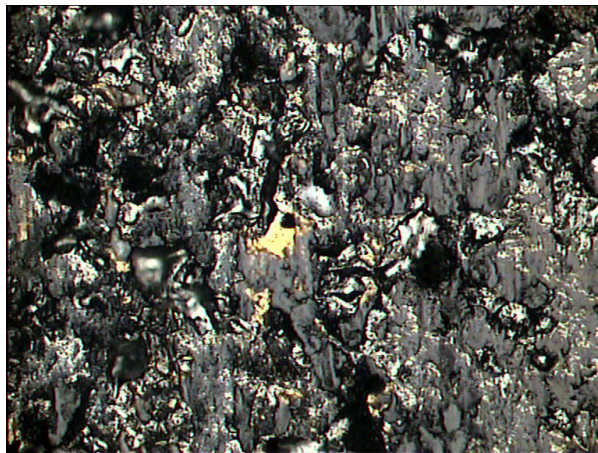**Fig. 85** - (MAG 500X) Load 20 N Speed 0.4 m/s

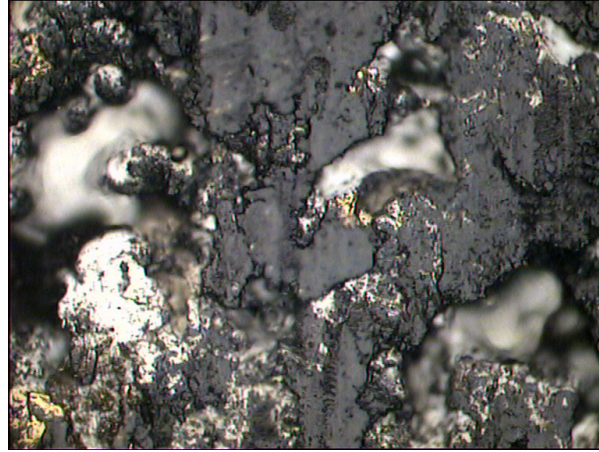**Fig. 86** - (MAG 200X) Load 30 N Speed 0.4 m/s

Fig. 87 - (MAG 500X) Load 30N Speed 0.4 m/s

SEM micrographs show the detachment of coating plates due to fatigue (see **Figures 88** and **89**). Also the thickness of the top TiN layer was assessed around 2-3 µm by a high (5000 X) magnification micrograph, shown in **Figure 90**.
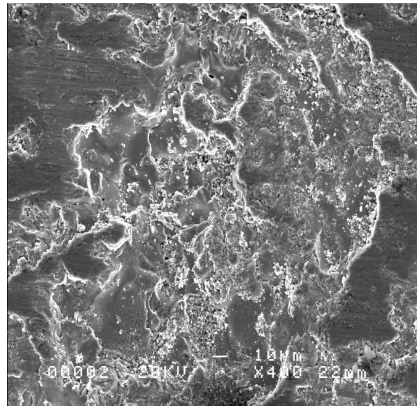

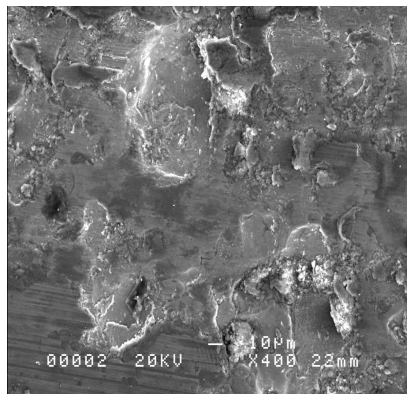**Fig. 88** – Ti/TiN RPS, Load 30N, Speed 0.4 m/s

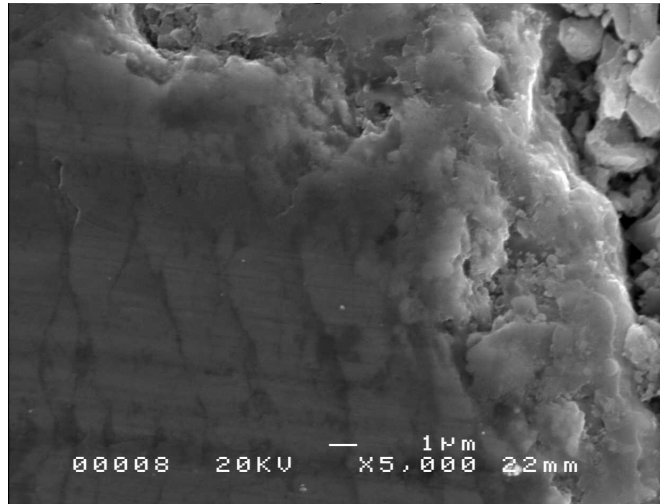**Fig. 89** – Ti/TiN RPS + TiN PVD, Load 30N, Speed 0.4 m/s

Fig. 90 – Detail of the border zone between undamaged TiN and open Ti/TiN RPS

In conclusion the results of optical and SEM suggest the following observations:

- at lower loads (10 N) adhesive and abrasive phenomena seem to coexist on both the RPS and RPS + PVD-arc coatings. Traces of Si_3N_4 were observed on the TiN intact surface. While the RPS undergoes a slight damage, the RPS + PVD-arc coating retains almost unchanged the TiN top layer.
- Increasing the load (20 N and 30 N) an extensive arising of surface fatigue phenomena (detachment of plates) is observed. The TiN top layer seems to show a progressive wear toward its almost complete removal. However, in every case the RPS under layer appears to be much less damaged with respect to the case when the TiN top layer is absent.

3. Realization and testing of mechanical component

The special holder, utilised for both RPS and PVD depositions on the sprocket (ϕ = 250 mm, 48 teeth), is shown in **Figure 91**.

Fig. 91 – Special sprocket holder utilized for RPS and PVD deposition process

The particular deposition procedure, which was developed for the RPS coating, consisted of three consecutive phases, illustrated in **Figure 92**. This approach was taken to minimize as much as possible the lack of uniformity in the thickness of the coating by a robot, on which the torch was assembled, moving in such a way to follow accurately the whole surface of each tooth. The three consecutive coating phases were the following:

- coating the tip and the bottom of each tooth
- coating the front of each tooth
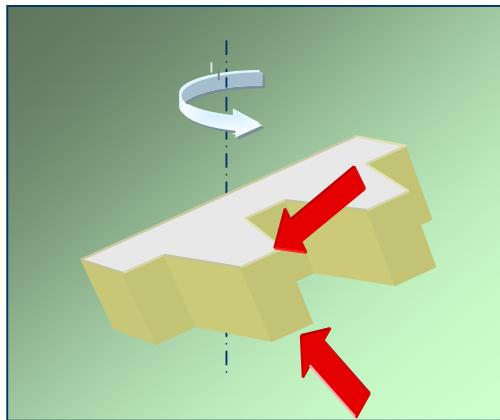- coating the flanks of each tooth
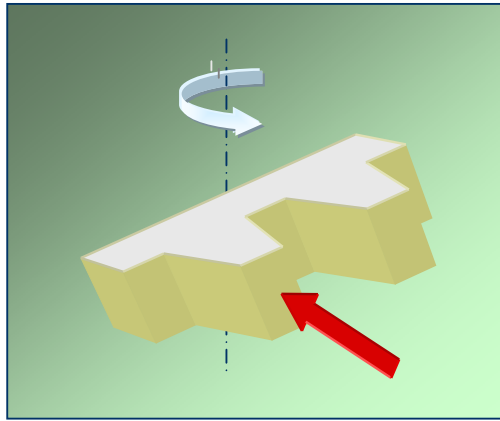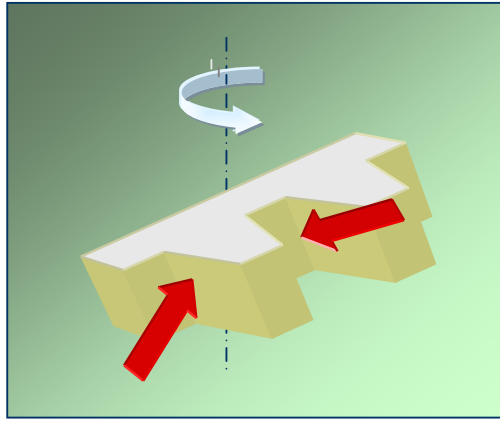
Fig. 92 – Deposition procedure adopted for RPS coating

Figure 93 shows the gears after the RPS deposition.

Fig. 93 – Sprocket after RPS deposition

Figures 94 and **95** show the coating around the teeth.
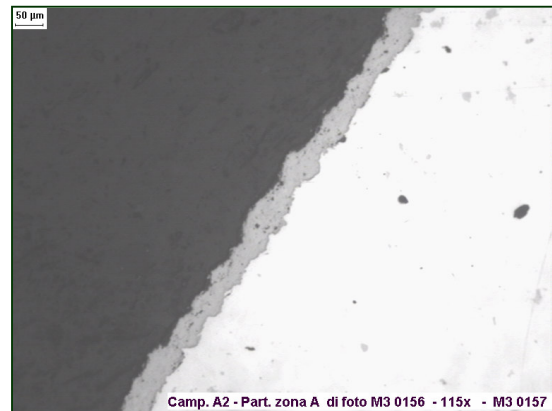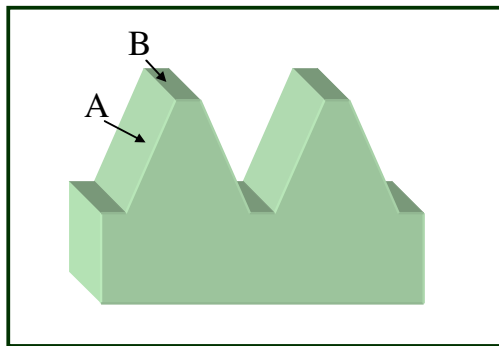
Fig. 94 – Coating on a tooth section (plane of section parallel to the sprocket plane). Zone A of the green scheme: tooth flank

Fig. 95 – Coating on a tooth section (plane of section parallel to the sprocket plane). Zone B of the green scheme (**Fig. 94**): tooth tip

Finally, **Figure 96** shows a sprocket coated with the multilayer system, RPS Ti/TiN + PVD TiN.

Fig. 96– Sprocket coated with the multilayer system, RPS Ti/TiN + PVD TiN

A specific test-bench (**Figures 97** and **98**) was utilised to preliminary assess the performances of the coated components.
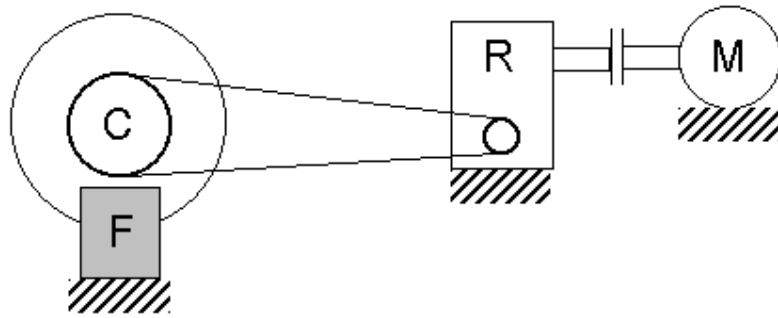
M: electrical engine

R: reducer

C: sprocket to be tested

F: brake

Fig. 97 – Scheme of the test bench for sprockets

Fig. 98 –Test-bench for sprockets

The following tests were carried out:

A) Test with constant mechanical rate, for 8 hours.
B) Test with variable mechanical rate, with the application of increasing resistant torque (by a brake).

During the test, the sprocket was in contact with a transmission chain made of carburized steel. A simple uncoated Ti6Al4V sprocket was tested too, to compare the results.

Table 34 summarizes tests and the measured torques.

Tab. 34 – Tests and measured torques for the coated sprocket on the test-bench

Test	Measured Current (A)	Electrical power (W)	Engine torque C_m (Nm)	Sprocket torque C (Nm)
A	3	1777	0	0
B1	3	1777	0	0
B2	6	3550	5.88	263
B3	9	5325	11.77	527
B4	11	6508	15.69	703

No visible damage (cracks, spall-out, etc.) was evidenced on the coatings after the above reported testing. **Figures 99**-**101** show a new uncoated tooth, a tested uncoated tooth, and a tested coated tooth, respectively.
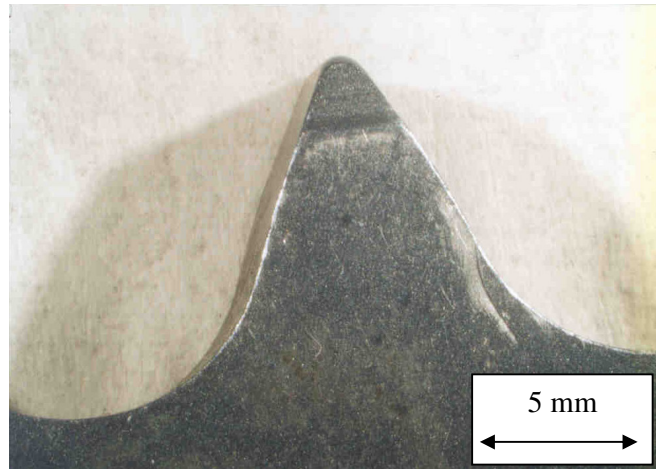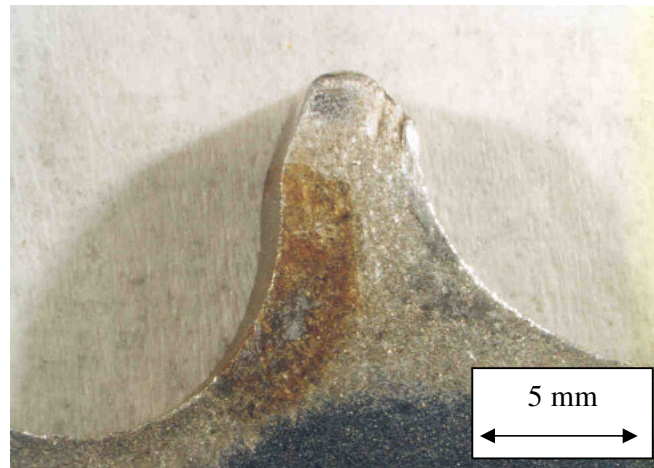
Fig. 99 – New uncoated tooth

Fig. 100 – Uncoated tooth after testing

Fig. 101 – Coated teeth after testing

On the base of the very promising results a coated sprocket was mounted on e real motorbike to run on the streets (**Figure 102**).

Fig. 102 – Sprocket on a motorbike

VI - DISCUSSION

At present there is a strong driving force to increase the use of lightweight titanium alloys for several applications within the aeronautical/aerospace, mechanical, and medical industrial sectors. These alloys possess some excellent properties, including low density, high strength, and corrosion resistance. On the other hand, their poor tribological characteristics have been improved significantly with the application of suitable hard coatings, either by electrochemical (Griffith et al., 2001) or vacuum deposition technologies (Peacock, 1997). However, a big drawback is the inability of the coated alloys to bear, for a satisfactory length of time, fluctuating and highly localised loads. In fact, under these conditions, severe fretting phenomena and excessive wear take place and they generally lead to early damage of the hardened surface layer, often manifesting itself in spalling and cracking.

Margaret W. Hunt, editor *of Advanced Materials and Processes*, devotes the editorial of the V. 166 N° 6 to the titanium world, introducing the Aeromat Conference 2008: "Because of the efforts put forth by a multitude of engineers and scientists, aerospace has become one of the few success stories in American manufacturing. It is a growing industry, with exports of both airplanes and their materials of construction. In particular, titanium alloy developments enable smaller, more powerful engines and lighted-weight structures. Composites, which were formerly considered too expensive for commercial aircrafts, are increasingly the material of choice for many aircraft structures. Titanium's compatibility with composites has increased its use on advanced aircrafts, but has also raised concerns about reliable supply." Dr. Hunt recognizes that the poor surface characteristics of the titanium alloys are yet a major problem; studies and researches of R&D centres and private companies are strongly concentrating in these topics: "Plasma Transferred Arc welding torches that serve as the high energy source for additive manufacturing have been designed by MER Corp. In addition, to the low cost fabrication of metallic structures, this technology has also been used to form very hard surface layers that are functionally graded to the substrate of a cermet composition".

Today's other technical solution in order to prevent fretting, for example on titanium dovetails (the contact between fan blade and disc) is to use the combined effects of shot peening and the application of a soft coating such as CuNiIn applied by plasma spraying, followed by an overlay of MoS_2 varnish applied by brush. The MoS_2 acts as a

friction reducer and it is contained within the porous CuNiIn coating. Behaviour of such a system is satisfactory for some thousand hours of service, but it is followed by coating degradation by wear and spallation and, in the extent, crack initiation. This implies coating stripping and re-coating on the fan blades, and machining of the disc component. Longer life times and better control of the fretting mechanisms on these components are required in order to reach similar life times as other engine components, and to provide more cost-efficient, competitive and safer engines. On the other hand, the tribological limitations have been tackled with a number of other alternative routes: to prevent fretting and wear or to reduce the friction coefficient are being tried electrolytic, thermally sprayed, or PVD coatings. In general, electrolytic coatings include cobalt or nickel with some strengthening phase such as chromium carbide. Apart from the environmental problem that these coating processes represent, and the fact that such coatings cannot be utilized in very important sectors such as the bio-medical, their main failure mode, especially under high contact pressures, is by flaking off. Thermally sprayed wear resistant coatings usually include a hard phase in a metallic matrix (e.g. WC/Co), but adhesion on titanium substrates is difficult to manage, especially due to the machining of the coatings which is required in order to reach thickness tolerances and tribological properties. PVD hard coatings are generally successful, but at higher concentrated loads spalling occurs. Also, a too hard coating risks to induce crack initiation.

These limits are currently tackled by utilising "duplex" processes (Meletis, Erdemir, Fenske, 1995) (runs of diffusion treatments and coating operations) or multilayer coatings (Leyland, Matthews, 1994). The underlying idea is to form layers having mechanical properties changing gradually from the substrate/coating interface to the outermost surface.

Such an idea was at the base of this research work. To this end, a combination of a graded thick coating and a thin top film was developed. The graded coating was obtained by reactive plasma spray (RPS) deposition of a Ti-4,5Al-3V-2Mo-2Fe powder onto a Ti6Al4V alloy substrate. The top thin film was deposited by a physical vapour deposition (PVD) – arc technique - and it was comprised of stoichiometric TiN.

RPS is a technological variant of thermal spraying. This technique allows coatings to be obtained with a thickness of several hundreds of micrometers and, in some cases, up to

a few millimetres. In thermal spraying, the material to be deposited is melted in the interior of an energetic source and then accelerated toward the substrate, where it quickly solidifies. The RPS process uses gaseous plasma (generated by an electric arc in the interior of a torch) as the thermal source for melting and accelerating the particles to be deposited. This technique, however, differs from the parent technology, since it is based on the reaction between a gas and the melted material being sprayed. Therefore, this method can be utilised for synthesizing, directly on the substrate, a variety of compounds such as nitrides, carbides, and borides.

The characterization of the RPS coatings confirmed some previous results in the same field (Tului et al., 2002) but new information was obtained relating the synthesis of the coating. In particular, the effects of major deposition parameters, such as N_2 concentration in the plasma gas mixture, substrate temperature and bias, N_2 pressure inside the spraying chamber, have been understood. The synthesis of TiN takes place mainly in the plasma stream while the nitriding in situ (that's on the substrate, enhanced by its temperature) promotes formation of the Ti_2N phase. A specific experiment showed that the application of a transferred arc during the RPS process increases the quality of the coatings microstructure and their hardness, when the depositions are carried out at high percentages of $N_2\%$, in both plasma gas and spraying chamber, and elevated substrate temperature.

Relating the PVD top layer, a mathematical statistics program - to relate various properties such as hardness, thickness, and scratch characteristics – has been applied successfully. A very important piece of information is represented by the maximum value of the coating adhesion calculated from the regression curves. Such a maximum, in fact, corresponds to a bias of 135 V. If it is considered that, at least at lower temperatures, a bias increase leads to an increase of the TiN absolute hardness, it is legitimate to conclude that an excessive bias increase (that's a higher intensity of ions bombardment) rises the residual stress within the PVD coating, lowering its adhesion to the substrate. In other words, this confirms again that: the higher the bias, the higher the coating hardness; however, an excessive increase of the bias leads to a decrease of the coating adhesion.

The experimental results on the multilayered coating shown that the PVD film formation on the RPS coating did not follow the usual course. In fact, SEM observations, corresponding to preset steps of the PVD process, have pointed out a

rapid growth, inside the RPS cavities until their partial filling, of species morphologically distinguishable from the materials deposited by both RPS and PVD. This was an unexpected result since it indicated some kind of chemical interactions between the PVD film, in its nucleation phase, and the RPS substrate. The growth of these new species seemed to be favoured by the presence of oxygen and carbon inside the pores of the RPS coating. The surface cleaning treatment with oxygenated solvents such as acetone was suspected as a possible source of oxygen. But, this hypothesis did not stand alone, since no differences were noticed when in place of acetone, trichloroethane was used. However, there are other possible oxygen sources such as contaminants (e.g. traces of water) in the gases, Ar and N_2, utilised in the pre-treatment and deposition process, and adsorbed species on the walls of the PVD apparatus which were not completely removed by the outgassing operation.

The presence of oxygen and carbon along with nitrogen and titanium, in the GDOES profiles and in the XPS analyses, suggested that titanium oxynitrides were mainly responsible for the filling of the pores and their formation was likely triggered by the ionic bombardment energy. The oxinitride species inside the cavities was likely favoured by the higher probability of entrapped oxygen bearing species and the effect of electric field concentration, due to the large amount of asperities. In fact, the presence of an electric field with suitable characteristics may enhance significantly the localized plasma activity, improving the likeness of chemical reactions and, thus, the effectiveness of the PVD process.

This piece of work is important because it opens a new field of study relating the thin films nucleation and deposition. In contrast with the usual course of a PVD deposition, in our case interactions involving chemical reactions between the PVD film and the RPS coating were observed. Undoubtedly, these interactions, if well controlled, may contribute to the conferring graded properties and the outstanding adhesion to the multilayer system.

The characterization results, and in particular those related to tribological performance of the newly developed graded coatings, reached so far in this on-going work, represent an important step in conferring to the titanium alloys outstanding tribological properties, as discussed below.

175

An important piece of information is related to the tribological characterization of the uncoated Ti6Al4V alloy in contact with Si_3N_4, contributing to the growth of the know-how in this field.

The behaviour of the wear rate of Ti6Al4V alloy, reported in Figure 68, may be due to physical and chemical changes of the sliding surfaces. In fact, at different sliding speeds, friction will fluctuate according to the junction population changes. Sliding speed is also correlated with surface temperature of the materials and it promotes the interactions between sliding materials as well as between them and environment. Regarding the initial portion of the curve, the increase of speed and, as a consequence, temperature, may favour the arising of oxidation phenomena which are able to protect the sliding surfaces. The change in the curve slope may be due to a breakdown of the surface oxides, contributing to abrasive wear phenomena.

Relating the wear coefficients assessed (in the order of 10^{-4}), it is worth to remind that they will have values at different operating conditions as long as the lubrication mechanism is unchanged. In absence of any lubricant, K represents the probability that a free wear particle forms from a junction. High values of K ($> 10^{-2}$) are usually considered unacceptable in engineering practice. Lower values of K are usually taken to imply that if rubbing consists of repeated asperity contacts, then the vast majority occur without wear or surface damage and that only a very small proportion of contacts result in the production of a worn particle. In some cases the wear coefficient may be negative due to transfer of material from one specimen to another and thus can increase the volume.

Results of the tribological testing showed generally that, increasing the load, the wear mechanism changes and becomes a combination of abrasion and adhesion, before the starting of delamination/surface fatigue phenomena. In this case the type of wear can be ascribed to two factors: one based on the strong adhesive forces set up whenever atoms of the two sliding materials come into intimate contact according to Bowden and Tabor theory and the other one on the ploughing by the harder material a series of grooves on the surface of the softer one or breakdown of oxides. The material from the grooves or the oxides is displaced eventually in the form of wear particles, generally loose ones.

TiN coating on Ti6Al4V alloy demonstrated its very poor performances, also at lower loads. As soon as the TiN layer was damaged across its full thickness, the friction coefficient from the typical contact TiN/Si_3N_4 changed to that of the Ti6Al4V/ Si_3N_4

176

pair. It was possible to determine the instant of the coating complete removal by analysing the friction coefficient curves; friction coefficient at both loads of 5 N and 10 N changed sharply around the fifth minute of test and the curves almost overlap that relative to the Ti6Al4V alloy. Since the coating at the completion of the test resulted to be completely damaged, the sharp change in the friction coefficient indicates the instant the TiN coating is broken down to its interface with the Ti6Al4V alloy. When the same pin on disk test was run at a load of 2 N only, no sharp change in the friction coefficient was observed, as shown by the relative curve and by the coating remaining undamaged.

Performance of the Ti/TiN (RPS) and Ti/TiN + TiN (RPS + PVD-arc) coatings was much better than the PVD-arc TiN coating alone; in fact, for these coatings higher loads were necessary to observe any visible damage.

Damage for the RPS coatings was slight and it increased a little bit by increasing the load with weight losses in the order of a thousandth of gram, close to the limit of the balance precision.

RPS + PVD-arc coatings exhibited a continuous damage by increasing the applied load, but they too had negligible weight losses. These coatings remained undamaged at loads equal to 10 N, while they showed severe damage at 30 N loads.

The tribological behaviour of the multilayered system has to be better understood in the future work, in particular utilising different testing configurations. The tribological performance in case of the fretting conditions is very important for these types of coatings, because there is a direct correlation to specific operating conditions (i.e. coatings on mechanical components for landing gears, etc.).

After the deposition processes development, as a further scaling up, RPS and PVD depositions were carried out for depositing the multilayer Ti/TiN + TiN coating on real components: two motor-bike transmission chain sprockets made up of Ti6-4 alloy, each one with 42 teeth. The gear transmits the motion to the wheel by the teeth contacting a case-hardened steel chain. Thus, the multilayer coating was realised on the toothed gear, utilising the same deposition apparatus and the optimized parameters.

The sprockets were tested on a specific test bench and, on the base of the very promising results a coated sprocket was mounted on e real motorbike.

The system studied in the present program of research introduces a strong character of originality in the context of the coatings and the surface treatments for components in light alloy. Beside the multilayer coatings and the duplex processes, a new class of systems process/product (meaning with *process* the technology of deposition and with *product* the materials of the surface layers) seems to be able to show with success on scientific/technical panorama, thanks to preliminary results that are quite encouraging. Such class of systems consist in the combination in succession of thick coatings obtained by means of thermal-spraying and of thin films deposited through PVD. If in the present work it has been developed a specific combination (Reactive Plasma Spray-PVD), this does not exhaust the potentialities of such typologies of approach; in relation to the physical/chemical and morphologic characteristics of the substrate and of the specific requirements, in principle it would be possible combining all the technological variants of thermal-spraying (Plasma-Spray, Arc-Spray, HVOF, PTA) and of the PVD (arc, sputtering, EB), for the planning and the realization of surface systems, with graded mechanical characteristics.

VII - CONCLUSIONS

A new graded coating system, obtained by combining Reactive Plasma Spray (RPS) and Physical Vapour Deposition (PVD) techniques, has been developed. The graded system consists of a Ti/Ti_xN_y (by RPS) composite coating on Ti6Al4V substrate and a stoichiometric TiN (by PVD-arc) top layer.

A basic parametric understanding, with the contribution of a DOE statistical analysis, of both the RPS and PVD processes, to form the multilayer graded coating, has been achieved.

- In regard to the RPS, the effects of major deposition parameters, such as N_2 concentration in the plasma gas mixture, substrate temperature and bias, N_2 pressure inside the spraying chamber, have been understood. In particular:

  ▪ nitride formation, coating hardness and particles melting are enhanced by increasing pressure in the spraying chamber. However, brittleness and porosity of the coatings tend to increase too.

  ▪ Particles melting is enhanced by increasing N_2 in the gaseous plasma. This is likely due to the higher enthalpy conferred by N_2 to the plasma, with respect to the contribution of Ar.

  ▪ Extent of nitriding increases by increasing nitrogen content in both spraying atmosphere and plasma gas mixture. This generally results in higher hardness of the coatings.

  ▪ The synthesis of TiN takes place mainly in the plasma stream while the nitriding in situ (that's on the substrate, enhanced by its temperature) promotes formation of the Ti_2N phase.

  ▪ The application of a transferred arc during the RPS process increases the quality of the coatings microstructure and their hardness, when the depositions are carried out at high percentages of $N_2\%$, in both plasma gas and spraying chamber, and elevated substrate temperature

- Relating the PVD, a mathematical statistics program - to relate various properties such as hardness, thickness, and scratch characteristics – has been applied successfully.

  By the regression curves it was observed that the TiN highest absolute hardness value was obtained at a temperature of 400°C and a negative bias of 165 V. A very important piece of information is represented by the maximum value of the coating adhesion. Such a maximum, in fact, corresponds to a bias of 135 V. If it is considered that, at least at lower temperatures, a bias increase leads to an increase of the TiN absolute hardness, it is legitimate to conclude that an excessive bias increase (that's a higher intensity of ions bombardment) rises the residual stress within the PVD coating. In other words, this confirms again that: the higher the bias, the higher the coating hardness; however, an excessive increase of the bias leads to a decrease of the coating adhesion.

However, more important, interactions involving chemical reactions between the TiN top layer and the RPS coating were observed. Such interactions, promoted by the presence of oxygenated species inside the pores of the RPS underlayer, led to the formation of titanium oxinitrides. These last ones, during the nucleation phase of the PVD film, grew rapidly, filling up partially the RPS cavities.

PVD leaves generally a thin uniform layer on the substrate surface without altering its topography. In this case, on the contrary, the chemical reactions leading to the formation of oxinitrides, showed a significant alteration of the RPS surface topography with synergic effects.

The results of characterization and tribological testing - which have indicated this graded system to possess a much improved structural integrity and higher load carrying capacity, over current solutions - open up a possible enlargement of the number of applications and industrial sectors where titanium based materials could be employed.

Finally, a real mechanical component, a motor-bike toothed gear, was coated with the developed graded system. Preliminary results of its in evaluation have been very encouraging.

VIII - FUTURE WORK

The system studied in the present program of research introduces a strong character of originality in the context of the coatings and the surface treatments for components in light alloy. Beside the multilayer coatings and the duplex processes, a new class of systems process /product (meaning with *process* the technology of deposition and with *product* the materials of the surface layers) seems to be able to show with success on scientific/technical panorama, thanks to preliminary results that are quite encouraging. Such class of systems consist in the combination in succession of thick coatings obtained by means of thermal-spraying (RPS) and of thin films deposited through PVD.

Relating the specific system RPS+PVD, the following topics would be further investigated in the future work:

- the nucleation of the PVD thin films on the thermal sprayed surface structures. If in this work a specific Ti based system was considered, it is worth to investigate the nucleation and the growth of other coating materials with interesting tribological properties (CrN, ZrN, TiAl, TiAlBN, DLC, etc.).
- The tribological behaviour of the multilayered system has to be better understood, in particular utilising different testing configurations. In particular, the tribological performance in case of the fretting conditions is very important for these types of coatings, because there is a direct correlation to specific operating conditions (i.e. coatings on mechanical components for landing gears, etc.).

If in the present work it has been developed a specific combination (Reactive Plasma Spray-PVD), this does not exhaust the potentialities of such typologies of approach; in relation to the physical/chemical and morphologic characteristics of the substrate and of the specific requirements, in principle it would be possible combining all the technological variants of thermal-spraying (Plasma-Spray, Arc-Spray, HVOF, PTA) and of the PVD (arc, sputtering, EB), for the planning and the realization of surface systems, with graded mechanical characteristics.

In this context, first experiments combining HVOF and Arc-PVD, were carried out relating piston pins for sport automotive, made of steel. The objective is the realization

of a multilayered coating resistant to the concentrated loads, with a surface roughness very low (about 0.06 μm Ra). Only HVOF coatings, among the thermal-spray technologies, can be machined up this roughness and the main research work would be concentrated on this topic.

Finally, the development of each new system has to take into account the cost-analysis process, to demonstrate its convenience, also from the economical point of view.

IX - REFERENCES

Arthur, G. ed. (1985), *Wear resistant surfaces in engineering*, London: Department of Trade and Industry, Her Majesty's Stationery Office

ASM Handbook (1980), *Metals Handbook, Properties and Selection: Stainless Steels, Tool Materials, and Special-Purpose Materials*, Vol 3, 9th ed.

ASM Handbook (1990), *Metals Handbook, Properties and Selection: Nonferrous Alloys and Special-Pourpose Metals*, Vol 2, 10th ed.

ASMI Handbook (1994), *Materials Properties Handbook: Titanium Alloys*

ASTM E 3-01: *Standard Guide for Preparation of Metallographic Specimens*

ASTM E 766-98 (Reapproved 2003): *Standard Practice for Calibrating the Magnification of Scanning Electron Microscope*

ASTM E 986-97: *Standard Practice for Scanning Electron Microscope Beam Size Characterization*

ASTM E 1508-98 (Reapproved 2003): *Standard Guide for Quantitative Analysis by Energy-Dispersive Spectroscopy*

ASTM B 748-90 (Reapproved 2001) *Standard Test Method for Measurement of Thickness of Metallic Coatings by Measurement of Cross Section with a Scanning Electron Microscope*

Batista, J.C.A., Godoy, C., Matthews, A. (2002), 'Micro-scale abrasive wear testing of duplex and non-duplex (single layered) PVD (Ti, Al)N, TiN and Cr-N coatings', *Tribology International*, 35, pp.363-372

Battelle Columbus Laboratories ed. (1963), *Aerospace Structural Metals Handbook*, Vol. 4

Bell, T., Dong, H., Sun, Y. (1998), 'Realising the potential of duplex surface engineering', *Tribology International*, 31 (1-3), pp. 127-137

Bill, R.C. (1985), 'Selected Fretting-WearResistant Coatings for Ti-6%Al-4%V Alloy', *Wear*, 106, pp. 283-301

Bolster, R.N. et al. (1991), 'Preparation by ion-beam-assisted deposition, analysis and tribological behavior of MoS_2 films', *Surf. Coat. Tech.*, 46, p. 207

Breyfogle, F. W. (1992), *Statistical Methods for testing, development and manufacturing*, Wiley-Interscience publication, p. 176

Broekaert, J.A.C. (1987), 'State of the Art of Glow Discharge Lamp Spectrometry', *Journal of Analytical Atomic Spectrometry*, 2, p. 537

Buchholtz, B.W., Kustas, F.M. (1996), 'Effects of surface pretreatment of Ti-6AI-4V on the adhesion and wear lifetimes of sputtered MoS_2 coatings', *Tribol. Trans.,* 39 (2), pp. 330-337

Buckley, D.H. (1981), *Surface Effects in Adhesion, Friction, Wear and Lubrication,* New York: Elsevier Scient., p. 353

Budinski, K.G. (1991), 'Tribological properties of titanium alloys',*Wear*, 151, p. 203

Bull, S.J., Berasetegui, E.G., Page, T.F. (2004), 'Modelling of the indentation response of coatings and surface treatments', *Wear*, 256, pp. 857-866.

Carassiti, F. et al. (1995), 'Presentation of the first Italian CAPS and preliminary experiences', in proc. 4th Euro Ceramics Conference, Riccione (I)

Chamont et al. (1988), 'Wear Problems in Small Displacements Encountered in Titanium Alloys Parts in Aircraft Turbomachines', in proc. Sixth World Conf. on Titanium, Cannes, pp. 1883-1888

Chicot, D., Lesage, J. (1995), 'Absolute hardness of film and coating', *Thin Solid Films,* 254, pp. 123-130

Conrad, H. (1981), 'Effect of interstitial solutes on the strength and ductility of titanium'*, Prog. Mat. Sci.*, Vol 26, pp.123-403

Covington, L.C. (1975), 'Factors Affecting the Hydrogen Embrittlement of Titanium', *Corrosion/75*, Toronto

Covington, L.C., Schutz, R.W. (1981), 'Effects of Iron on the Corrosion Resistance of Titanium', *Industrial Applications of Titanium and Zirconium*, pp. 163-180

Covington, L.C., Schutz, R.W. (1982), *Corrosion Resistence of Titanium*, TIMET Corporation Brochure

Davanloo, F., Park, H., Collins, C.B. (1996), 'Protective Coatings of Nanophase Diamond Deposited Directly on Stainless Steel Substrates'*, J. Mater. Res.,* 11 (8), pp. 2042-2050

De Las Heras, E., et al. (2008), 'Duplex surface treatment of an AISI 316L stainless steel; microstructure and tribological behaviour', *Surface & Coating Technology*, 202, 2945-2954

Donachie, M. J. Jr., ed. (1988), *Titanium: A Technical Guide*, Materials Park, OH: ASM International

Dong, H., Bell, T. (1998), 'Designer surfaces for titanium components', *Industrial Lubrication and Tribology*, 50, 282-289

Finlayand, W.L., Synder, J.A. (1950), 'Effect of three interstitial solutes (Nitrogen, Oxygen, and Carbon) on the mechanical properties of high-purity, Alpha Titanium', *Trans. AIME*, Vol. 188; pp. 277-285

Gicquel, A. et al. (1990), 'Plasma and Nitrides: Application to the Nitriding of Titanium', *Pure Appl. Chem.*, 62(9) pp. 1743-1750

Gilmore, C.M., Imam, M.A. (1982), *Titanium and Titanium Alloys*, J.C. Williams and A.F. Belov eds., Plenum Press, p. 637

Gissler, W. (1994), 'Structure and properties of Ti-B-N coatings', *Surf. Coat. Technol.*, 68/69, p. 556

Griffiths, L.E. et al (2001), 'Low temperature electrochemical synthesis of titanium nitride', *Chem. Commun.*, pp. 579-580

He, J.L., Chen, K.C., Davison A. (2005), 'Improvements in the understanding and application of duplex coating systems using arc plasma technology', *Surface & Coating Technology*, 2005, pp. 1464-1471

Hertz, H. (1882), Zeitschrift fur Reine und Angewandte Mathematik, Vol. 92, p. 156.

Huang et al. (1992), 'Microstructural and Identation Characterization of Ti/TiN Multilayer Films', *Surf. Coat. Technol.*, 50, pp. 97-101

Hunt, M. W. (2008), 'Welcome to Aeromat 2008', *Advanced Materials and Processes*, 166, N° 6, p. 3

Ignatiev, M., Kovalev, E., Melekhin, I. (1993), 'Investigation of the Hardening of Titanium Alloy by Laser Nitriding', *Wear*, 166, pp. 233-236

Jamal, T. et al. (1980), 'Friction and Adhesive Wear of Titanium Carbide and Titanium Nitride Overlay Coatings', *Thin Solid Films*, Vol 73, pp. 245-254

Je, J.H. et al. (1966), *J. Mat. Res.*, rapid communication

Knotek, O. et al. (1990), 'Superhard Ti-B-C-N coatings', *Surf. Coat. Technol*., 43/44, p. 107

Kolachev, B.A., et al. (1978), 'Hydrogen Influence on Deformability of Titanium Alloys of Different Phase Compositions, Titanium Physical Metallurgy and Technology', in proc. 3rd Int. Conf. VILS, vol.3, Moscow, pp. 61-68

Kolachev, B.A. et al. (1993), 'Hydrogen Technology of Titanium Alloys', *Titanium,* N°1, pp. 27-30

Kustas, F.M. et al. (1992), 'High Temperature Nitrogen Implantation of Ti-6Al-4V; Part I: Microstructure Characterization; Part II: Tribological Properties*, Surf. Coat. Technol.*, 51 pp. 100-105, 106-111

Kustas, F.M. et al. (1993), 'Diamondlike carbon coatings on Ti-6Al-4V', *Tribol. Trans.*, 36 (1), pp. 113-119

Kwietniewski, C, et. al. (2001), 'Duplex surface treatment of high strength Timetal 550 alloy towards high load-bearing capacity', *Surface & Coating Technology*, 139, pp. 284-292

Kwietniewski, C., et al. (2004), 'Nitrided layers embrittlement due to edge effect on duplex treated AISI M2 high-speed steel', *Surface & Coating Technology*, 179, 27-32

Lanagan, J. (1988), 'Properties of Plasma Nitrided Titanium Alloys', in proc. Sixth World Conf. on Titanium, Cannes, pp. 1957-1962

Lee, S.Y., Kim, S.D., Hong, Y.S. (2005), 'Application of the duplex TiN coatings to improve the tribological properties of Electro Hydrostatic Actuator pump parts', *Surface & Coating Technology*, 193, pp. 266-271

Leyland, A., Matthews, A. (1994), 'Thick Ti/TiN Multilayered Coatings for Abrasive and Erosive Wear Resistance', *Surf. Coat. Technol.*, 70, pp. 19-25

Lin, J., et al. (2006), 'Design methodology for optimized die coatings: the case for aluminium pressure die casting', *Surface & Coating Technology*, 201, pp. 2930-2941

Luo, J., Dong, H., Bell, T. (2006), 'Model-based contact fatigue design of surface engineered titanium gears', *Computational Materials Science*, 35, pp. 447-457

Mao, K., Sun, Y., Bell, T. (2007), 'An initial approach to the link of multi-layer coatings contact stresses and the surface engineered gears', *Surface & Coating Technology*, 201, pp. 5796-5803

Matthes, B. et al. (1991), 'Corrosion performance of some titanium-based hard coatings', *Surf. Coat. Technol.*, 49, p. 489

Matthes, B., Broszeit, E., Kloos, K. H. (1993), 'Tribological behaviour and corrosion performance of Ti-B-N hard coatings under plastic manufacturing conditions', *Surf. Coat. Technol.*, 57, p. 97

Matthews, A., Murawa, V. (1985), **'**Latest work with TiN coating extends tool life', *Chart. Mech. Eng.*, 32, p. 31

Matthews, A. et al. (1991), *IMechE Publication,* C412/038 (1991) p. 213

McQuillan, A.D. (1956), *Titanium*, New York: Academic Press

Meletis, E.I., Erdemir, A., Fenske, G.R. (1995), 'Tribological Characteristics of DLC Films and Duplex Plasma Nitriding/DLC Coating Treatments', *Surf. Coat. Technol.*, 73, pp. 39-45

MIL-HDBK 5, 1 (1991)

Miyoshi, K., Buckley, D.H. (1982), 'Correlation of Tensile and Shear Strengths of Metals with their Friction Properties', *ASLE Trans.*, Vol 27 (N°1), pp. 15-23

Molchanova, E.K. (1965), *Phase Diagrams of Titanium Alloys (translation of Atlas Diagram Sostoyaniya Titanovyk Splavov)*, Jerusalem: Israel Program for Scientific Translations

Moody, N. R., Costa, J. E. (1991), 'A Review of Microstructural Effects on Hydrogen-induced Sustained Load Cracking in Structural Titanium Alloys', in proc. Symp. Properties/Structure Relationships in Titanium Alloys and Titanium Aluminides

Motte, P. et al. (1976), 'A Comparative Study of the Oxidation with Water Vapour of Pure Titanium and Ti-6Al-4V', *Oxd. Met.*, Vol 10, pp. 113-125

Murray, J.L., Wriedt, H. A. (1987), *Phase Diagrams of Bynary Titanium Alloys*, OH: ASM International

Oh, U.C. Je, J.H. (1993), 'Effects of strain energy on the preferred orientation of TiN thin films', *J. Appl. Phys.*, 74, p. 1692

Ohring, M. (1992), *The Materials Science of Thin Films*, Academic Press

Oliver, W.C. et al. (1984), 'Ion Implanted Ti-6Al-4V', in proc. Mat. Res. Soc. Symp., Vol 27, pp. 699-704

Peacock, D.K. (1997), 'The Selection and Application of Coatings for Titanium and Titanium Alloys', in proc. Eurocorr '97 Vol. II, Trondheim, Norway, pp. 22-25

Pelleg, J., Zevin, L.Z., Lungo, S. (1991), 'Reactive-Sputter-Deposited TiN Films on Glass Substrates', *Thin Solid Films*, 197, p. 117

Podgornik, B. (2001), 'Coated machine elements – fiction or reality?', *Surface & Coating Technology*, 146-147, pp.b318-323

Podgornik, B., Vizintin, J. (2003), 'Tribology of thin films and their use in the field of machine elements', *Vacuum*, 68, pp. 39-47

Pons, F. et al. (1987), 'Inibition of Tribo-Oxidation Preciding Wear by Single-Phased TiN_x Films Formed by Ion Implantation into Ti-6Al-4V', *J. Mater. Res.*, Vol 2 (N°5), pp. 580-587

Rahman, M., et al. (2005), 'Investigation of mechanical properties of TiN + MoSx coating on plasma-nitrided substrate', *Surface & Coating Technology*, 200, 1451-1457

Rahman, M., et al. (2007), 'Continuously deposited duplex biomedical coatings', *Surface & Coating Technology*, 201, 5310-5317

Rassmann G., L. Illgen (1972), *Neue Hutte*, vol 17, pp. 321-328

Rebholz, C. et al. (1998), 'Structure, mechanical and tribological properties of Ti–B–N and Ti–Al–B–N multiphase thin films produced by electron-beam evaporation', *J. Vac.Sci. Technol.*, A 16 (5) p. 2851

Rebholz, C. et al. (1999), 'Deposition and characterisation of TiAlBN coatings produced by direct electron-beam evaporation of Ti and Ti-Al-B-N material from a twin crucible source', *Thin Solid Films.*, 343/344, p. 242

Rebholz, C et al. (1999), 'The effect of boron additions on the tribological behaviour of TiN coatings produced by electron-beam evaporative PVD', *Surf. Coat. Technol.*, 116-119, pp. 648-653

Ronkainen, H. et al. (1990), 'Comparative tribological and adhesion studies of some titanium-based ceramic coatings', *Surf. Coat. Technol.*, 43/44, p. 888

Rosemberg, H.W. (1970), 'Titanium Alloying in Theory and Practice in The Science', in proc. 1st Int. Conf. on Titanium, London, pp. 851-859

Rother, B. et al. (1997), 'Applicative characterization of cathodic arc-deposited Ti–B–N coatings', *Surf. Coat. Technol.*, 97, p. 564

Rother, B., Kappl, H. (1997), 'Effects of low boron concentrations on the thermal stability of hard coatings', *Surf. Coat. Technol.*, 96, p. 163

Salmon, D.R. (1979), *Low Temperature Data Handbook, Titanium and Titanium Alloys*, Nat. Phis. Lab. NPL Report QU53 (N80 23448)

Seitzman, L.E., Bolster, R.N., Singer, I.L. (1992), 'Effects of temperature and ion-to-atom ratio on the orientation of IBAD MoS_2 coatings', *Surf. Coat. Tech.,* 51, p. 232

Seitzman, L.E., Bolster, R.N., Singer, I.L. (1996), 'IBAD MoS_2 Lubrication of Titanium Alloys', *Surf. Coat. Tech.*, 78, pp. 10-13

Smith, J., Liu, C. (1953), 'Stresses due to tangential and normal loads on an elastic solid with application to some contact stress problems', *J. Appl. Mech.*, ASME 20, p. 157

Snyder, C.E., Dolle, R.E. (1975), 'Development of Polyperfluoroalchylehters as High Temperature Lubricants and Hydraulic Fluids', *ASME Trans.*, Vol 19 (N°3), pp.171-180

Tamura, M., Kubo, H. (1992), 'Ti-B-N coatings deposited by magnetron arc evaporation', *Surf. Coat. Technol.*, 54/55, p. 255

Taylor, D. (1981), *Fretting Fatigue,* London: Waterhouse R. Ed., Applied Science Publishers, Ltd., p. 177

Tian, H., Saka, N., Suh N.P. (1989), 'Boundary Lubrication of undulated metal surfaces at elevated temperature', *Tribology Transaction,* 32 (3), p. 289

Toth, L.E. (1971), *Transition Metal Carbides and Nitrides*, New York and London: Academic Press, p. 248

Tului, M. et al. (2002), 'Analytical characterization of various titanium nitride based coatings obtained by reactive plasma spraying' in proc. ITSC – Essen (D)

Vardiman, R.G. et al. (1983), 'The Effect of Ion Implantation on Fretting Fatigue in Ti-6Al-4V', *Ion Implantation for Materials Processing*, F.A. Smidt Ed., pp. 165-177

Vardiman, R.G. (1984), 'Wear Improvement in Ti-6Al-4V by Ion Implantation', in proc. Mat. Res. Soc. Symp., Vol 27, pp. 705-710

Wagner, C.D. et al. (1981), 'Spectroscopy for Chemical Analysis', *Surf. Interface Anal.*, 3, p. 211

Wasa, K., Hayakawa, S. (1991), *Handbook of sputter deposition technology*, New Jersey: Noyes Publication

Webster, M., Sayles, R. (1986), 'A numerical model for the elastic frictionless contact of real rough surfaces', *J. Tribol.*, ASME 108, p. 314

Weissmantel, C. (1983), 'Applications of ion beams for the preparation of thin films', in proc. IX IVC-VICES, Madrid, p. 300

Welsch, G. et al. (1977), 'Deformation characteristics of age hardened Ti-6Al-4V', *Met. Trans.*, Vol 8A, pp. 169-177

Wierzchon, T. (2004), 'Structure and properties of multicomponent and composite layers produced by combined surface engineering methods', *Surface and Coating Technology*, 180, pp. 458-464

Wierzchon, et al. (2000), 'Structure and Properties of Composite Layers Produced by Combined Methods of Surface Treatments', in proc. 12th International Federation for Heat Treatments and Surf. Eng. Congress, Melbourne, vol. 2, pp.31-35

Wilson, A. et al. (1993), 'A Comparison of the Wear and Fatigue Properties of Plasma-Assisted Physical Vapour Deposition TiN, CrN and Duplex Coatings on Ti-6Al-4V', *Surf. Coat. Technol.*, 62, pp. 600-607

Wu, L. et al. (2000), 'Analysis of Diamond-Like Carbon and Ti/MoS$_2$ Coatings on Ti-6Al-4V Substrates for Applicability to Turbine Engine Applications', *Surf. Coat. Technol.*, 130, pp. 207-217

Yang, Q.Q. et al. (1996), 'The microstructure of Ti-B-N film-substrate interfaces', *Surf. Coat. Technol.*, 81, p. 287

Yongqing, F., et al. (2000), 'Friction and wear behaviour of carbon nitride films deposited on plasma nitrided Ti-6Al-4V', *Wear*, pp. 12-19

Yongqing, F., et al. (2000), 'Characterization and tribological evaluation of duplex treatment by depositing carbon nitride films on plasma nitrided Ti-6Al-4V', *Journal of Materials Science*, 35, pp. 2215-2227

Yongqing, F., Hejun, D. (2001), 'Effects of the counterface materials on the tribological characteristics of CrN$_x$ coating deposited on plasma-nitrided Ti-6Al-4V', *Materials Science and Engineering*, A298, pp. 16-25

Zhang, Z. X., Dong, H., Bell, T. (2006), The load bearing capacity of hydrogen-free Cr-DLC coatings on deep-case oxygen hardened Ti6Al4V', *Surface & Coating Technology*, 200, 5237-5244

Acknowledgements

This work is dedicated to the memory of Maria Grasso.

A first thanks to Dr. Roberto Bruno of Centro Sviluppo Materiali SpA to have sponsored and encouraged, from the beginning at the end, this special adventure.

A special thanks to Dr. Franco Arezzo, scientific and human mentor, during all these years. To him I owe the scientific formulation, the continuous tension to the knowledge, the courage for some decisions.

Special thanks for Prof. Allan Matthews, my Supervisor, and for his research group, from which I derived big part of the competences that today are at the base of our activities on PVD-batch and on Duplex Surface Engineering.

Thanks to Prof. Philip Rubini for his precious contribution and hospitality to the University of Hull.

Thanks to Ing. Dante Pocci, to have before born and then literally adopted the present work, and me.

The support of the Dr. Mario Tului has been of big importance for the finalization of the most remarkable results. Mario has thought particularly me in the final phase of the job, especially in the formulation of the defence of the thesis.

The technical/scientific/moral support of my group of research has represented a conclusive factor for the good result of the work. Thank you, Edoardo, Roberta, Domenico, Rosanna, Carlo, Franco, Valerio, Marcello, Romano, Manuela.

To Valeria and Fabio Massimo I will communicate in the next years the great enthusiasm and the importance that this work represented for me.

To Claudia I will return the time, the patience, the support.

Finally, thanks to Marilena and Giovanni, to have always believed in me, in these last, very beautiful 40 years.